



**MARYLAND  
ENVIRONMENTAL  
SERVICE**

Parris N. Glendening  
Governor

James W. Peck  
Director

October 2, 2002

Dr. Stephen Storms  
Maryland Port Administration  
Maritime Center II  
2310 Broening Highway  
Baltimore, MD 21224



REF: MPA Contract No. 500912, PIN No. 600105P, MES Contract 99-07-30  
Environmental, Planning, and Technical Services

SUBJ: Task 21.2: Draft Hydrodynamics and Sedimentation Modeling Report for  
Reconnaissance Studies of James Island as a Potential Beneficial Use and Habitat  
Restoration Project

Dear Dr. Storms:

Enclosed please find two copies of the Draft Hydrodynamics and Sedimentation  
Modeling Report for James Island submitted by Moffatt & Nichol. This draft is for your  
review and consideration. Please provide any comments you may have to MES by  
October 16<sup>th</sup>.

Please do not hesitate to contact me at 410-974-7261 if you have any questions or  
comments regarding this report.

Sincerely,

*Rebecca Halloran*

Rebecca Halloran, Natural Resource Planner  
Environmental Dredging

Enclosures



**From:** Steve Storms  
**To:** Halloran, Rebecca  
**Date:** 10/15/02 7:06PM  
**Subject:** James draft hydro report (10/2/02) comments

Rebecca:

My comments are -

I have no technical comments, just a few to achieve internal consistency:

Pg 2-2, line 12: Schubel 1987 in text - does this refer to Schubel and Pritchard 1987 in Ch 9? (may appear elsewhere too, best do a search).

Pg 2-7, line 1: Need to add USACE 1984 to Ch 9.

Pg 2-7, line 14: Need to add E2CR 2002 to Ch 9.

Pg 3-1, line 5: Thomas and McAnally 1985 in text - is it the same as Thomas, McAnally, and Adamec 1985 in Ch 9?

Pg 3-4, line 1 and 2. Add the two Ariaturai references to the ref list in Ch 9.

Pg 3-6, lines 13, 15, 16: more citations to be included in Ch 9.

Pg 3-7, lines 8, 9: ditto.

Pg 3-8, line 12: ditto.

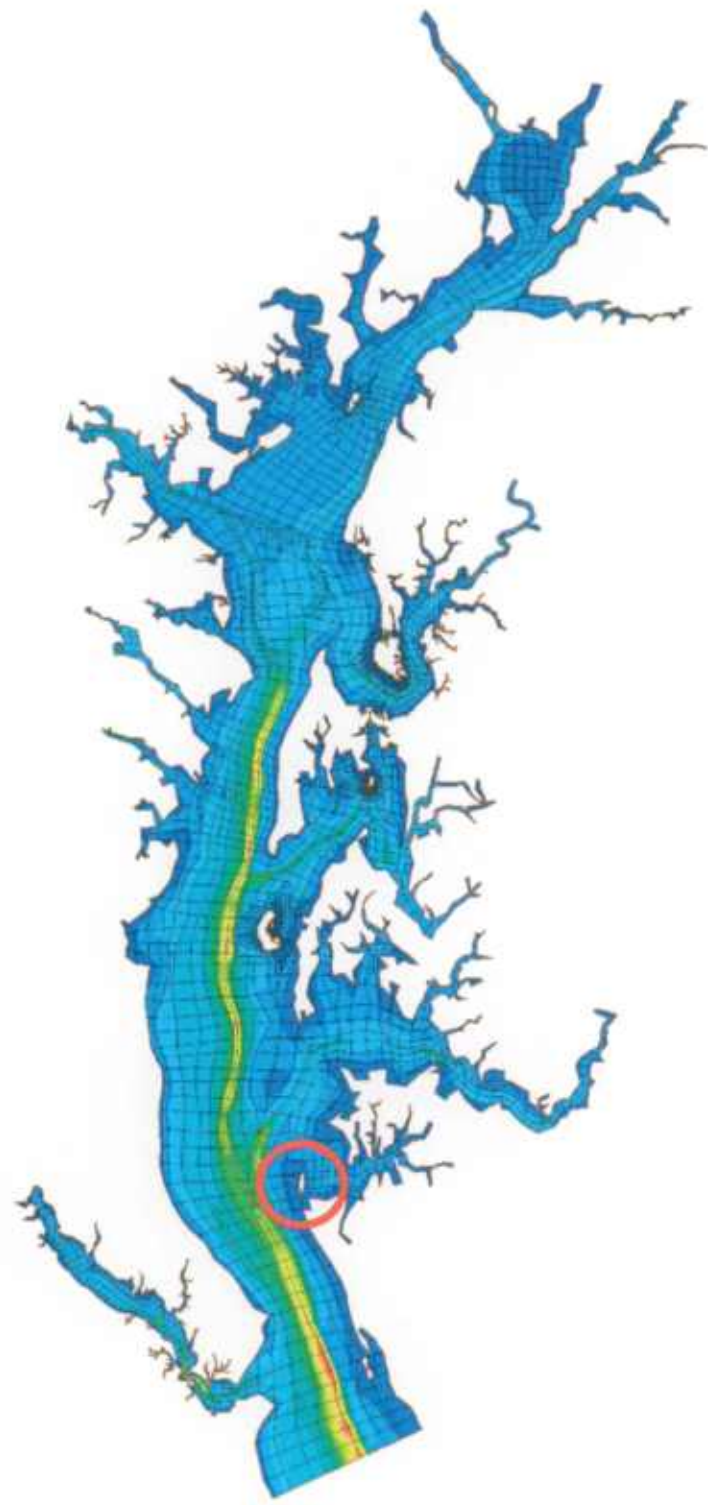
Pg 3-9, line 5: ditto.

Pg 5-10, Fig 5-1: Patapsco is mis-spelled.

Pg 8-24, line 9: there may be a comma missing at the end of the line.

Thanks!

# JAMES ISLAND RECONNAISSANCE STUDY



## HYDRODYNAMICS AND SEDIMENTATION MODELING

**DRAFT REPORT  
SEPTEMBER 30, 2002**

Maryland Port Administration  
MPA Contract Number: 500912  
MPA Pin Number: 600105-P



Maryland Environmental Services  
MES Contract Number: 02-07-49



*Prepared by*



Moffatt & Nichol Engineers  
2700 Lighthouse Point East  
Suite 501  
Baltimore, MD 21224



## EXECUTIVE SUMMARY

The purpose of this Hydrodynamics and Sedimentation Modeling Reconnaissance Study is to evaluate the impacts due to construction of the James Island Beneficial Use of Dredged Material Facility. Moffatt & Nichol Engineers' (MNE) Upper Chesapeake Bay – Finite Element Model (UCB-FEM) (MNE, 2000) was used to predict existing conditions and with-project hydrodynamics and sedimentation. This report summarizes the calibration and implementation of the UCB-FEM two-dimensional numerical model of the Chesapeake Bay and evaluation of hydrodynamic and sedimentation output including time-varying flow velocity, water surface elevations, and patterns of erosion and accretion.

A summary of site conditions that are relevant to the project is provided below:

- **Bathymetry and Topography.** Water depths in the area where the dikes would be located range from –2 to –12 ft MLLW, with an average depth along the exterior dikes ranging from –3 to –12 MLLW. Water depths in the deeper portions of the Bay west of James Island are as great as –93 ft MLLW.
- **Freshwater Inflow.** The drainage area of the Chesapeake Bay is approximately 64,000 square miles and includes portions of Maryland, Virginia, West Virginia, Pennsylvania, New York and the District of Columbia. Freshwater enters the Chesapeake Bay via approximately 150 major rivers and streams at approximately 80,000 cubic feet per second (Schubel, 1987).
- **Tides.** Water levels in the Chesapeake Bay are dominated by a semidiurnal lunar tide. Tides enter the Bay via the Chesapeake Bay entrance and the Chesapeake and Delaware (C&D) Canal. The mean range of tides throughout the entire Chesapeake Bay is generally 1 to 3 ft (NOS, 1988). In the project vicinity, the mean tide level is 0.9 ft above MLLW; the mean tidal range is 1.3 ft and the spring tidal range is 1.8 ft (NOS 1997).
- **Currents.** In the project vicinity, approximately 2.5 miles west of James Island, peak flood currents are about 1.0 ft/sec, and peak ebb currents are about 0.8 ft/sec (NOS,

1 1996). Currents are not considered important for shore protection design at this project  
2 site.

- 3 • **Wind and Wave Conditions.** Design winds for the site were developed on the basis of  
4 data collected at Baltimore-Washington International (BWI) airport. These winds, which  
5 can exceed 90 miles per hour during a 100-year storm event, were used to develop design  
6 wave conditions. James Island is exposed to wind-generated waves approaching from all  
7 directions.
- 8 • **Site Soil Characteristics.** Results of the preliminary study indicate that the underlying  
9 soil consists of silty sand, suitable for supporting the dike. Areas with soft silty clays at  
10 the mud line, however, would need to be undercut and backfilled with sand.

11 The numerical modeling system used in this study consists of the US Army Corps of Engineers  
12 finite element hydrodynamics (RMA-2) and sedimentation (SED-2D) models – collectively  
13 known as TABS-2 (Thomas and McAnally, 1985). The numerical modeling system uses a  
14 bathymetric mesh of water depths, represented by nodes located in the horizontal plane that are  
15 interconnected to create elements.

16 Correlation of the hydrodynamic model calibration results to NOAA predicted data for tidal  
17 elevations and current velocities is generally better than 90%. Predicted percent error is typically  
18 less than 10% for tidal elevations and less than 15% for current velocity.

19 The non-cohesive sediment model was run using 0.1mm (.004 inch) sediment under no-wind  
20 conditions. Analysis of results shows negligible sand transport due to tidal currents. Modeled  
21 non-cohesive sediment transport for existing conditions is negligible for 4- and 13-mph winds  
22 for all directions. Sixteen-mph winds, when taken cumulatively with lower wind speeds, account  
23 for nearly 90% of the yearly wind occurrences and cause significant sediment transport for winds  
24 from the NNW and SSE directions with less sediment transport for winds from other directions.

25 The cohesive sediment model was run for a 6-month simulation period at which point the model  
26 achieved a dynamic equilibrium (average values and rates remain steady over time). The  
27 cohesive sediment model was then run for each of 16 wind directions for wind speeds of 4 and  
28 13-mph.

1 Hydrodynamics and sedimentation numerical modeling for the James Island Reconnaissance  
2 Study show minimal impacts on local tidal elevations, which are essentially unchanged. Current  
3 velocities are impacted following island construction, with maximum increase or decrease in  
4 current velocity of about 0.4 ft/sec. Construction of James Island also would have beneficial  
5 effects on sedimentation rates and patterns, with less erosion of the James Island shoreline and  
6 the shallow areas surrounding the remnant James Islands. Some protection would also be  
7 afforded to the shoreline of Taylors Island from wind and waves coming from the N, NNW, and  
8 NW directions. This reduction in erosion would likely cause reduced suspended sediment and  
9 improved water quality.

10

## TABLE OF CONTENTS

1	<b>TABLE OF CONTENTS</b>		
2	<b>EXECUTIVE SUMMARY</b>		
3	<b>TABLE OF CONTENTS</b>		
4	<b>LIST OF TABLES</b>		
5	<b>LIST OF FIGURES</b>		
6	<b>1. INTRODUCTION.....</b>		<b>1-1</b>
7	1.1 STUDY PURPOSE AND OBJECTIVES.....		1-1
8	1.2 PROJECT SCOPE .....		1-1
9	1.3 STUDY DESCRIPTION .....		1-2
10	<b>2. PROJECT SITE PHYSICAL CONDITIONS.....</b>		<b>2-1</b>
11	2.1 GENERAL .....		2-1
12	2.2 BATHYMETRY AND TOPOGRAPHY.....		2-1
13	2.3 FRESHWATER INFLOW.....		2-2
14	2.4 TIDES .....		2-2
15	2.5 CURRENTS.....		2-4
16	2.6 WIND AND WAVE CONDITIONS.....		2-4
17	2.6.1 Wind Conditions .....		2-4
18	2.6.2 Wave Conditions.....		2-6
19	2.7 SITE SOIL CHARACTERISTICS .....		2-7
20	<b>3. SIMULATION MODELS.....</b>		<b>3-1</b>
21	3.1 GENERAL.....		3-1
22	3.2 HYDRODYNAMIC MODEL .....		3-2
23	3.3 SEDIMENTATION MODEL.....		3-3
24	3.3.1 Convection-Diffusion Governing Equation.....		3-4
25	3.3.2 Bed Shear Stress.....		3-5
26	3.3.3 Source/Sink Terms .....		3-6
27	3.3.3.1 Sand Transport.....		3-6
28	3.3.3.2 Clay Transport .....		3-8
29	3.3.4 Bed Strata Discretization.....		3-9
30	3.3.4.1 Sand Beds .....		3-9
31	3.3.4.2 Clay Beds.....		3-10
32	<b>4. FINITE ELEMENT MESH.....</b>		<b>4-1</b>
33	4.1 GENERAL.....		4-1
34	4.2 ELEMENTS.....		4-1
35	4.2.1 Two Dimensional Elements .....		4-1
36	4.2.2 One Dimensional Elements .....		4-2
37	4.2.3 Special Elements .....		4-2
38	4.3 MODEL EXTENTS.....		4-2
39	<b>5. MODEL CALIBRATION.....</b>		<b>5-1</b>
40	5.1 GENERAL.....		5-1
41	5.2 HYDRODYNAMIC MODEL .....		5-1

1	5.3	SEDIMENTATION MODEL .....	5-6
2	5.3.1	Non-Cohesive Sediment (Sand) .....	5-6
3	5.3.2	Cohesive Sediment (Clay and Silt) .....	5-7
4	<b>6.</b>	<b>HYDRODYNAMIC MODELING RESULTS .....</b>	<b>6-1</b>
5	6.1	GENERAL .....	6-1
6	6.2	HABITAT ISLAND IMPACTS .....	6-1
7	6.2.1	Alignment 1 .....	6-1
8	6.2.2	Alignment 2 .....	6-2
9	6.2.3	Alignment 3 .....	6-3
10	6.2.4	Alignment 4 .....	6-4
11	6.2.5	Alignment 5 .....	6-5
12	<b>7.</b>	<b>SEDIMENTATION MODELING RESULTS.....</b>	<b>7-1</b>
13	7.1	GENERAL .....	7-1
14	7.2	ALTERNATIVE 1 IMPACTS .....	7-1
15	7.2.1	Non-Cohesive Sediment .....	7-2
16	7.2.2	Cohesive Sediment .....	7-2
17	7.3	ALTERNATIVE 2 IMPACTS .....	7-3
18	7.3.1	Cohesive Sediment .....	7-4
19	7.4	ALTERNATIVE 3 IMPACTS .....	7-4
20	7.4.1	Non-Cohesive Sediment .....	7-4
21	7.4.2	Cohesive Sediment .....	7-5
22	7.5	ALTERNATIVE 4 IMPACTS .....	7-5
23	7.5.1	Non-Cohesive Sediment .....	7-5
24	7.5.2	Cohesive Sediment .....	7-6
25	7.6	ALTERNATIVE 5 IMPACTS .....	7-7
26	7.6.1	Non-Cohesive Sediment .....	7-7
27	7.6.2	Cohesive Sediment .....	7-8
28	<b>8.</b>	<b>CONCLUSIONS AND RECOMMENDATIONS.....</b>	<b>8-24</b>
29	8.1	CONCLUSIONS .....	8-24
30	8.2	RECOMMENDATIONS .....	8-24
31	<b>9.</b>	<b>REFERENCES.....</b>	<b>9-1</b>
32			
33			

**LIST OF TABLES**

1

2

3 TABLE 2-1: CHESAPEAKE BAY TIDAL RANGES ..... 2-3

4 TABLE 2-2: WIND SPEED (% OCCURRENCE) BY DIRECTION FOR BWI AIRPORT, 1951-1982 ..... 2-5

5 TABLE 2-3: ANNUAL EXTREME WIND SPEED (MPH) PER DIRECTION FOR BWI AIRPORT,

6 1951-1982 ..... 2-6

7 TABLE 2-4: RADIAL FETCH DISTANCE AND MEAN WATER DEPTH AT JAMES ISLAND ..... 2-7

8 TABLE 5-1: FRESHWATER INFLOW BOUNDARIES ..... 5-2

9 TABLE 5-2: WATER SURFACE ELEVATION CALIBRATION STATISTICS ..... 5-3

10 TABLE 5-3: CURRENT VELOCITY CALIBRATION STATISTICS ..... 5-4

11 TABLE 5-4: SEDIMENT MODEL INITIAL BED LAYERING ..... 5-8

12 TABLE 6-1: HYDRODYNAMIC MODELING RESULTS – ALTERNATIVE 1 ..... 6-2

13 TABLE 6-2: HYDRODYNAMIC MODELING RESULTS – ALTERNATIVE 2 ..... 6-3

14 TABLE 6-3: HYDRODYNAMIC MODELING RESULTS – ALTERNATIVE 3 ..... 6-4

15 TABLE 6-4: HYDRODYNAMIC MODELING RESULTS – ALTERNATIVE 4 ..... 6-5

16 TABLE 6-5: HYDRODYNAMIC MODELING RESULTS – ALTERNATIVE 5 ..... 6-6

17

**LIST OF FIGURES**

1		
2		
3	FIGURE 2-1:	JAMES ISLAND LOCATION MAP ..... 2-8
4	FIGURE 2-2:	JAMES ISLAND AUGUST 2002 AERIAL PHOTOGRAPH LOOKING SOUTHEAST ..... 2-9
5	FIGURE 2-3:	JAMES ISLAND FIVE ALIGNMENTS AND SURROUNDING BATHYMETRY ..... 2-10
6	FIGURE 2-4:	BALTIMORE-WASHINGTON INTERNATIONAL AIRPORT (BWI) WIND ROSE ..... 2-11
7	FIGURE 2-5:	JAMES ISLAND RADIALLY-AVERAGED FETCH DISTANCES ..... 2-12
8	FIGURE 2-6:	OFFSHORE SIGNIFICANT WAVE HEIGHTS (FT) FOR JAMES ISLAND ..... 2-13
9	FIGURE 2-7:	PEAK SPECTRAL WAVE PERIODS (SEC) FOR JAMES ISLAND ..... 2-13
10	FIGURE 3-1:	TABS-2 SCHEMATIC ..... 3-1
11	FIGURE 4-1:	FINITE ELEMENT SHAPES ..... 4-2
12	FIGURE 4-2:	UPPER CHESAPEAKE BAY FINITE ELEMENT MODEL (UCB-FEM) ..... 4-4
13	FIGURE 4-3:	UCB-FEM – JAMES ISLAND EXISTING CONDITIONS ..... 4-5
14	FIGURE 4-4:	UCB-FEM – JAMES ISLAND ALTERNATIVE 1 ..... 4-6
15	FIGURE 4-5:	UCB-FEM – JAMES ISLAND ALTERNATIVE 2 ..... 4-7
16	FIGURE 4-6:	UCB-FEM – JAMES ISLAND ALTERNATIVE 3 ..... 4-8
17	FIGURE 4-7:	UCB-FEM – JAMES ISLAND ALTERNATIVE 4 ..... 4-9
18	FIGURE 4-8:	UCB-FEM – JAMES ISLAND ALTERNATIVE 5 ..... 4-10
19	FIGURE 5-1:	UCB-FEM BOUNDARY CONDITION LOCATIONS ..... 5-10
20	FIGURE 5-2:	UCB-FEM BOUNDARY CONDITIONS ..... 5-11
21	FIGURE 5-3:	UCB-FEM TIDAL ELEVATION CALIBRATION POINTS ..... 5-12
22	FIGURE 5-4:	UCB-FEM CURRENT VELOCITY CALIBRATION POINTS ..... 5-13
23	FIGURE 5-5:	TIDAL ELEVATION CALIBRATION RESULTS ..... 5-14
24	FIGURE 5-6:	CURRENT VELOCITY CALIBRATION RESULTS ..... 5-14
25	FIGURE 5-7:	NON-COHESIVE SEDIMENT – NNW WIND 16 MPH – EXISTING CONDITIONS ..... 5-15
26	FIGURE 5-8:	NON-COHESIVE SEDIMENT – SSE WIND 16 MPH – EXISTING CONDITIONS ..... 5-16
27	FIGURE 5-9:	NON-COHESIVE SEDIMENT – WNW WIND 16 MPH – EXISTING CONDITIONS ..... 5-17
28	FIGURE 5-10:	COHESIVE SEDIMENT – NNW WIND 13 MPH – EXISTING CONDITIONS ..... 5-18
29	FIGURE 5-11:	COHESIVE SEDIMENT – SSE WIND 13 MPH – EXISTING CONDITIONS ..... 5-19
30	FIGURE 5-12:	COHESIVE SEDIMENT – WNW WIND 13 MPH – EXISTING CONDITIONS ..... 5-20
31	FIGURE 6-1:	RESULTS COMPARISON LOCATIONS FOR ALIGNMENT 1 ..... 6-7
32	FIGURE 6-2:	JAMES ISLAND TIDAL RESULTS COMPARISON FOR ALIGNMENT 1 ..... 6-8
33	FIGURE 6-3:	PEAK EBB CURRENT VELOCITY – ALIGNMENT 1 VS. EXISTING CONDITIONS ..... 6-9
34	FIGURE 6-4:	PEAK FLOOD CURRENT VELOCITY – ALIGNMENT 1 VS. EXISTING
35		CONDITIONS ..... 6-9
36	FIGURE 6-5:	RESULTS COMPARISON LOCATIONS FOR ALIGNMENT 2 ..... 6-10
37	FIGURE 6-6:	JAMES ISLAND TIDAL RESULTS COMPARISON FOR ALIGNMENT 2 ..... 6-11
38	FIGURE 6-7:	PEAK EBB CURRENT VELOCITY – ALIGNMENT 2 VS. EXISTING CONDITIONS ..... 6-12
39	FIGURE 6-8:	PEAK FLOOD CURRENT VELOCITY – ALIGNMENT 2 VS. EXISTING
40		CONDITIONS ..... 6-12
41	FIGURE 6-9:	RESULTS COMPARISON LOCATIONS FOR ALIGNMENT 3 ..... 6-13
42	FIGURE 6-10:	JAMES ISLAND TIDAL RESULTS COMPARISON FOR ALIGNMENT 3 ..... 6-14
43	FIGURE 6-11:	PEAK EBB CURRENT VELOCITY – ALIGNMENT 3 VS. EXISTING CONDITIONS ..... 6-15
44	FIGURE 6-12:	PEAK FLOOD CURRENT VELOCITY – ALIGNMENT 3 VS. EXISTING
45		CONDITIONS ..... 6-15
46	FIGURE 6-13:	RESULTS COMPARISON LOCATIONS FOR ALIGNMENT 4 ..... 6-16
47	FIGURE 6-14:	JAMES ISLAND TIDAL RESULTS COMPARISON FOR ALIGNMENT 4 ..... 6-17
48	FIGURE 6-15:	PEAK EBB CURRENT VELOCITY – ALIGNMENT 4 VS. EXISTING CONDITIONS ..... 6-18
49	FIGURE 6-16:	PEAK FLOOD CURRENT VELOCITY – ALIGNMENT 4 VS. EXISTING
50		CONDITIONS ..... 6-18
51	FIGURE 6-17:	RESULTS COMPARISON LOCATIONS FOR ALIGNMENT 5 ..... 6-19
52	FIGURE 6-18:	JAMES ISLAND TIDAL RESULTS COMPARISON FOR ALIGNMENT 5 ..... 6-20
53	FIGURE 6-19:	PEAK EBB CURRENT VELOCITY – ALIGNMENT 5 VS. EXISTING CONDITIONS ..... 6-21

1	FIGURE 6-20: PEAK FLOOD CURRENT VELOCITY – ALIGNMENT 5 VS. EXISTING	
2	CONDITIONS.....	6-21
3	FIGURE 7-1: NON-COHESIVE SEDIMENT – NORTH-NORTHWEST WIND 16 MPH –	
4	ALIGNMENT 1 VS. EXISTING CONDITIONS.....	7-9
5	FIGURE 7-2: NON-COHESIVE SEDIMENT – SOUTH-SOUTHEAST WIND 16 MPH –	
6	ALIGNMENT 1 VS. EXISTING CONDITIONS.....	7-9
7	FIGURE 7-3: NON-COHESIVE SEDIMENT – WEST -NORTHWEST WIND 16 MPH –	
8	ALIGNMENT 1 VS. EXISTING CONDITIONS.....	7-10
9	FIGURE 7-4: COHESIVE SEDIMENT – NORTH-NORTHWEST WIND 13 MPH ALIGNMENT 1	
10	VS. EXISTING CONDITIONS.....	7-10
11	FIGURE 7-5: COHESIVE SEDIMENT – SOUTH-SOUTHEAST WIND 13 MPH – ALIGNMENT 1	
12	VS. EXISTING CONDITIONS.....	7-11
13	FIGURE 7-6: COHESIVE SEDIMENT – WEST-NORTHWEST WIND 13 MPH – ALIGNMENT 1	
14	VS. EXISTING CONDITIONS.....	7-11
15	FIGURE 7-7: NON-COHESIVE SEDIMENT – NORTH-NORTHWEST WIND 16 MPH –	
16	ALIGNMENT 2 VS. EXISTING CONDITIONS.....	7-12
17	FIGURE 7-8: NON-COHESIVE SEDIMENT – SOUTH-SOUTHEAST WIND 16 MPH –	
18	ALIGNMENT 2 VS. EXISTING CONDITIONS.....	7-12
19	FIGURE 7-9: NON-COHESIVE SEDIMENT – WEST -NORTHWEST WIND 16 MPH –	
20	ALIGNMENT 2 VS. EXISTING CONDITIONS.....	7-13
21	FIGURE 7-10: COHESIVE SEDIMENT – NORTH-NORTHWEST WIND 13 MPH ALIGNMENT 2	
22	VS. EXISTING CONDITIONS.....	7-13
23	FIGURE 7-11: COHESIVE SEDIMENT – SOUTH-SOUTHEAST WIND 13 MPH – ALIGNMENT 2	
24	VS. EXISTING CONDITIONS.....	7-14
25	FIGURE 7-12: COHESIVE SEDIMENT – WEST-NORTHWEST WIND 13 MPH – ALIGNMENT 2	
26	VS. EXISTING CONDITIONS.....	7-14
27	FIGURE 7-13: NON-COHESIVE SEDIMENT – NORTH-NORTHWEST WIND 16 MPH –	
28	ALIGNMENT 3 VS. EXISTING CONDITIONS.....	7-15
29	FIGURE 7-14: NON-COHESIVE SEDIMENT – SOUTH-SOUTHEAST WIND 16 MPH –	
30	ALIGNMENT 3 VS. EXISTING CONDITIONS.....	7-15
31	FIGURE 7-15: NON-COHESIVE SEDIMENT – WEST -NORTHWEST WIND 16 MPH –	
32	ALIGNMENT 3 VS. EXISTING CONDITIONS.....	7-16
33	FIGURE 7-16: COHESIVE SEDIMENT – NORTH-NORTHWEST WIND 13 MPH ALIGNMENT 3	
34	VS. EXISTING CONDITIONS.....	7-16
35	FIGURE 7-17: COHESIVE SEDIMENT – SOUTH-SOUTHEAST WIND 13 MPH – ALIGNMENT 3	
36	VS. EXISTING CONDITIONS.....	7-17
37	FIGURE 7-18: COHESIVE SEDIMENT – WEST-NORTHWEST WIND 13 MPH – ALIGNMENT 3	
38	VS. EXISTING CONDITIONS.....	7-17
39	FIGURE 7-19: NON-COHESIVE SEDIMENT – NORTH-NORTHWEST WIND 16 MPH –	
40	ALIGNMENT 4 VS. EXISTING CONDITIONS.....	7-18
41	FIGURE 7-20: NON-COHESIVE SEDIMENT – SOUTH-SOUTHEAST WIND 16 MPH –	
42	ALIGNMENT 4 VS. EXISTING CONDITIONS.....	7-18
43	FIGURE 7-21: NON-COHESIVE SEDIMENT – WEST -NORTHWEST WIND 16 MPH –	
44	ALIGNMENT 4 VS. EXISTING CONDITIONS.....	7-19
45	FIGURE 7-22: COHESIVE SEDIMENT – NORTH-NORTHWEST WIND 13 MPH ALIGNMENT 4	
46	VS. EXISTING CONDITIONS.....	7-19
47	FIGURE 7-23: COHESIVE SEDIMENT – SOUTH-SOUTHEAST WIND 13 MPH – ALIGNMENT 4	
48	VS. EXISTING CONDITIONS.....	7-20
49	FIGURE 7-24: COHESIVE SEDIMENT – WEST-NORTHWEST WIND 13 MPH – ALIGNMENT 4	
50	VS. EXISTING CONDITIONS.....	7-20
51	FIGURE 7-25: NON-COHESIVE SEDIMENT – NORTH-NORTHWEST WIND 16 MPH –	
52	ALIGNMENT 5 VS. EXISTING CONDITIONS.....	7-21
53	FIGURE 7-26: NON-COHESIVE SEDIMENT – SOUTH-SOUTHEAST WIND 16 MPH –	
54	ALIGNMENT 5 VS. EXISTING CONDITIONS.....	7-21
55	FIGURE 7-27: NON-COHESIVE SEDIMENT – WEST -NORTHWEST WIND 16 MPH –	
56	ALIGNMENT 5 VS. EXISTING CONDITIONS.....	7-22

1 FIGURE 7-28: COHESIVE SEDIMENT – NORTH-NORTHWEST WIND 13 MPH ALIGNMENT 5  
2 VS. EXISTING CONDITIONS..... 7-22  
3 FIGURE 7-29: COHESIVE SEDIMENT – SOUTH-SOUTHEAST WIND 13 MPH – ALIGNMENT 5  
4 VS. EXISTING CONDITIONS..... 7-23  
5 FIGURE 7-30: COHESIVE SEDIMENT – WEST-NORTHWEST WIND 13 MPH – ALIGNMENT 5  
6 VS. EXISTING CONDITIONS..... 7-23  
7

# 1. INTRODUCTION

## 1.1 STUDY PURPOSE AND OBJECTIVES

The purpose of this Hydrodynamics and Sedimentation Numerical Modeling Reconnaissance Study report is to analyze impacts due to construction of the James Island Beneficial Use of Dredged Material Facility as regards hydrodynamics and sedimentation in the site vicinity. Moffatt & Nichol Engineers' (MNE) Upper Chesapeake Bay – Finite Element Model (UCB-FEM) (MNE, 2000) was modified to include James Island and used to predict with- and without-project hydrodynamics and sedimentation.

Study objectives include the following:

- Comparison of with- and without-project tidal elevations
- Comparison of with- and without-project current velocities
- Comparison of with- and without-project relative sedimentation rates and patterns for non-cohesive and cohesive sediments

The proposed five alignments are compared to existing conditions, both graphically and numerically, to determine both specific and relative impacts.

## 1.2 PROJECT SCOPE

James Island is being studied as a potential site for beneficial use of dredged material. Benefits of this project include:

- Protection of the remnant James Island and Taylors Island shorelines from additional erosion
- Protection of the shallow water surrounding James Island to provide improved water quality and subsequently promote the re-establishment of subaquatic vegetation
- Creation of additional desirable habitats for fish, vegetation and wildlife

1 To accomplish these objectives, the project consists of the construction of armored dikes that  
2 would serve to contain clean sediments dredged from the Baltimore Harbor approach channels  
3 located within the Chesapeake Bay.

### 4 **1.3 STUDY DESCRIPTION**

5 This report summarizes the calibration and implementation of a two-dimensional numerical  
6 model of the Chesapeake Bay to evaluate the impacts of construction of the James Island facility  
7 on tidal elevations, current velocity conditions, and sedimentation patterns.

8 The existing UCB-FEM model was modified to provide additional detail near James Island and  
9 was re-calibrated to published data, including astronomical tidal information, tidal current  
10 velocity information, and streamflow discharge for existing conditions. The calibrated model  
11 was used to compare hydrodynamic and sedimentation conditions within the model domain for  
12 the proposed construction alignment.

13 The UCB-FEM model was developed based on the following U.S. Army Corps of Engineers  
14 (USACE) numerical models:

- 15       ➤ RMA-2: A depth-averaged finite element model for the simulation of velocities and  
16       water elevations for river systems, estuaries and other shallow water bodies. The  
17       model can be applied in either a one- or two-dimensional mode.
- 18       ➤ SED-2D: A two-dimensional flow model for sediment transport related to unsteady  
19       flows. The model is based on the solution of the depth-averaged convection-diffusion  
20       equations of sediment with bed sources terms. SED-2D is capable of modeling  
21       cohesive and non-cohesive sediment transport.

22 Assumptions critical to these numerical modeling efforts include:

- 23       ➤ Calibration and application of the UCB-FEM hydrodynamic model was performed  
24       based on available data for normal tide and freshwater discharge conditions for  
25       existing conditions.
- 26       ➤ Hydrodynamic conditions are analyzed to ascertain potential changes arising from

- 1 construction of the James Island project.
- 2       ➤ Sedimentation modeling was performed to estimate the change in bay sedimentation  
3 and scouring patterns and relative rates due to construction of the James Island  
4 project.
- 5       ➤ All results are subject to limitations of existing data, modeling capabilities and  
6 existing information regarding environmental resources and historical records.  
7 Hence, results depicted herein may be subject to modification in any additional future  
8 study stages as additional information is made available.
- 9 UCB-FEM hydrodynamic output includes time-varying flow velocity and water surface  
10 elevation fields. The UCB-FEM model also evaluates and predicts areas where erosion and  
11 accretion are likely to occur.

12

## 2. PROJECT SITE PHYSICAL CONDITIONS

### 2.1 GENERAL

James Island is located in the Chesapeake Bay at the mouth of the Little Choptank River. It is located in Dorchester County at approximately 38° 31' N latitude and 76° 20' W longitude (Maryland State Plane Coordinates N 310,000 E 1,503,000) as shown in Figure 2-1. Figure 2-2 is an aerial photograph of James Island taken in August 2002. Figure 2-3 shows the proposed five alignments for James Island.

Site conditions germane to project design include bathymetry and topography, water levels, currents, wind and wave conditions, and site soil characteristics. A discussion of each of these factors is presented in the following paragraphs.

### 2.2 BATHYMETRY AND TOPOGRAPHY

The Chesapeake Bay is the largest estuary in the United States, extending over 200 miles from its seaward end at Cape Charles and Cape Henry in Virginia to the mouth of the Susquehanna River at Havre de Grace, Maryland. The Chesapeake Bay (including tributaries) has a surface area of approximately 4,500 square miles. Water depths in the Bay, including all of its tidal tributaries, average approximately 21 feet with a few deep troughs reaching a maximum depth of 174 feet (Schubel, 1987).

Chesapeake Bay bathymetric data was obtained from the National Ocean Service (NOS) Digital Elevation Models (NOS, 2000) and Charts 12230, 12263, 12264, 12266, 12268, 12270, 12272, 12273, 12274, and 12278. Vertical and horizontal data in this report are referenced to mean lower low water (MLLW) based on the 1960 to 1978 tidal epoch, and the Maryland State Plane, North American Datum 1983, respectively.

The bathymetry surrounding James Island is shown in Figure 2-3. Water depths within the project vicinity vary from -2 ft to -12 ft MLLW; maximum water depths in which the new containment dikes would be constructed is -12 ft MLLW. Water depths approximately one mile west of James Island are as great as -93 ft MLLW.

### 1    2.3    FRESHWATER INFLOW

2    The drainage area of the Chesapeake Bay is approximately 64,000 square miles and includes  
3    portions of Maryland, Virginia, West Virginia, Pennsylvania, New York and the District of  
4    Columbia. Freshwater enters the Chesapeake Bay via approximately one-hundred and fifty  
5    major rivers and streams at approximately 80,000 cubic feet per second (Schubel, 1987). The  
6    primary rivers within the Chesapeake Bay drainage basin are the Susquehanna, Chester, Severn,  
7    Choptank, Patuxent, Nanticoke, Potomac, Rappahannock, York, and James Rivers. The  
8    Susquehanna River provides approximately 48.2% of the total freshwater inflow into the bay.  
9    Additional rivers on the western shore of the Bay, which contribute significant flows are the  
10   Potomac, James, Rappahannock, York, and Patuxent, contributing 13.6%, 12.5%, 3.1% 3.0%  
11   and 1.2%, respectively. Two significant sources of freshwater flow on the eastern shore of  
12   Maryland and Virginia are the Choptank (1.2%) and Nanticoke (1.1%) Rivers (Schubel, 1987).

### 13   2.4    TIDES

14   Water levels in the Chesapeake Bay are dominated by a semidiurnal lunar tide. Tides enter the  
15   Bay via the Chesapeake Bay Entrance and the Chesapeake and Delaware (C&D) Canal. The  
16   Bay is sufficiently long to contain one complete wavelength of the semidiurnal tide (NOS, 1988).  
17   The combination of tides and freshwater inflow creates a spring tide approximately 30-40%  
18   larger than mean tide and a neap tide approximately 30-40% smaller than the mean tide  
19   (Schubel, 1987).

20   The mean range of tides throughout the entire Chesapeake Bay is generally 1 to 3 feet (NOS,  
21   1988). Tides are amplified in some tributaries as the tide progresses from the mouth of the  
22   tributary to the limit of the tide.

23   Average and spring tidal ranges, as published by NOS for the Bay north of the Potomac River  
24   (NOS Chart Nos. 12263, 12266, 12268, 12270, 12272), are listed in Table 2-1.

25

<b>Table 2-1: Chesapeake Bay Tidal Ranges</b>		
<b>Location</b>	<b>Mean Tidal Range (ft)</b>	<b>Spring Tidal Range (ft)</b>
<b>Main Chesapeake Bay</b>		
Cove Point	1.3	2.0
Bloody Point Bar Light	1.3	1.6
Pooles Island	1.2	1.8
Sevenfoot Knoll Light	0.9	1.3
<b>Western Chesapeake Bay</b>		
Fairhaven, Herring Bay	0.9	1.3
Thomas Point Shoal Light	0.9	1.4
Annapolis	0.9	1.4
Sandy Point	0.8	1.2
Baltimore (Ft. McHenry)	1.2	1.7
Pond Point	1.4	2.1
<b>Choptank River</b>		
Cambridge	1.7	2.4
Chesapeake Beach	1.0	1.5
<b>Eastern Bay</b>		
St. Michaels, Miles River	1.2	1.8
Kent Island Narrows	1.2	1.8
<b>Chester River</b>		
Love Point	1.2	1.7
Queenstown	1.3	2.0
Cliffs Wharf	1.5	2.2
Chestertown	1.8	2.7
<b>Sassafras River</b>		
Betterton	1.6	2.4
<b>C &amp; D Canal</b>		
Chesapeake City	2.8	2.9
<b>Susquehanna River</b>		
Havre de Grace	1.8	2.6

- 1
- 2 Average tides range from 0.8 ft in various locations on the western shore to 2.8 ft in the C & D
- 3 Canal. Spring tides (tides occurring at or near the time of new or full moon which rise highest
- 4 and fall lowest from the mean sea level) range from 1.3 ft at Fairhaven on Herring Bay to 2.9 ft
- 5 in the C & D Canal. Near James Island, mean tide range is approximately 1.3 ft (NOS, 1996).

1 Additionally, tides in the Chesapeake Bay are influenced by Coriolis forces (momentum forces  
2 due to the rotation of the Earth). Browne and Fisher (NOS, 1988) found a significant west to  
3 east tide range differential due to Coriolis forces throughout the bay with peak differences of 1.0  
4 foot in the region between Smith Point (1 foot range, western shore) and Tangier Sound (2 foot  
5 range, eastern shore).

## 6 2.5 CURRENTS

7 Currents in the Chesapeake Bay are tidally driven and range in values up to a maximum velocity  
8 of over 3 ft/sec near the Bay entrance (NOS, 1988). Peak current velocities in the Bay north of  
9 Kent Island approach 1.5 ft/sec and average 1.2 ft/sec. Phasing of current velocity is influenced  
10 by bottom friction. Browne and Fisher (NOS, 1988) determined that during a given tidal cycle  
11 the peak current velocity occurs first in the center of the bay over the deepest channels, whereas  
12 peak velocity occurs later closer to shore in shallower water.

13 In the project vicinity, approximately 2.5 miles west of James Island, peak tidal current velocities  
14 are approximately 1.0 ft/sec for flood currents and 0.8 ft/sec for ebb currents (NOS, 1996).

## 15 2.6 WIND AND WAVE CONDITIONS

16 The frictional force of air on water as wind blows generates waves. Higher winds, deeper water,  
17 and longer distances over which the wind travels result in larger waves. Wind and wave  
18 conditions representative of the James Island vicinity are discussed in the following paragraphs.

### 19 2.6.1 Wind Conditions

20 Average annual wind speeds at James Island are represented by the wind rose shown in Figure 2-  
21 4. The wind rose represents percent occurrence of wind speeds and directions at Baltimore-  
22 Washington International (BWI) Airport as reported by the National Oceanic and Atmospheric  
23 Administration (NOAA), National Climatic Data Center (NOS, 1982 and NCDC, 1994). Table  
24 2-2 shows the data used to generate the wind rose.

25 On average, nearly 90% of the yearly wind occurrences are less than 16 mph and only 1-2% of  
26 wind occurrences are greater than 25 mph.

1

**Table 2-2: Wind Speed (% Occurrence) By Direction for BWI Airport, 1951-1982**

Direction	0-3 MPH	4-13 MPH	13-16 MPH	16-19 MPH	19-25 MPH	25-32 MPH	>32 MPH
N		3.6	0.6	0.3	0.1	0	0
NNE		2.1	0.4	0.2	0.1	0	0
NE		3.3	0.5	0.2	0.1	0	0
ENE		3.3	0.6	0.3	0.1	0	0
E		4.3	0.5	0.2	0	0	0
ESE		2.3	0.2	0.1	0	0	0
SE		3.1	0.4	0.2	0.1	0	0
SSE		3.2	0.5	0.2	0.1	0	0
S		5.2	0.6	0.3	0.1	0	0
SSW		3.5	0.7	0.3	0.2	0	0
SW		4.7	0.8	0.4	0.2	0	0
WSW		4.7	0.6	0.3	0.1	0	0
W		9.4	1.4	1.0	0.7	0.2	0
WNW		5.9	1.8	1.5	1.3	0.4	0
NW		4.4	1.6	1.2	0.7	0.2	0
NNW		3.0	0.8	0.5	0.2	0	0
ALL	10.2						

2

3 Annual extreme wind speed data from the NOAA, NCDC for BWI Airport for the period 1951  
 4 through 1982 (NOS, 1982 and NCDC, 1994) are presented in Table 2-3 as fastest mile winds.  
 5 Fastest mile winds are defined as the highest recorded wind speeds that last long enough to travel  
 6 one mile during a 24-hour recording period. For example, a fastest mile wind speed of 60 miles  
 7 per hour would have a duration of 60 seconds, a fastest mile wind speed of 50 miles per hour  
 8 would have a duration of 72 seconds, etc.

9

**Table 2-3: Annual Extreme Wind Speed (mph) Per Direction for BWI Airport, 1951-1982**

Year	North	Northeast	East	Southeast	South	Southwest	West	Northwest
1951	24	41	27	34	39	29	42	46
1952	66	25	47	66	41	66	46	43
1953	20	28	22	27	34	39	47	43
1954	31	27	22	60	28	39	57	44
1955	21	43	29	28	43	53	40	43
1956	29	34	25	24	28	34	56	40
1957	29	53	35	33	33	30	46	46
1958	30	52	25	33	37	43	40	43
1959	28	26	20	27	23	38	46	43
1960	26	38	28	27	25	35	40	53
1961	45	28	28	29	24	70	41	54
1962	56	41	28	17	25	36	42	61
1963	38	32	18	34	25	28	44	60
1964	34	31	23	24	47	23	48	61
1965	36	26	28	34	36	54	44	44
1966	32	25	29	24	47	43	50	48
1967	30	29	25	39	27	46	53	43
1968	45	30	36	26	19	45	48	50
1969	28	21	20	34	26	45	45	53
1970	28	28	18	21	39	34	48	60
1971	31	45	26	18	21	41	39	58
1972	28	25	35	26	20	41	41	41
1973	40	26	26	38	26	35	49	33
1974	32	23	46	29	33	33	45	41
1975	40	26	21	24	25	38	54	45
1976	31	18	20	28	32	28	45	54
1977	32	31	19	28	26	25	49	48
1978	39	28	36	28	19	52	33	45
1979	32	25	27	36	32	32	45	47
1980	33	27	18	32	20	32	45	50
1981	24	24	19	26	23	28	41	42
1982	31	20	23	23	29	34	40	48

1 Note: Data adjusted to 10 meter height.

## 2 2.6.2 Wave Conditions

3 James Island is exposed to wind-generated waves approaching from all directions. In accordance  
4 with procedures recommended by the U.S. Army Corps of Engineers (USACE), Shore

1 Protection Manual (SPM) (USACE, 1984), a radially averaged fetch distance was computed for  
2 the eight directions, namely N, NE, E, SE, S, SW, W and NW. The radially averaged fetch  
3 distances for these directions are shown in Table 2-4 and Figure 2-5.

4  
**Table 2-4: Radial Fetch Distance and Mean Water  
Depth at James Island**

Direction	Mean Distance (Miles)	Mean Water Depth (ft, MLLW)
North	26.9	34.2
Northeast	5.3	9.6
East	5.3	12.2
Southeast	2.4	3.7
South	29.5	43.1
Southwest	6.9	39.8
West	8.3	35.4
Northwest	8.0	28.5

5  
6 Wave conditions were hindcast along each fetch direction for the design winds presented in  
7 Table 2-3 (adjusted appropriately for duration) and the mean water depths along the fetch  
8 directions as shown in Table 2-4 using methods published in the SPM (1984). Wave hindcast  
9 results are presented in Figure 2-6 (Significant Wave Height,  $H_s$ ) and Figure 2-7 (Peak Wave  
10 Period,  $T_p$ ). These figures present a summary of  $H_s$  and  $T_p$  showing the directions from which  
11 the highest waves and longest periods approach the site.

## 12 2.7 SITE SOIL CHARACTERISTICS

13 An evaluation of the soil characteristics at the project site was performed by Engineering  
14 Consultation Construction Remediation, Inc. (E2CR, 2002). The evaluation included performing  
15 soil borings, preparing soil boring profiles, identifying soil strata thickness, location and  
16 characteristics, and conducting a preliminary slope stability analysis. Results of the preliminary  
17 study indicate that the underlying soil consists of silty sand suitable for supporting the dike.,  
18 Areas with soft silty clays at the mud line, however, would need to be undercut and backfilled  
19 with sand.

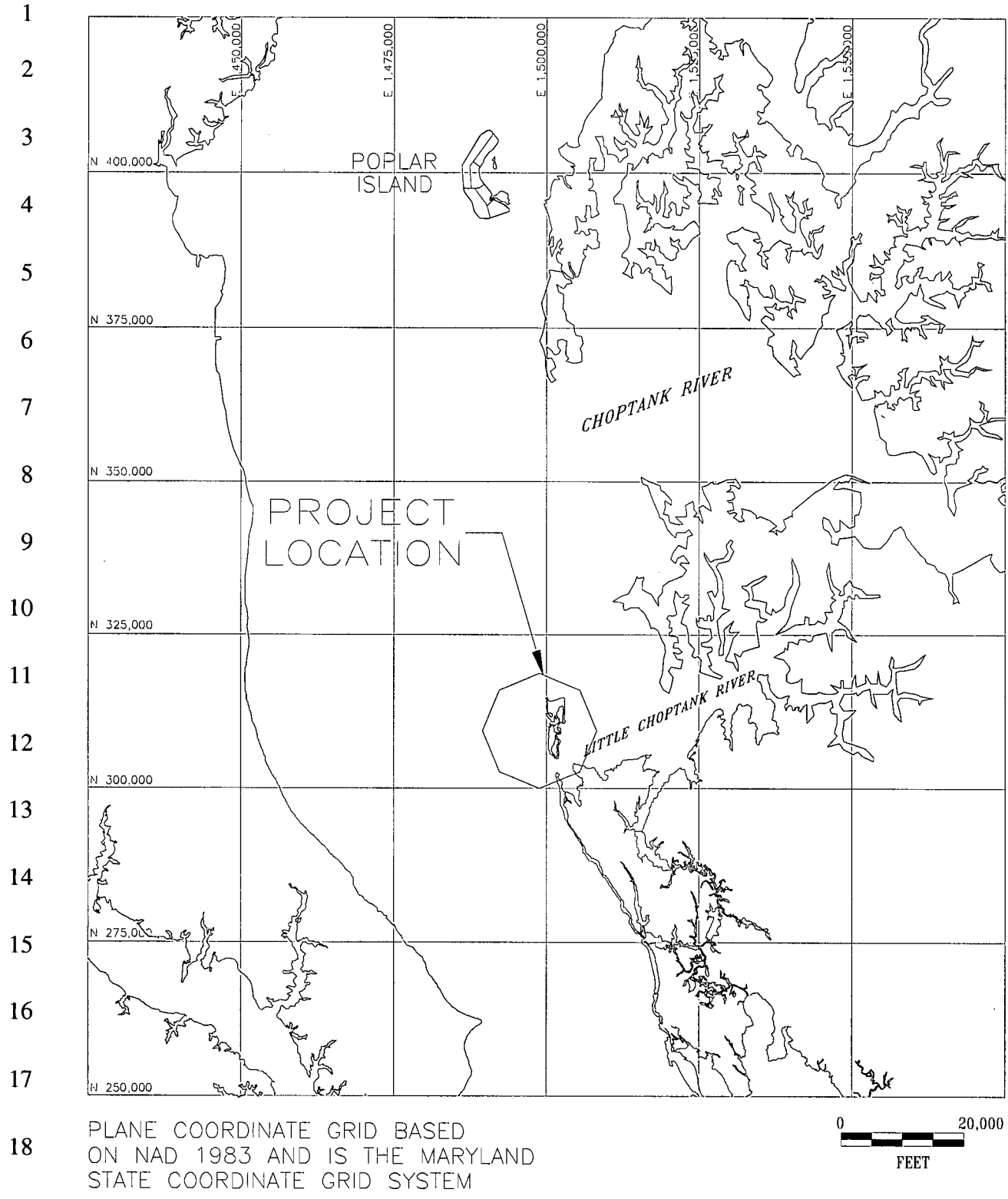


Figure 2-1: James Island Location Map

1

2

3

4

5

6

7

8

9

10

11

12

13

14

15

16

17

18



Figure 2-2: James Island August 2002 Aerial Photograph Looking Southeast

1  
2  
3  
4  
5  
6  
7  
8  
9  
10  
11  
12  
13  
14  
15  
16  
17  
18  
19  
20  
21  
22  
23  
24  
25  
26  
27  
28  
29  
30  
31  
32  
33  
34  
35

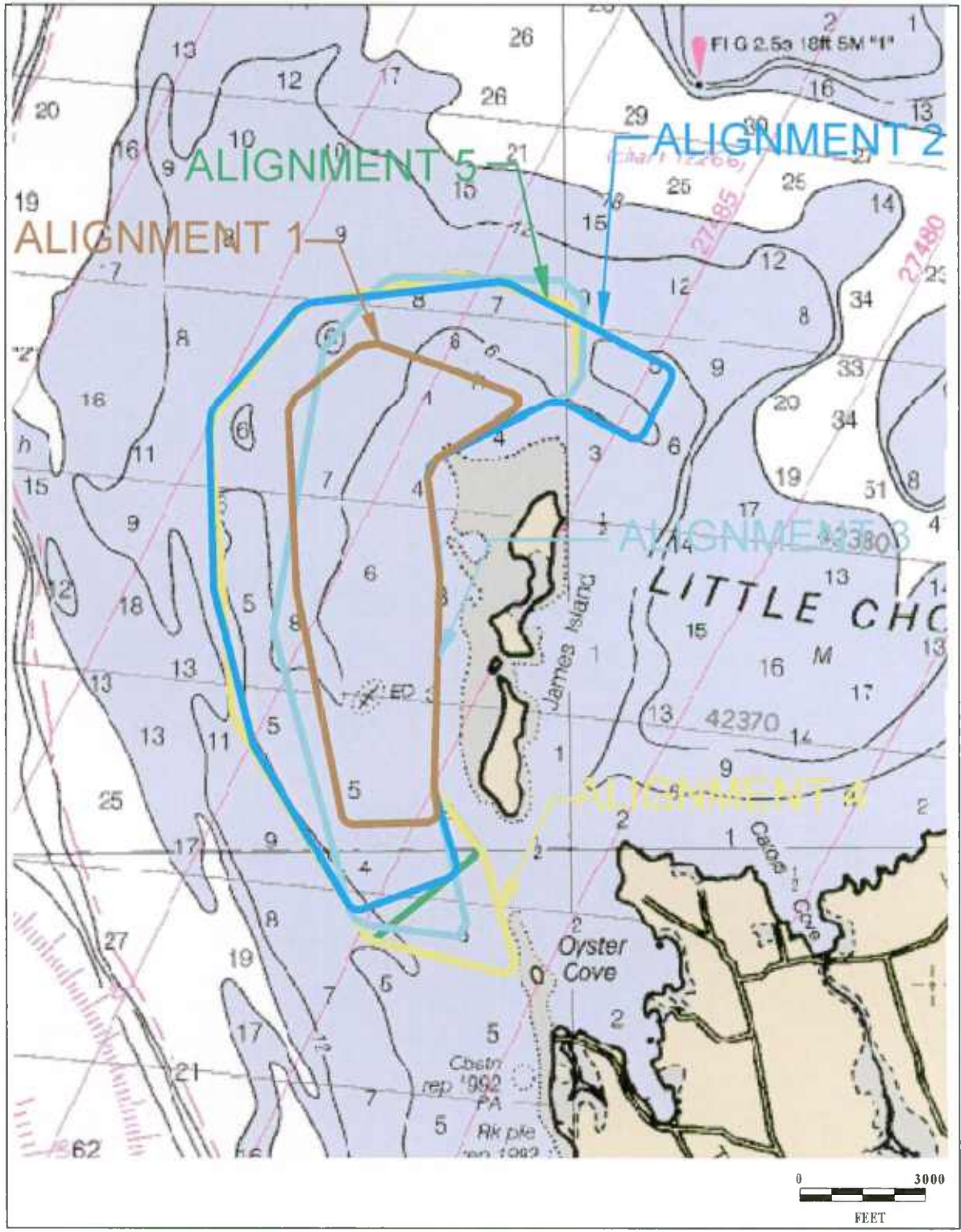


Figure 2-3: James Island Five Alignments and Surrounding Bathymetry

1  
2  
3  
4  
5  
6  
7  
8  
9  
10  
11  
12  
13  
14  
15  
16  
17  
18  
19  
20  
21  
22  
23  
24  
25  
26

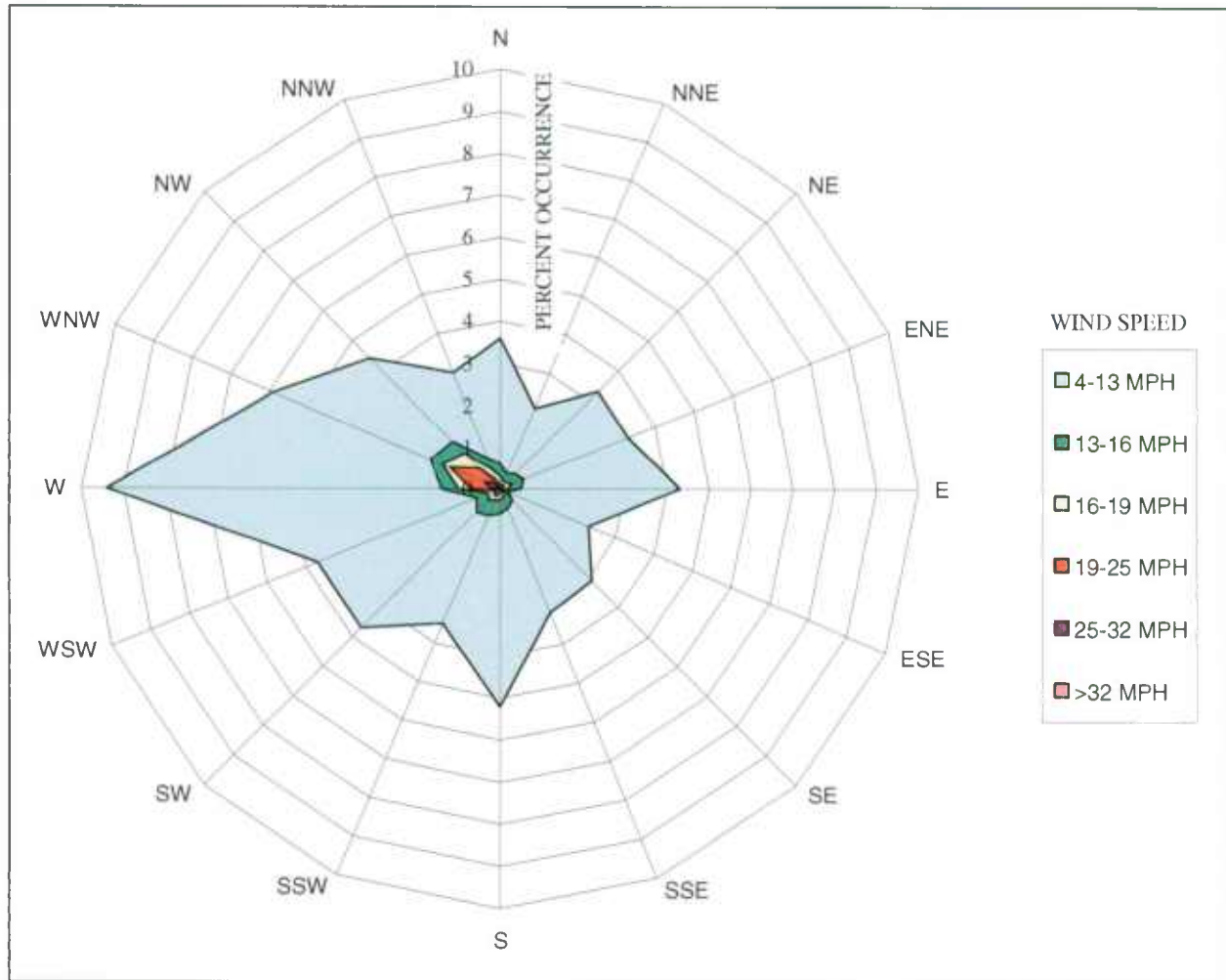


Figure 2-4: Baltimore-Washington International Airport (BWI) Wind Rose

1  
2  
3  
4  
5  
6  
7  
8  
9  
10  
11  
12  
13  
14  
15  
16  
17  
18  
19  
20

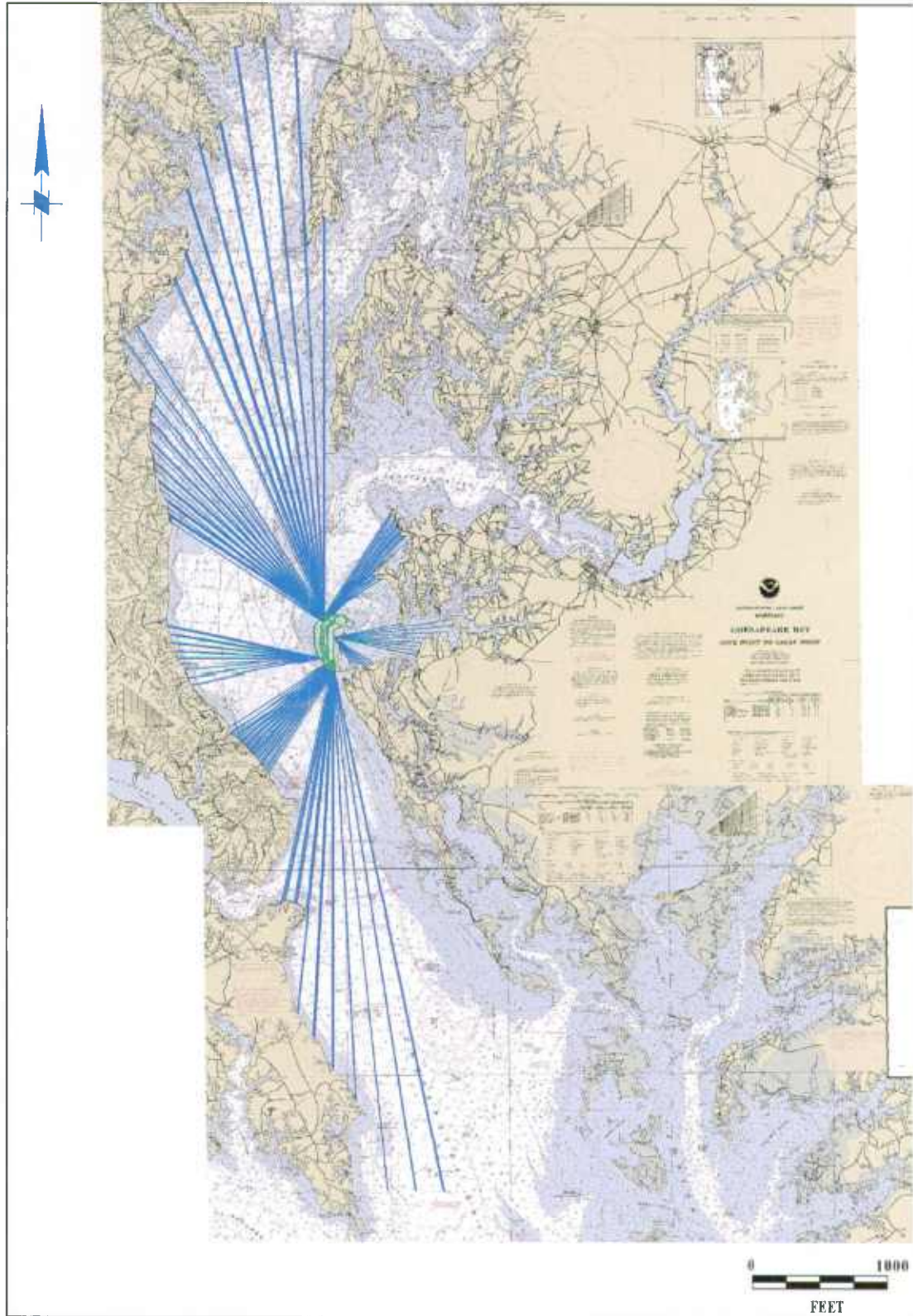
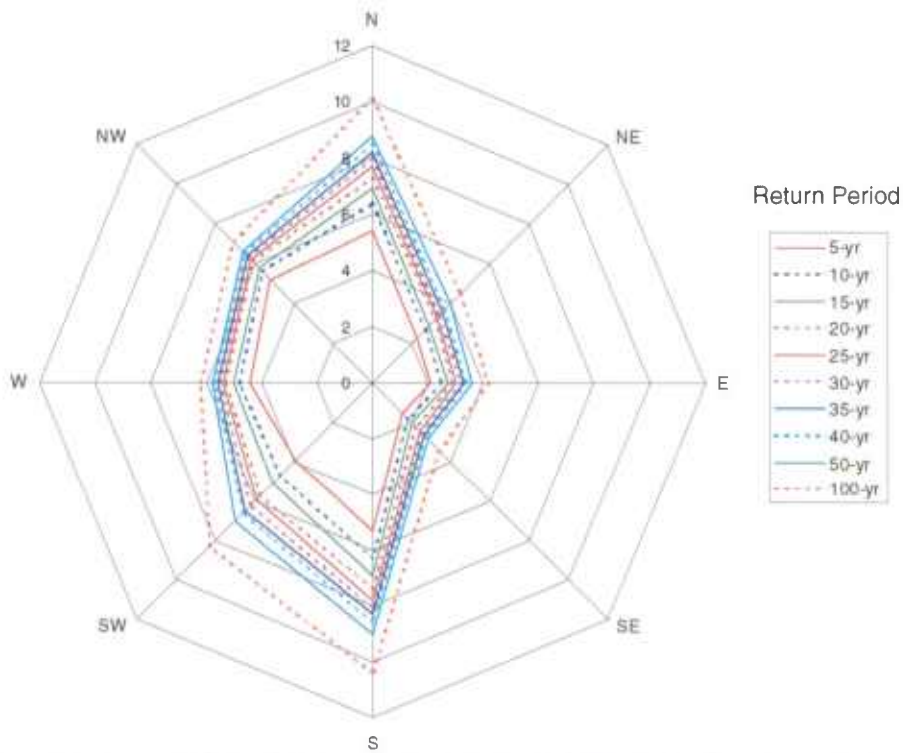
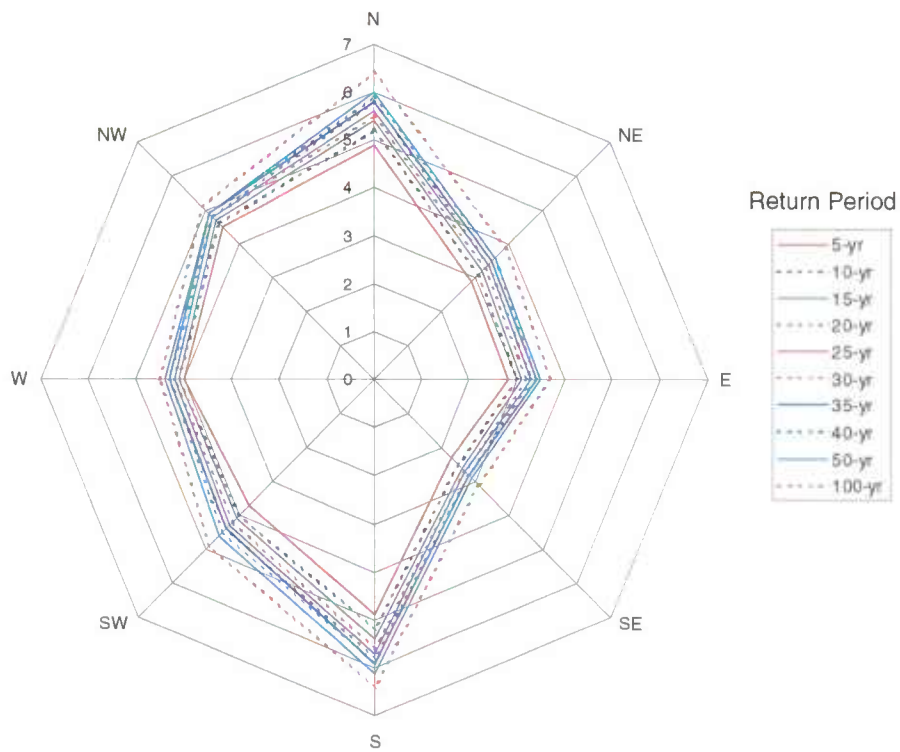


Figure 2-5: James Island Radially-Averaged Fetch Distances



1 **Figure 2-6: Offshore Significant Wave Heights (ft) for James Island**



2 **Figure 2-7: Peak Spectral Wave Periods (sec) for James Island**

### 3. SIMULATION MODELS

#### 3.1 GENERAL

The numerical modeling system used in this study is the US Army Corps of Engineers (USACE), Waterways Experiment Station (WES) finite element hydrodynamics (RMA-2) and sedimentation (SED-2D) models – collectively known as TABS-2 (Thomas and McAnally, 1985). TABS-2 is a collection of generalized computer programs and pre- and post-processor utility codes integrated into a numerical modeling system for studying two-dimensional depth-averaged hydrodynamics, constituent transport, and sedimentation problems in rivers, reservoirs, bays, and estuaries. The finite element method provides a means of obtaining an approximate solution to a system of governing equations by dividing the area of interest into smaller sub-areas called elements.

Time-varying partial differential equations are transformed into finite element form and then solved in a global matrix system for the modeled area of interest. The solution is smooth across each element and continuous over the computational area. This modeling system is capable of simulating wetting and drying of marsh and intertidal areas of the estuarine system.

A schematic representation of the system is shown in Figure 3-1. It can be used either as a stand-alone solution technique or as a step in the hybrid modeling approach. The model calculates water surface elevations, current patterns, constituent transport, sediment erosion and deposition, the resulting bed surface elevations, and the feedback to hydraulics. Existing conditions can be analyzed to determine the impacts of project construction at James Island on flow circulation and sedimentation. All models are depth-averaged and are solved by the finite element method using Galerkin weighted residuals.

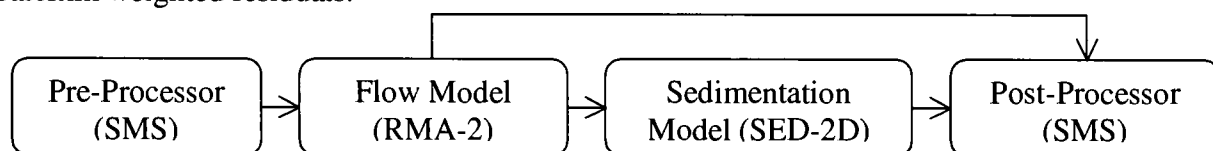


Figure 3-1: TABS-2 Schematic

### 3.2 HYDRODYNAMIC MODEL

RMA-2 is a two-dimensional, depth-averaged, finite element, hydrodynamic numerical model. It computes water surface elevations and horizontal velocity components for subcritical, free-surface flow in two dimensional flow fields. RMA-2 computes a finite element solution of the Reynolds form of the Navier-Stokes equations for turbulent flows. Friction is calculated with the Manning's or Chezy equation, and eddy viscosity coefficients are used to define turbulence characteristics. The equations also account for Coriolis forces and surface wind stresses. Both steady and unsteady state (dynamic) problems can be analyzed. The general governing equations are:

$$h \frac{\partial u}{\partial t} + hu \frac{\partial u}{\partial x} + hv \frac{\partial u}{\partial y} - \frac{h}{\rho} \left( E_{xx} \frac{\partial^2 u}{\partial x^2} + E_{xy} \frac{\partial^2 u}{\partial y^2} \right) + gh \left( \frac{\partial a}{\partial x} + \frac{\partial h}{\partial x} \right) + \frac{gun^2}{(1.486h^{1/6})^2} + (u^2 + v^2)^{1/2} - \zeta V_a^2 \cos \psi - 2h\omega v \sin \phi = 0$$

$$h \frac{\partial v}{\partial t} + hu \frac{\partial v}{\partial x} + hv \frac{\partial v}{\partial y} - \frac{h}{\rho} \left( E_{yx} \frac{\partial^2 v}{\partial x^2} + E_{yy} \frac{\partial^2 v}{\partial y^2} \right) + gh \left( \frac{\partial a}{\partial y} + \frac{\partial h}{\partial y} \right) + \frac{gvn^2}{(1.486h^{1/6})^2} + (u^2 + v^2)^{1/2} - \zeta V_a^2 \sin \psi - 2h\omega u \sin \phi = 0$$

$$\frac{\partial h}{\partial t} + h \left( \frac{\partial u}{\partial x} + \frac{\partial v}{\partial y} \right) + u \frac{\partial h}{\partial x} + v \frac{\partial h}{\partial y} = 0$$

where:

$h$  = Depth

$u, v$  = Velocities in Cartesian directions

$x, y, t$  = Cartesian coordinates and time

$\rho$  = Density of fluid

$E$  = Eddy viscosity coefficient

for  $xx$  = normal direction on  $x$ -axis surface

- 1 for  $yy$  = normal direction on y-axis surface  
2 for  $xy$  and  $yx$  = shear direction on each surface  
3  $g$  = Acceleration due to gravity  
4  $a$  = Elevation of Bottom  
5  $n$  = Manning's roughness n-value  
6 1.486 = Conversion from SI (metric) to non-SI units  
7  $\zeta$  = Empirical wind shear coefficient  
8  $V_a$  = Wind speed  
9  $\psi$  = Wind direction  
10  $\omega$  = Rate of Earth's angular rotation  
11  $\phi$  = Local latitude  
12

13 RMA-2 operates under the hydrostatic assumption, meaning accelerations in the vertical  
14 direction are negligible. RMA-2 is two dimensional in the horizontal plane and is not intended  
15 for use in near field problems where vortices, vibrations, or vertical accelerations are of primary  
16 interest. Vertically stratified flow effects are beyond the capabilities of RMA-2.

### 17 3.3 SEDIMENTATION MODEL

18 The sedimentation model, SED-2D, can be applied to sediments where flow velocities can be  
19 considered two-dimensional in the horizontal plane (i.e., the speed and direction can be  
20 satisfactorily represented as a depth-averaged velocity). It is useful for both deposition and  
21 erosion studies. The program treats two categories of sediment: 1) noncohesive, which is  
22 referred to as sand herein; and 2) cohesive, which is referred to as clay.

23 Both clay and sand may be analyzed, but the model considers a single, effective grain size during  
24 each simulation. Therefore, a separate model run is required for each effective grain size. Fall  
25 velocity must be prescribed along with the water surface elevations, x-velocity, y-velocity,  
26 diffusion coefficients bed density, critical shear stresses for erosion, erosion rate constants, and  
27 critical shear stress for deposition.

1 The derivation of the basic finite element formulation is presented in Ariathurai (1974) and  
2 Ariathurai, MacArthur, and Krone (1977) and is summarized below.

3 There are four major computations.

- 4 1. Convection-Diffusion Governing Equation
- 5 2. Bed Shear Stress Calculation
- 6 3. The Bed Source/Sink Term
- 7 4. The Bed Strata Discretization

### 8 3.3.1 Convection-Diffusion Governing Equation

9 The mesh employed for the hydrodynamic model is used for the sedimentation model. The  
10 convection-dispersion equation in two horizontal dimensions for a single sediment constitute  
11 solved by the model is:

$$12 \quad \frac{\partial C}{\partial t} + u \frac{\partial C}{\partial x} + v \frac{\partial C}{\partial y} = D_x \frac{\partial^2 C}{\partial x^2} + D_y \frac{\partial^2 C}{\partial y^2} + \alpha_1^C + \alpha_2$$

13 where:

14  $u, v$  = depth-averaged sediment velocity components

15  $C$  = suspended sediment concentration

16  $D_x$  = effective diffusion coefficient in X-direction

17  $D_y$  = effective diffusion coefficient in Y-direction

18  $\alpha_1$  = concentration-dependent source/sink term

19  $\alpha_2$  = coefficient of source/sink term

20

21 The source/sink terms in the above equation are computed in routines that treat the interaction of  
22 the flow and the bed. Separate sections of the code handle computations for clay bed and sand  
23 bed problems as described below.

### 1 3.3.2 Bed Shear Stress

2 Bed shear stresses are calculated from the flow speed according to one of four optional  
 3 equations: the smooth-wall log velocity profile or Manning equation for flows alone; and a  
 4 smooth bed or rippled bed equation for combined currents and wind waves. Shear stresses are  
 5 calculated using the shear velocity concept where

$$6 \quad \tau_b = \rho u_*^2$$

7 where:

8  $\tau_b$  = bed shear stress

9  $u_*$  = shear velocity

10

11 and the shear velocity is calculated by one of four methods:

12 a. Smooth-wall log velocity profiles

$$13 \quad \frac{\bar{u}}{u_*} = 5.75 \log \left( 3.32 \frac{u_* h}{\nu} \right)$$

14 which is applicable to the lower 15 percent of the boundary layer when

$$15 \quad \frac{u_* h}{\nu} > 30$$

16 where  $\bar{u}$  is the mean flow velocity (resultant of u and v components)

17 b. The Manning shear stress equation

$$18 \quad u_* = \frac{(\bar{u} n) \sqrt{g}}{CME(h)^{1/6}}$$

19 where CME is a coefficient of 1 for SI (metric units) and 1.486 for non-SI units of

1 measurement.

2 c. A Jonsson-type equation for surface shear stress (plane beds) caused by waves and  
3 currents

$$4 \quad u_* = \sqrt{\frac{1}{2} \left( \frac{f_w u_{om} + f_c \bar{u}}{u_{om} + u} \right) \left( \bar{u} + \frac{u_{om}}{2} \right)}$$

5 where

6  $f_w$  = shear stress coefficient for waves

7  $u_{om}$  = maximum orbital velocity of waves

8  $f_c$  = shear stress coefficient for currents

9  
10 d. A Bijker-type equation for total shear stress caused by waves and current

$$11 \quad u_* = \sqrt{\frac{1}{2} f_c \bar{u}^{-2} + \frac{1}{4} f_w u_{om}^2}$$

### 12 3.3.3 Source/Sink Terms

13 The Ackers-White (1973) procedure is used to calculate a sediment transport potential for sand  
14 from which actual sand transport is calculated based on sediment availability. Model clay  
15 erosion is based on formulas by Partheniades (1962) and Ariathurai while the deposition of clay  
16 utilizes Krone's equations (Ariathurai, MacArthur, and Krone, 1977).

#### 17 3.3.3.1 Sand Transport

18 For sand transport, the transport potential of the flow and availability of material in the bed  
19 control the supply of sediment from the bed. The bed source term is

$$20 \quad S = \frac{C_{eq} - C}{t_c}$$

1 where:

2  $S$  = source term

3  $C_{eq}$  = equilibrium concentration (transport potential)

4  $C$  = sediment concentration in the water column

5  $t_c$  = characteristic time for effecting the transition

6  
 7 There are many transport relations for calculating  $C_{eq}$  for sand size material. The Ackers-White  
 8 (1973) formula was adopted for this model because it performed satisfactorily in tests by WES  
 9 and others (White, Milli, and Crabbe 1975; Swart 1976), is relatively complete, and is reasonably  
 10 simple. The transport potential is related to sediment and flow parameters by the expressions in  
 11 the following paragraphs. The Ackers-White formula computes the total load, including  
 12 suspended load and bed load, and was developed originally for fine sand. The formulation was  
 13 later updated to include coarser sands and these revised coefficients are included in the current  
 14 model formulation. However, the appropriateness of the use of SED-2D with the Ackers-White  
 15 formula diminishes with coarsening of the sediment.

16 The characteristic time,  $t_c$ , is somewhat subjective. It should be the amount of time required for  
 17 the concentration in the flow field to change from  $C$  to  $C_{eq}$ . In the case of deposition,  $t_c$  is related  
 18 to fall velocity. The following expression was adopted.

19 
$$t_c = \text{the larger of } \left\{ \begin{array}{l} C_d \frac{h}{V_s} \\ \text{or} \\ DT \end{array} \right.$$

20 where:

21  $t_c$  = Characteristic time

22  $C_d$  = Coefficient for deposition

23  $V_s$  = Fall velocity of a sediment particle

24  $DT$  = Computational time interval

1

2 In the case of scour, there are no simple parameters to employ. The following expression is  
3 used.

4

$$t_c = \text{the larger of } \begin{cases} C_e \frac{h}{u} \\ or \\ DT \end{cases}$$

5

where:

6

$C_e$  = Coefficient for entrainment

7

$V$  = Flow speed

8

### 9 3.3.3.2 Clay Transport

10 Cohesive sediments (usually clays and some silts) are considered to be depositional if the bed  
11 shear stress exerted by the flow is less than a critical value  $\tau_d$ . When that value occurs, the  
12 deposition rate is given by Krone's (1962) equation

13

$$S = \begin{cases} -\frac{2V_s}{h} C \left(1 - \frac{\tau}{\tau_d}\right) & \text{for } C < C_c \\ -\frac{2V_s}{hC_c^{4/3}} C^{5/3} \left(1 - \frac{\tau}{\tau_d}\right) & \text{for } C > C_c \end{cases}$$

14

where:

15

$S$  = source term

16

$V_s$  = fall velocity of a sediment particle

17

$h$  = flow depth

18

$C$  = sediment concentration in water column

19

$\tau$  = bed shear stress

20

$\tau_d$  = critical shear stress for deposition

1  $C_c$  = critical concentration = 300 mg/ℓ

2

3 If the bed shear stress is greater than the critical value for particle erosion  $\tau_e$ , material is  
4 removed from the bed. The source term is then computed by Ariathurai's (Ariathurai,  
5 MacArthur, and Krone 1977) adaptation of Partheniades' (1962) findings:

6 
$$S = \frac{P}{h} \left( \frac{\tau}{\tau_e} - 1 \right) \text{ for } \tau > \tau_e$$

7 where  $P$  is the erosion rate constant, unless the shear stress is also greater than the critical value  
8 for mass erosion. When this value is exceeded, mass failure of a sediment layer occurs and

9 
$$S = \frac{T_L \rho_L}{h \Delta t} \text{ for } \tau > \tau_s$$

10 where:

11  $T_L$  = thickness of the failed layer

12  $\rho_L$  = density of the failed layer

13  $\Delta t$  = time interval over which failure occurs

14  $\tau_s$  = bulk shear strength of the layer

15

### 16 3.3.4 Bed Strata Discretization

17 The sink-source term in convection-diffusion equation becomes a source-sink term for the bed  
18 model, which keeps track of the elevation, composition, and character of the bed.

#### 19 3.3.4.1 Sand Beds

20 Sand beds are considered to consist of a sediment reservoir of finite thickness, below which is a  
21 nonerodible surface. Sediment is added to or removed from the bed at rate determined by the  
22 value of the sink/source term at the previous and present time-steps. The mass rate of exchange  
23 with the bed is converted to a volumetric rate of change by the bed porosity parameter.

1 **3.3.4.2 Clay Beds**

2 Clay beds are treated as a sequence of layers. Each layer has its own characteristics as follows:

- 3           ▪ Thickness.
- 4           ▪ Density.
- 5           ▪ Age.
- 6           ▪ Bulk shear strength.
- 7           ▪ Type.

8 In addition, the layer type specifies a second list of characteristics.

- 9           ▪ Critical shear stress for erosion.
- 10          ▪ Erosion rate constant.
- 11          ▪ Initial and 1-year densities.
- 12          ▪ Initial and 1-year bulk shear strengths.
- 13          ▪ Consolidation coefficient.
- 14          ▪ Clay or sand.

15 New clay deposits form layers up to a specified initial thickness and then increase in density and  
16 strength with increasing overburden pressure and age. Variation with overburden occurs by  
17 increasing the layer type value by one for each additional layer deposited above it.

18

## 1    4.    **FINITE ELEMENT MESH**

### 2    4.1    **GENERAL**

3    The numerical modeling system implemented herein requires that a database of water depths and  
4    bottom material properties represent the estuarial system. Water depths are represented by nodes  
5    located in the horizontal plane, which are interconnected to create elements. Two, three, or four  
6    nodes can be connected to form elements. The resulting nodal/element network is commonly  
7    called a finite element mesh and provides a computerized representation of the estuarial  
8    geometry and bathymetry.

### 9    4.2    **ELEMENTS**

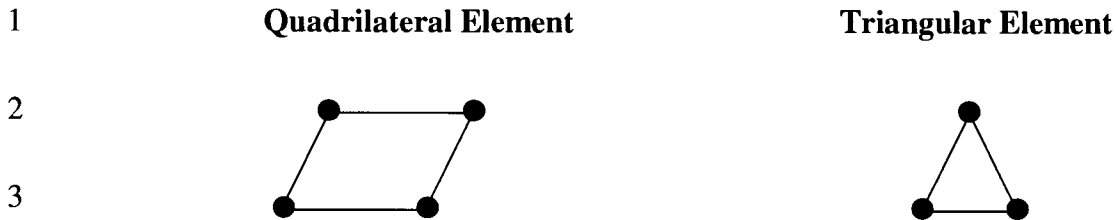
10   RMA-2 is capable of supporting different types of elements within the same computational finite  
11   element mesh. The types of elements fit into three basic categories:

- 12           ▪ Two Dimensional Elements
- 13           ▪ One Dimensional Elements
- 14           ▪ Special Elements

15   These element types are discussed briefly in the following sections.

#### 16   4.2.1    **Two Dimensional Elements**

17   Two-dimensional elements are the customary type used with RMA-2 and may be either  
18   triangular or quadrilateral in shape, as shown in Figure 4-1. A two dimensional element  
19   possesses a length and a width, determined by the positions of the corner nodes which define the  
20   element. The depth at any location within a two dimensional element is obtained by  
21   interpolating among the depths of the corner nodes which define the element.



5                      **Figure 4-1: Finite Element Shapes**

#### 6                      **4.2.2 One Dimensional Elements**

7                      A one-dimensional element is a simplified element which is composed of two corner nodes and  
8                      one midside node. The Finite Element Governing Equations for one-dimensional elements are  
9                      based on a trapezoidal cross section with side slopes, and an off channel storage area. The depth  
10                     at any location along a one-dimensional element is obtained by interpolating between the depths  
11                     of the two corner nodes defining the element.

#### 12                     **4.2.3 Special Elements**

13                     Special elements are one-dimensional elements that serve special purposes including transition  
14                     from one- to two-dimensional elements, junctions between multiple one-dimensional elements,  
15                     and flow control structures.

### 16                     **4.3 MODEL EXTENTS**

17                     The areal extent and the level of detail necessary to represent the project area are the parameters  
18                     that define a finite element mesh. The TABS-2 system, described in Section 3.0, is numerically  
19                     robust and capable of simulating tidal elevations, flows, and sediment transport over a mesh with  
20                     widely varying boundaries and levels of detail. Accordingly, the incorporation of significant  
21                     bathymetric features of the estuary generally dictates the level of detail for the mesh. However,  
22                     there are several factors used to guide decisions regarding the extents of the mesh. First, it is  
23                     desirable to extend the mesh to areas sufficiently distant from the project site such that the  
24                     boundary conditions do not directly influence the hydrodynamics at the site. Secondly, the  
25                     terminus of the mesh should be in a location where conditions can be reasonably measured and  
26                     described to the model. Additionally, it is preferable to locate boundaries in locations where  
                         flow characteristics have been measured or are known and can be accurately specified.

1 Geometric information for the UCB-FEM model was obtained from NOAA DEMs, nautical  
2 charts, and recently performed bathymetric surveys. NOAA DEM's are electronic maps of  
3 bathymetric elevations imposed on a 30-meter grid and are based on many years of hydrographic  
4 survey data acquired for production of navigational charts. For the areas not covered by the  
5 DEM, navigation charts were used to complete the mesh. The resulting mesh geometry was  
6 checked and alterations were made as deemed necessary to improve physical representation of  
7 the estuary and to improve model stability in areas of large depth gradients.

8 The UCB-FEM model finite element mesh used herein is shown in Figure 4-2. Quadrilateral and  
9 triangular 2-dimensional elements were used to represent the estuarial system. The southern  
10 boundary of the mesh is located in the Chesapeake Bay near the Hooper Island Light from which  
11 it extends north to its terminus at the Conowingo Dam on the Susquehanna River and  
12 Chesapeake City on the C & D Canal resulting in total mesh length of roughly 90 nautical miles.  
13 A dense mesh was created around James Island to provide a more accurate simulation of  
14 conditions at the project site.

15 Water depths were adjusted to represent both existing and with-project conditions. Figure 4-3  
16 depicts the finite element mesh developed for existing conditions in the vicinity of James Island.  
17 Figures 4-4 through 4-8 depict the finite element meshes developed for Alternatives 1 through 5,  
18 respectively.

19  
20

1  
2  
3  
4  
5  
6  
7  
8  
9  
10  
11  
12  
13  
14  
15  
16  
17  
18  
19  
20

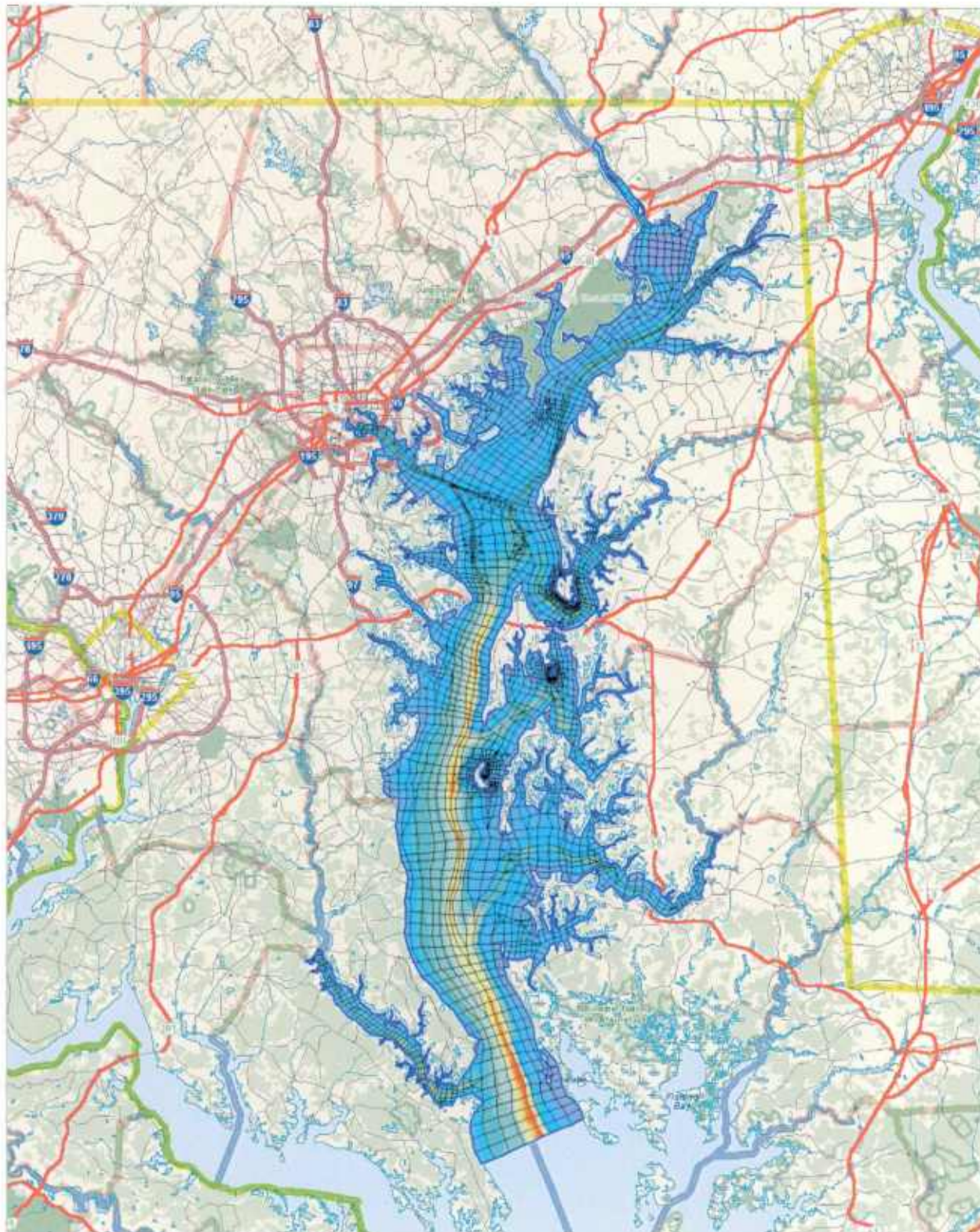


Figure 4-2: Upper Chesapeake Bay Finite Element Model (UCB-FEM)

1  
2  
3  
4  
5  
6  
7  
8  
9  
10  
11  
12  
13  
14  
15  
16  
17  
18  
19  
20

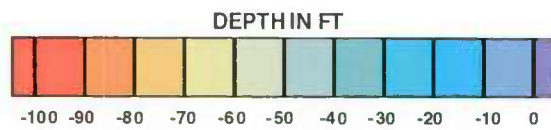
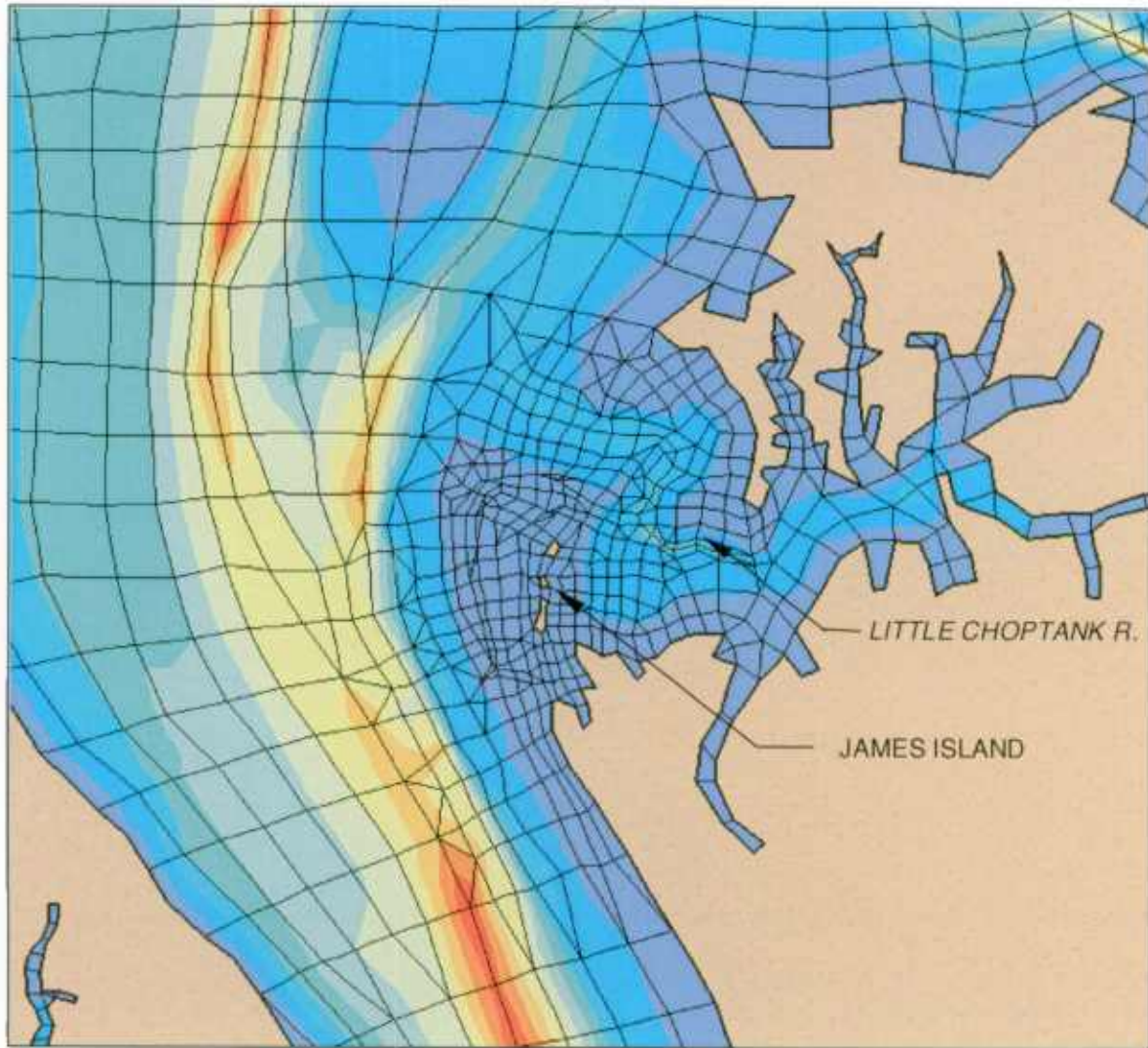


Figure 4-3: UCB-FEM – James Island Existing Conditions

1  
2  
3  
4  
5  
6  
7  
8  
9  
10  
11  
12  
13  
14  
15  
16  
17  
18  
19  
20  
21

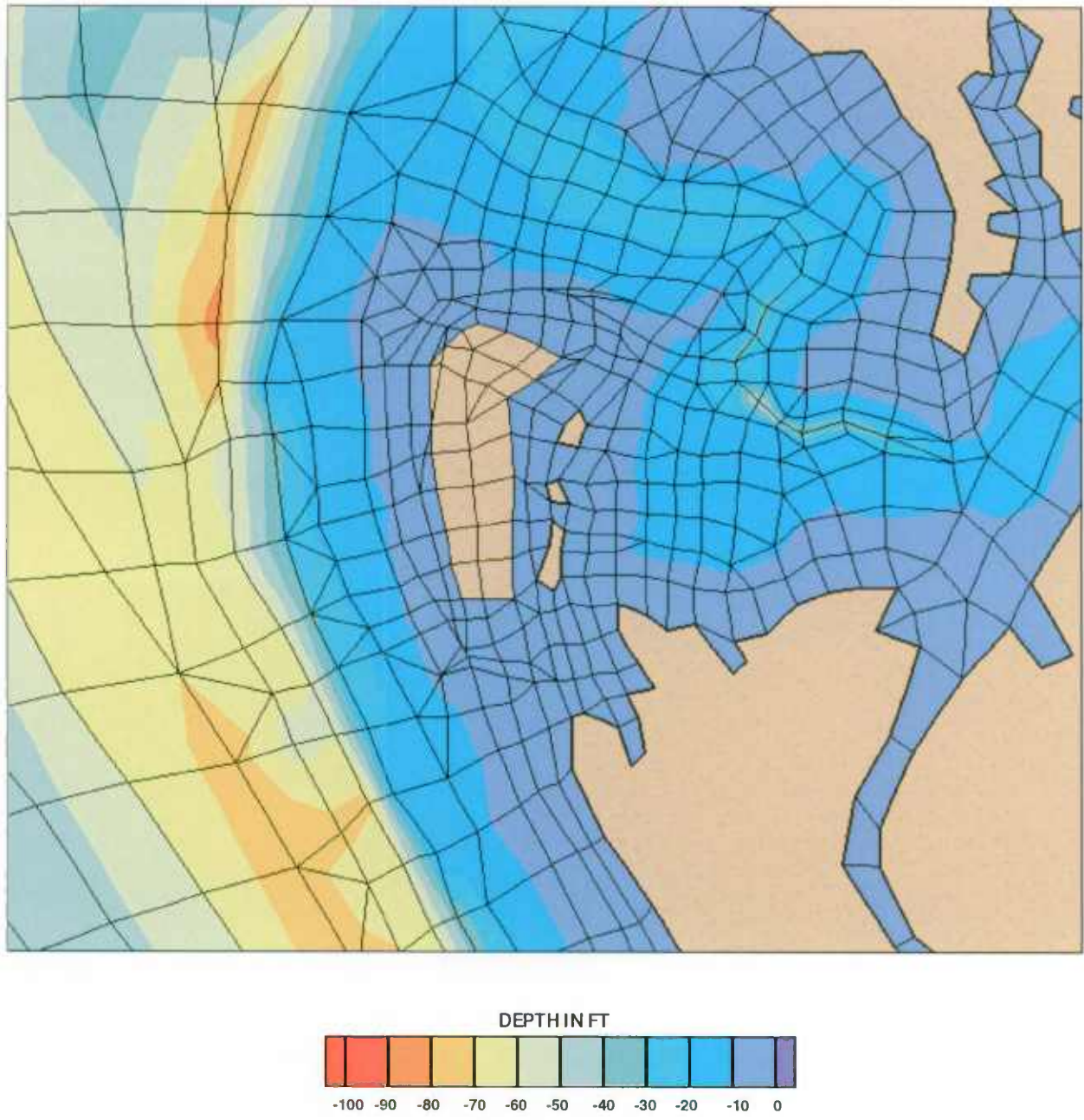


Figure 4-4: UCB-FEM – James Island Alternative 1

1  
2  
3  
4  
5  
6  
7  
8  
9  
10  
11  
12  
13  
14  
15  
16  
17  
18  
19  
20  
21  
22

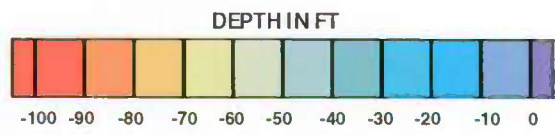
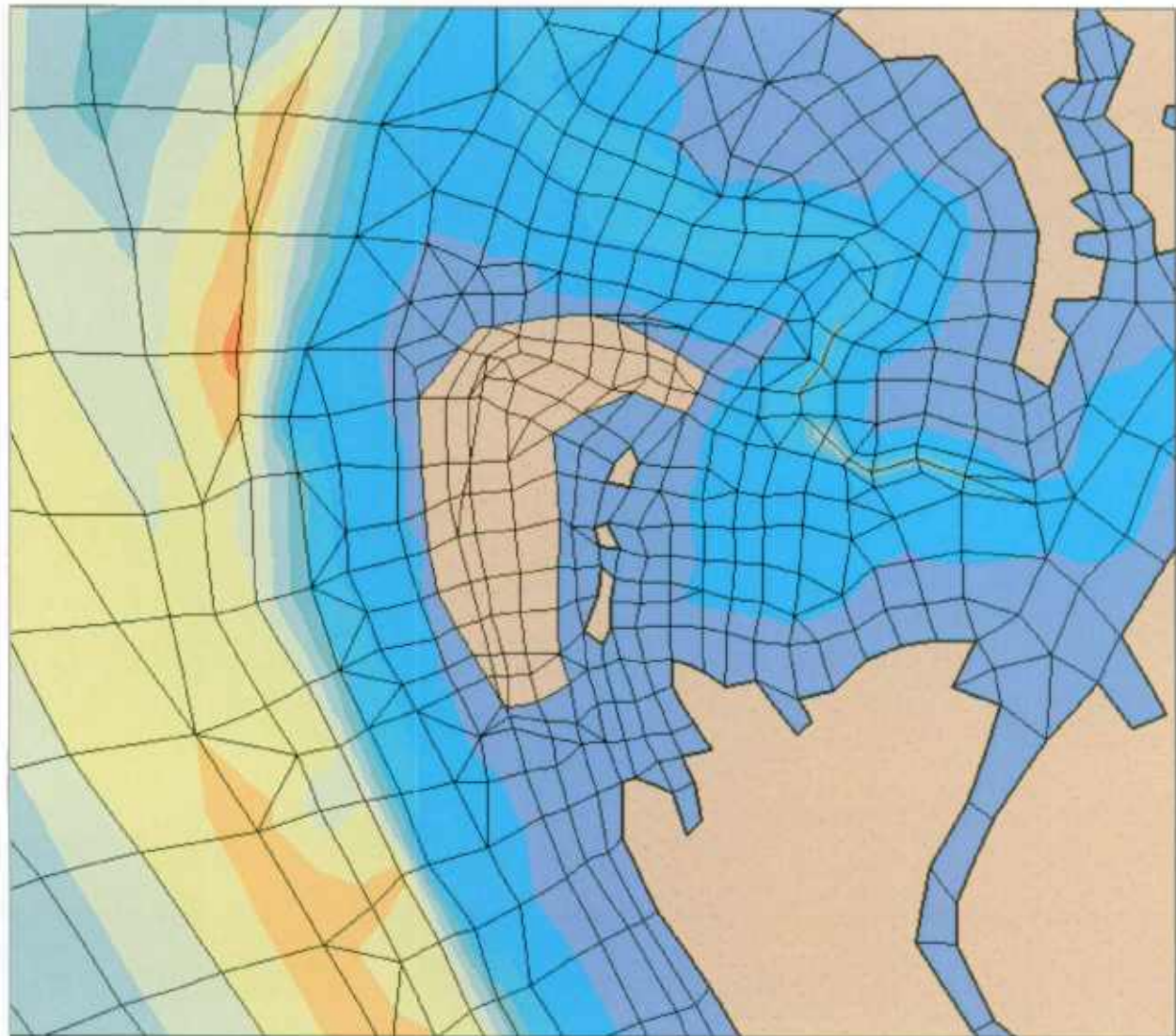


Figure 4-5: UCB-FEM – James Island Alternative 2

1  
2  
3  
4  
5  
6  
7  
8  
9  
10  
11  
12  
13  
14  
15  
16  
17  
18  
19  
20

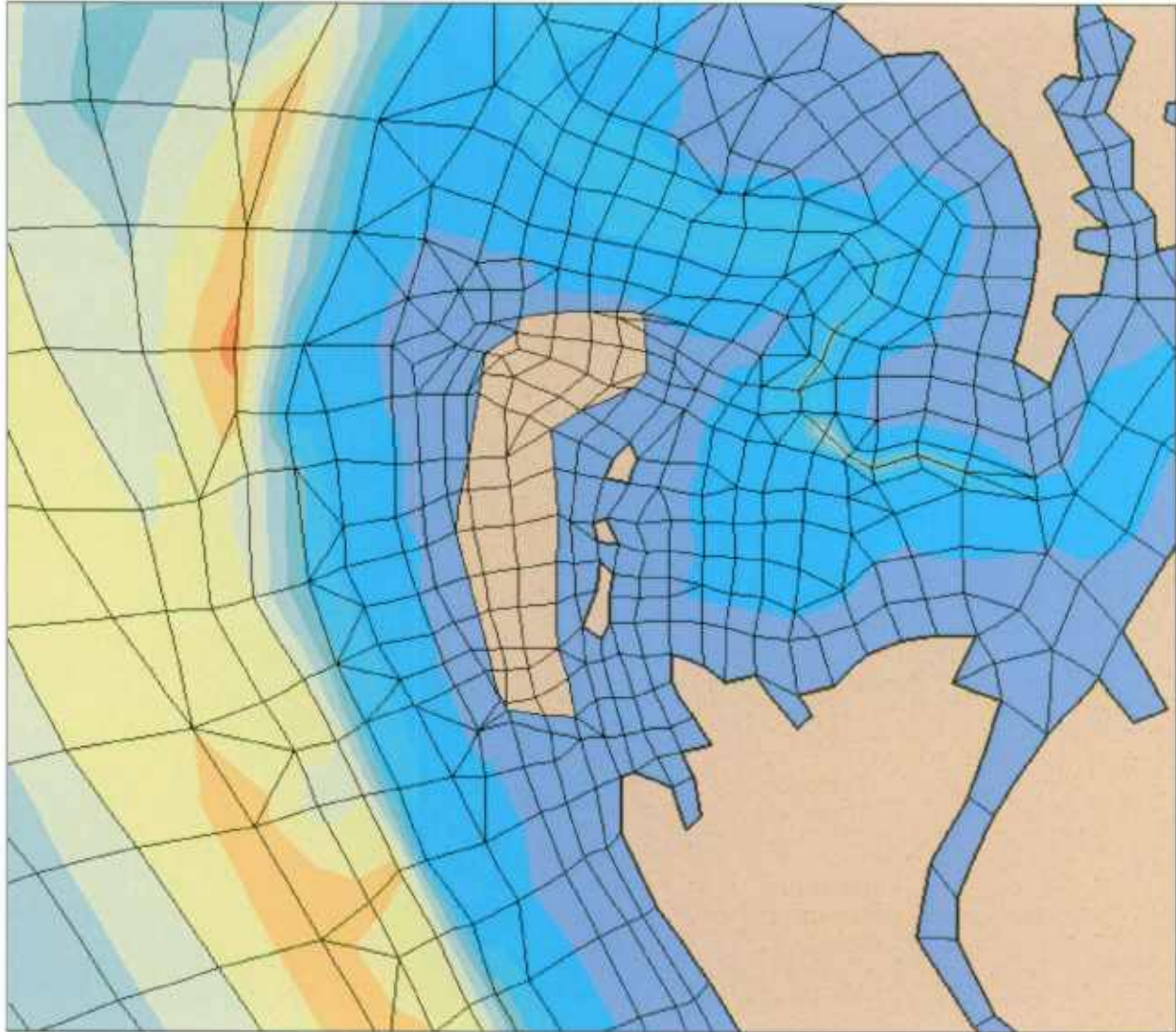


Figure 4-6: UCB-FEM – James Island Alternative 3

1  
2  
3  
4  
5  
6  
7  
8  
9  
10  
11  
12  
13  
14  
15  
16  
17  
18  
19  
20

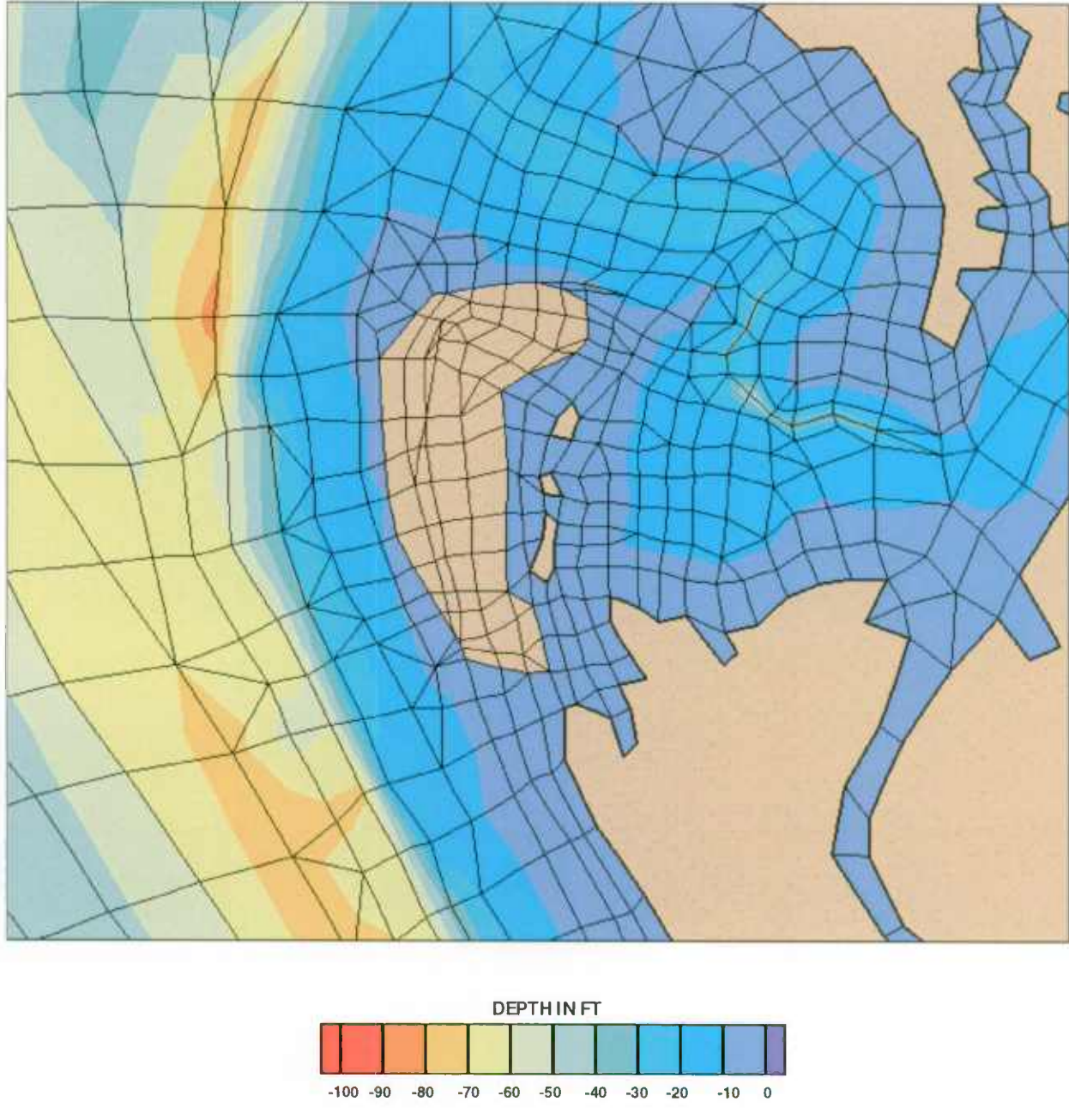


Figure 4-7: UCB-FEM – James Island Alternative 4

1  
2  
3  
4  
5  
6  
7  
8  
9  
10  
11  
12  
13  
14  
15  
16  
17  
18  
19

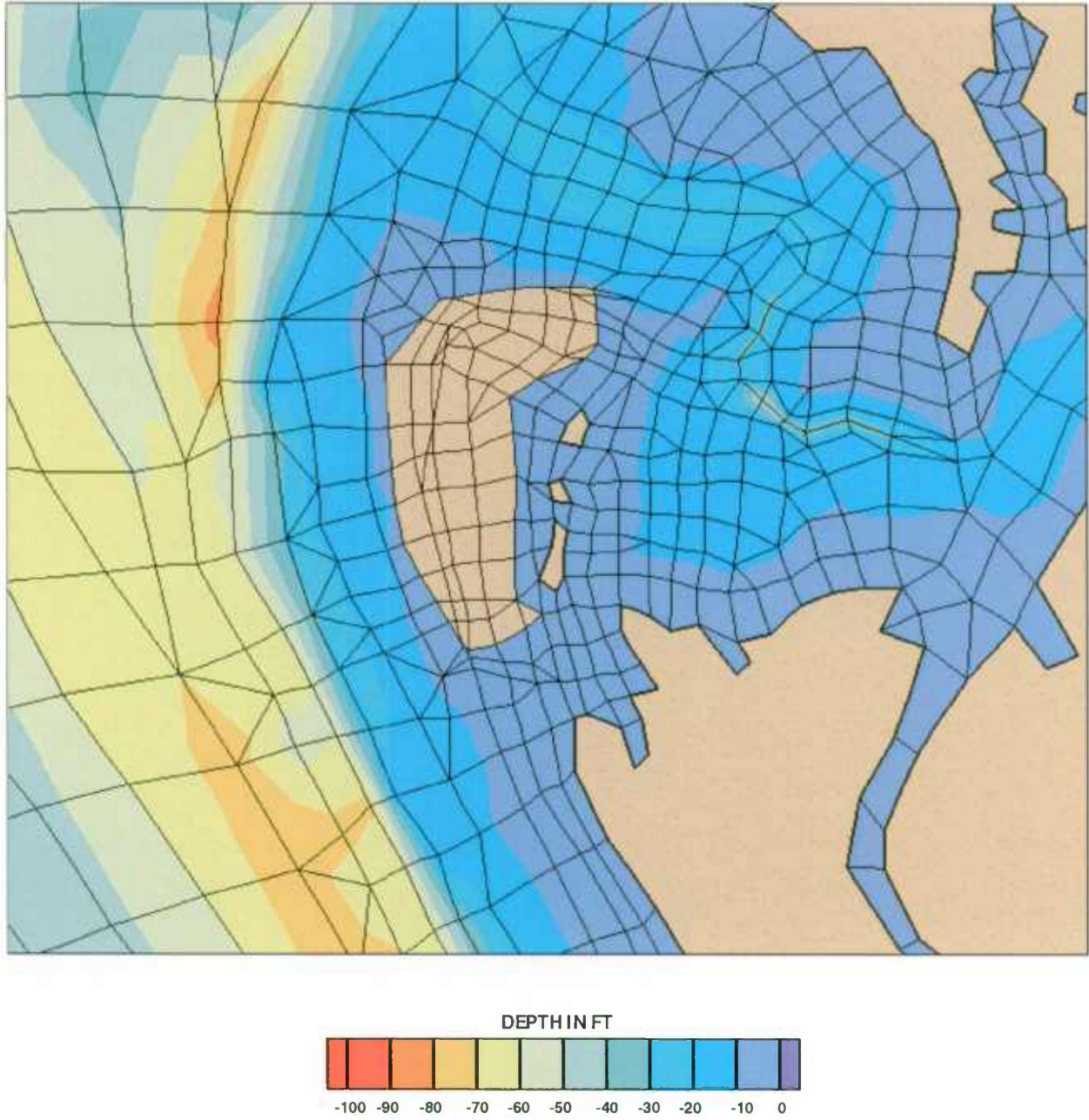


Figure 4-8: UCB-FEM – James Island Alternative 5

## 5. MODEL CALIBRATION

### 5.1 GENERAL

A measure of a finite element model's accuracy is the comparison of modeled tide elevations and currents with measured or known values. A properly calibrated model can be expected to produce current velocity and tidal elevation results with 80% to 100% accuracy. Model calibrations are adjusted by the refinement of the model bathymetry, the accurate representation of bottom structure (i.e. vegetation, mud, sand) and the stipulation of model parameters that are artifacts of the numerical formulation and are functions of element size and empirical constants. Upon satisfactory completion of calibration, the model can be used to evaluate the impacts of physical changes to the system.

Model calibration is best achieved by means of a set of simultaneous measurements both along the model boundaries and throughout the estuarial system. Boundary conditions important to the present study include tidal elevation, flow velocity, freshwater discharge, suspended sediment concentration, and bottom change over time. For a given set of boundary conditions, the model should be calibrated to reproduce tidal elevations, tidal velocities, or sedimentation rates and patterns within the estuary. The sediment transport model is driven by results obtained from the hydrodynamic model; therefore, the latter is calibrated first.

### 5.2 HYDRODYNAMIC MODEL

The UCB-FEM model is controlled by boundary conditions as shown in Figure 5-1. Boundary conditions are located on the southern boundary of the model in the vicinity of the Hooper Island Light and at the Conowingo Dam on the Susquehanna River and Chesapeake City on the C & D Canal on the northern boundaries. Additional boundary conditions are stipulated at tributaries throughout the model domain including the Patuxent, Choptank, Chester, and Susquehanna Rivers as well as the other smaller tributaries listed in Table 5-1. The type of boundary condition is based on the data available at each boundary. The Hooper Island Light boundary condition is comprised of tidal elevations while the C & D Canal, Patuxent River, Chester River and Choptank River boundary conditions consist of current velocities and directions and the

1 Conowingo Dam boundary condition is described by volume flux (flow). Boundary conditions  
 2 located at smaller tributaries are described as constant sources of flow into the bay based on  
 3 historic average measured flow. Calibration was performed for a two-week period of predicted  
 4 data from February 1-14, 2001, which is representative of an average tidal cycle and low  
 5 freshwater inflow.

6

<b>Location</b>	<b>Flowrate (cfs)</b>
Patapsco River	431
Gunpowder River	2888
Bush River	1149
Elk River	1874

7  
 8 Tide elevation and current velocity boundary conditions for the UCB-FEM model are based on  
 9 NOS tidal predictions. NOS tidal predictions are based on historic harmonic constituents and  
 10 represent idealized conditions which do not account for low frequency events including wind and  
 11 storms. Figure 5-2 shows the water surface elevations and current velocities used as boundary  
 12 conditions in the UCB-FEM model calibration.

13 Aside from the boundary conditions, the model is also influenced by bottom friction and eddy  
 14 viscosity. Physically, bottom friction varies by bottom material and vegetation type and density  
 15 and is best described by a map of Manning's roughness coefficient over the entire model domain.  
 16 As is often the case, detailed information regarding bottom material is not available for the entire  
 17 model domain. Standard practice is to then specify Manning's roughness relative to water depth  
 18 resulting in a loose correlation with vegetation density. Eddy viscosity, or lateral mixing, also  
 19 varies over the entire domain but is also dependent upon numerical element size and predicted  
 20 current velocity in the model. Eddy viscosity is, therefore, specified based on a function  
 21 calculated at each element for each time step. The final set of eddy viscosity and Manning's  
 22 roughness values which provided the best fit between measured and simulated water elevations  
 23 and flow velocities at measurement stations within the estuarial system were implemented.

24 NOS predicted tides and currents were used to check the model calibration at the locations  
 25 shown in Figures 5-3 and 5-4. Figures 5-5 and 5-6 show results for selected calibration

- 1 locations, for water surface elevations and current velocities, respectively.
- 2 Comparisons of the NOS predicted and UCB-FEM modeled data show excellent correlation to
- 3 both tidal phasing and amplitudes. Tables 5-2 and 5-3 show the statistical comparison of the
- 4 model results to NOS predicted data at each station subdivided by geographical regions.
- 5 Statistics are calculated for overall calibration correlation and peak condition amplitudes.
- 6 Percent error is calculated by dividing the RMS (root mean square) error by the calculated mean
- 7 range.
- 8

<b>Table 5-2: Water Surface Elevation Calibration Statistics</b>			
	<b>Time Series Statistics</b>		
	<b>Correlation</b>	<b>Peak RMS Error (ft)</b>	<b>Peak RMS Error %</b>
<b>Little Choptank River</b>			
Taylor's Island	1.00	0.07	5.5%
Hudson Creek	0.98	0.07	4.9%
<b>Choptank River</b>			
Broad Neck Creek	0.98	0.06	4.3%
Choptank River Light	0.95	0.05	3.4%
Cambridge	0.96	0.08	5.1%
Choptank	0.92	0.06	3.3%
<b>Eastern Bay</b>			
Claiborne	0.96	0.10	9.0%
Miles River	0.99	0.10	7.8%
<b>Chester River</b>			
Love Point	0.98	0.10	8.7%
Cliff's Point	0.98	0.09	5.8%
<b>Sassafras and Susquehanna River and C and D Canal</b>			
Betterton	0.92	0.26	15.1%
Courthouse Point	0.99	0.17	7.1%
Havre de Grace	0.92	0.27	14.4%
Port Deposit	0.96	0.44	19.6%
<b>Main Chesapeake Bay</b>			
Sharps Island Light	0.92	0.07	5.1%
Poplar Island	0.95	0.06	5.1%
Bloody Point Light	0.94	0.07	6.4%
Matapeake	0.97	0.12	12.3%
Pooles Island	0.94	0.18	14.0%

<b>Western Chesapeake Bay</b>			
Cedar Point	1.00	0.08	6.6%
Cove Point	1.00	0.08	5.7%
Long Beach	0.96	0.08	7.6%
Chesapeake Beach	0.97	0.08	8.1%
West River	0.98	0.14	14.6%
Thomas Light	0.96	0.14	15.3%
Sandy Point	0.96	0.20	25.2%
Seven Foot Knoll Light	0.96	0.15	16.0%
<b>Patapsco, Middle, and Gunpowder Rivers</b>			
Fort Carroll	0.97	0.10	8.8%
Rocky Point	0.95	0.12	9.9%
Bowley's Bar	0.95	0.16	12.5%
Battery Point	0.95	0.14	11.3%

1

2 The model calibration results shown in Table 5-2 show better than 90% correlation for all  
3 locations. Predicted tidal elevation percent error is typically less than 10% with the exception of  
4 some specific areas of the model domain which are under 20%. Under-prediction of the Coriolis  
5 force and over-simplification of the bottom friction in the bay result in higher percent errors for  
6 tides along the western shore of the Bay including the Middle and Gunpowder Rivers. Tides in  
7 the main Chesapeake Bay near James Island represent the project area and are well predicted.  
8 Correlation in the main Bay near James is about 92% at Sharps Island Light, 96% at Long  
9 Beach, and 100% at Cove Point, and the peak tide is under-predicted by 0.07 to 0.08 ft.

10

<b>Table 5-3: Current Velocity Calibration Statistics</b>			
	<b>Time Series Statistics</b>		
	<b>Correlation</b>	<b>RMS Error (ft/s)</b>	<b>RMS Error %</b>
<b>Main Cedar Point</b>			
Cedar Point 1.1 nmi ENE	0.93	0.28	15.7%
Cedar Point 2.9 nmi ENE	0.96	0.34	19.7%
<b>Main Cove Point</b>			
Cove Point 1.1 nmi E	0.97	0.18	7.9%
Cove Point 2.7 nmi E	0.96	0.17	12.3%
Cove Point 3.9 nmi E	0.97	0.22	10.5%

<b>Main James Island</b>			
Kenwood Beach 1.5mi NE	0.94	0.16	19.1%
James Island 3.4 mi W	0.97	0.15	12.3%
James Island 2.5 mi WNW	0.87	0.16	10.5%
<b>Main Sharps Island</b>			
Plum Pt 2.1 mi N	0.96	0.11	9.1%
Sharps Is Lt. 3.4 mi W	0.95	0.15	12.8%
Sharps Is Lt. 2.1 W	0.92	0.11	9.1%
<b>Main Poplar Island</b>			
Holland Pt 2 mi E	0.95	0.15	18.4%
Poplar Is 2.2 mi WSW	0.96	0.20	10.2%
Poplar Island E of S end	0.90	0.54	19.7%
<b>Main Thomas Point Shoal</b>			
Thomas Pt Shoal Lt 1.8 mi SW	0.92	0.10	8.1%
Thomas Pt Shoal Lt 0.5 m SE	0.95	0.19	10.3%
Thomas Pt Shoal Lt 2 mi E	0.97	0.11	6.6%
<b>Main Sandy Point</b>			
Sandy Point 0.8 nmi ESE	0.97	0.43	13.8%
Sandy Point 2.3 nmi E	0.98	0.17	7.8%
<b>Main Baltimore</b>			
Brewerton Channel Eastern Ext, Buoy 7	0.97	0.24	18.7%
Swan Point 1.6 mi NW	0.98	0.42	17.7%
<b>Main Pooles Island</b>			
Gunpowder River Entrance	0.94	0.48	38.1%
Robins Point 0.7 mi ESE	0.89	0.59	17.6%
Pooles Island 1.6 nmi E	0.98	0.23	7.6%
<b>Main Upper</b>			
Howell Point 0.4 mi NNW	0.97	0.49	15.8%
Turkey Point 1.2 nmi W	0.88	0.33	19.4%
<b>Patuxent River</b>			
Hog Point 0.6 mi N	0.92	0.09	6.9%
<b>Choptank River</b>			
Sharps Is Lt. 2.3 mi SE	0.97	0.19	9.0%
Holland Pt 2 mi SSW	0.94	0.09	12.9%
Chlora Pt 0.5 mi SSW	0.93	0.16	11.8%
Cambridge Highway Bridge W of Swingspan	0.97	0.28	22.6%
Poplar Pt S of	1.00	0.08	3.1%

<b>Eastern Bay</b>			
Long Point 1 mi SE	0.88	0.21	13.5%
Tilghman Point 1 mi N of	0.92	0.12	10.9%
Parson's Island 0.7 NNE of	0.94	0.08	15.1%
Kent Island Narrows Highway Bridge	0.95	0.53	16.9%
<b>Chester River</b>			
Love Point 1.6 nmi E	0.95	0.29	21.0%
Hail Point 0.7 nmi E	0.96	0.17	11.0%
<b>C &amp; D Canal</b>			
Arnold Point 0.4 mi W	0.87	0.21	12.95%
C & D Canal, Chesapeake City Bridge	1.00	0.01	0.13%

1

2 The above model calibration results show better than 90% correlation for most currents with the  
 3 remaining better than 85%. Predicted current velocity percent error is typically less than 15%  
 4 with the exception of some specific areas of the model which are closer to 20%. Near James  
 5 Island, the correlation is between 87% to 97%. The factors affecting tidal elevation calibration,  
 6 compounded with depth averaging in the model not reflecting the variation of currents with  
 7 depth in the Bay, cause the discrepancies between predicted and modeled currents.

### 8 **5.3 SEDIMENTATION MODEL**

9 Sedimentation model calibration typically requires historic sedimentation and erosion rates and  
 10 detailed suspended sediment data. When these data are not available, the model can be used  
 11 empirically to determine patterns and relative rates of sedimentation and erosion.

#### 12 **5.3.1 Non-Cohesive Sediment (Sand)**

13 Studies performed by E2CR show fine surface sand in the vicinity of James Island. The non-  
 14 cohesive sediment model was run using 0.1mm (.004 inch) sediment under no-wind conditions.  
 15 Analysis of results shows negligible sand transport due to tidal currents. The non-cohesive  
 16 sediment model was then run for each of 16 wind directions (E, ENE, NE, NNE, N, NNW, NW,  
 17 WNW, W, WSW, SW, SSW, S, SSE, SE, and ESE) for wind speeds of 4-, 13-, and 16-mph  
 18 corresponding to wind speed ranges from the wind rose shown in Figure 2-4.

1 Modeled non-cohesive sediment transport for existing conditions is negligible for 4- and 13-mph  
2 winds for all directions. Sixteen-mph winds, when taken cumulatively with lower wind speeds,  
3 account for nearly 90% of the yearly wind occurrences and cause significant sediment transport  
4 for winds from the NNW, SSE and WNW directions with negligible to moderate sediment  
5 transport for winds from other directions.

6 Model results for 16-mph winds from the NNW, SSE and WNW directions are shown in Figures  
7 5-7, 5-8 and 5-9, respectively. Results are shown using a normalized unitless scale due to the  
8 empirical use of the sedimentation model and the lack of available data to verify model  
9 calibration.

10 Figure 5-7 shows areas of both erosion (green to blue) and accretion (yellow to orange) due to  
11 NNW winds. As shown in the figure, erosion generally occurs in the shallow waters around  
12 James Island, along the eastern shore of Taylors Island to the south, and within the Little  
13 Choptank River. Areas of accretion occur in the adjacent deeper areas west of James Island and  
14 Taylors Island, and within the Little Choptank River. To the north of James Island, erosion is  
15 observed in the shallows around Sharps Island Light, with accretion in the deeper waters east of  
16 the light. Figure 5-8 shows increased erosion and accretion potential due to SSE winds,  
17 indicated by the more extensive blue areas and patches of red. Similar to the NNW winds,  
18 erosion occurs in the shallow waters with accretion in the adjacent deeper waters. Impacts to the  
19 bottom sediment are west of James Island, with no effects in the Little Choptank River. Figure  
20 5-9 shows erosion and accretion patterns due to WNW winds. As shown in this figure, erosion is  
21 not as pronounced, as the fetch distance from this direction is much shorter than the previous two  
22 directions. Erosion occurs mainly in the shallows close to James Island, along the Taylors Island  
23 shore, near Ragged Island in the Little Choptank River, and off Cook Point in Trippe Bay.  
24 Accretion again occurs in the deeper areas adjacent to the eroded shallow waters regions.

### 25 **5.3.2 Cohesive Sediment (Clay and Silt)**

26 Detailed cohesive sediment data, including suspended sediment concentrations, sedimentation  
27 and erosion rates, and spatial maps of specific surface sediment properties are not available for  
28 the project area. Since these data are unavailable, the sedimentation model was used empirically  
29 by assigning multiple thin layers of cohesive material with increasing cohesion and density over

1 the entire domain. The layers erode and accrete in response to tidal current forcing and reach a  
2 dynamic equilibrium, meaning zero net sediment transport over a full lunar tidal cycle.

3 The UCB-FEM sedimentation model was initialized with nine cohesive layers of uniform  
4 thickness throughout the model domain. Layer calibration parameters include critical shear  
5 stresses of deposition ( $\tau_{cd}$ ) and erosion ( $\tau_{ce}$ ), erosion rate constant ( $E$ ), bulk density ( $\rho$ ), and  
6 settling velocity ( $w_s$ ). The critical shear stress for deposition was set constant to  $0.07 \text{ N/m}^2$  and  
7 settling velocity was set to  $0.4 \text{ mm/second}$  and increases as a function of concentration  
8 (Winterwerp, 1999). Other model layer parameters are shown in Table 5-4.

9 Sensitivity analyses show that sediment model boundary conditions are sufficiently far from the  
10 project area and have minimal impact on sediment transport in the project vicinity. Sediment  
11 model boundary conditions were set equal to the background values in the Bay. The resulting set  
12 of initial layer thicknesses shows the complete erosion of the upper layers in areas of high shear  
13 stress and deposition in quiescent areas.

14

**Table 5-4: Sediment Model Initial Bed Layering**

Layer Number	Thickness (inches)	Critical Shear Strength, $\tau_{ce}$ ( $\text{N/m}^2$ )	Erosion Rate Constant, $E$ ( $\text{g/m}^2/\text{sec}$ )	Dry Density, $\rho_{\text{dry}}$ ( $\text{kg/m}^3$ )
1	0.25	0.07	0.200	334
2	0.25	0.16	0.200	450
3	0.25	0.21	0.200	500
4	0.5	0.27	0.100	550
5	0.5	0.33	0.100	600
6	0.5	0.45	0.100	650
7	1.0	0.57	0.050	650
8	1.0	0.69	0.050	650
9	1.0	0.82	0.050	650

15

16 The cohesive sediment model was run for a 6-month simulation period at which point the model  
17 was operating in a dynamic equilibrium. Ensuing with-project simulations show negligible  
18 erosion and accretion due to tidal currents. The cohesive sediment model was then run for each  
19 of 16 wind directions for wind speeds of 4- and 13-mph corresponding to wind speed ranges

1 from the wind rose shown in Figure 2-4.

2 Modeled cohesive sediment transport is negligible for 4-mph. Thirteen-mph winds cause  
3 significant sediment transport for winds from the NNW, SSE, and WNW as shown in Figures 5-  
4 10 through 5-12, respectively, with negligible to moderate sediment transport for winds from  
5 other directions. Results are shown using a normalized unitless scale due to the empirical use of  
6 the sedimentation model and the lack of available data to verify model calibration. In general,  
7 for cohesive sediments the areas of erosion and accretion are larger than for non-cohesive  
8 sediment, as properties of cohesive sediment (shape, plasticity, electric charge) cause the  
9 particles to remain in suspension for relatively long periods of time before they settle out.

10 Figure 5-10 shows erosion due to NNW winds in the shallow areas west of James Island and  
11 Taylors Island, in the shallow regions of the Little Choptank River and Trippe Bay, and at Sharps  
12 Island Light. Accretion occurs southeast of James Island due to its sheltering effect from the  
13 NNW. Accretion also occurs in the adjacent deeper waters, but extends over a greater distance  
14 across the Bay to the Western Shore, south past Cove Point and north to the Choptank River.  
15 Figure 5-11 presents results from SSE winds, and shows a greater area of erosion west of James  
16 Island and south along Taylors Island extending to Barren Island and Hooper Island. Erosion is  
17 also greater around Sharps Island Light. Accretion is not as wide spread as with NNW winds,  
18 but has higher potential in the central deep waters of the Bay. Increased accretion potential  
19 exists in the Little Choptank River with winds from the SSE. Figure 5-12 shows model results  
20 for WNW winds. As shown in this figure, although erosion occurs along the entire shoreline that  
21 is exposed to this direction, the erosion potential is not as great as the previous two conditions.  
22 Accretion occurs in the deeper waters adjacent to the erosional areas within the Bay, the Little  
23 Choptank River, Trippe Bay, and the Choptank River.

24

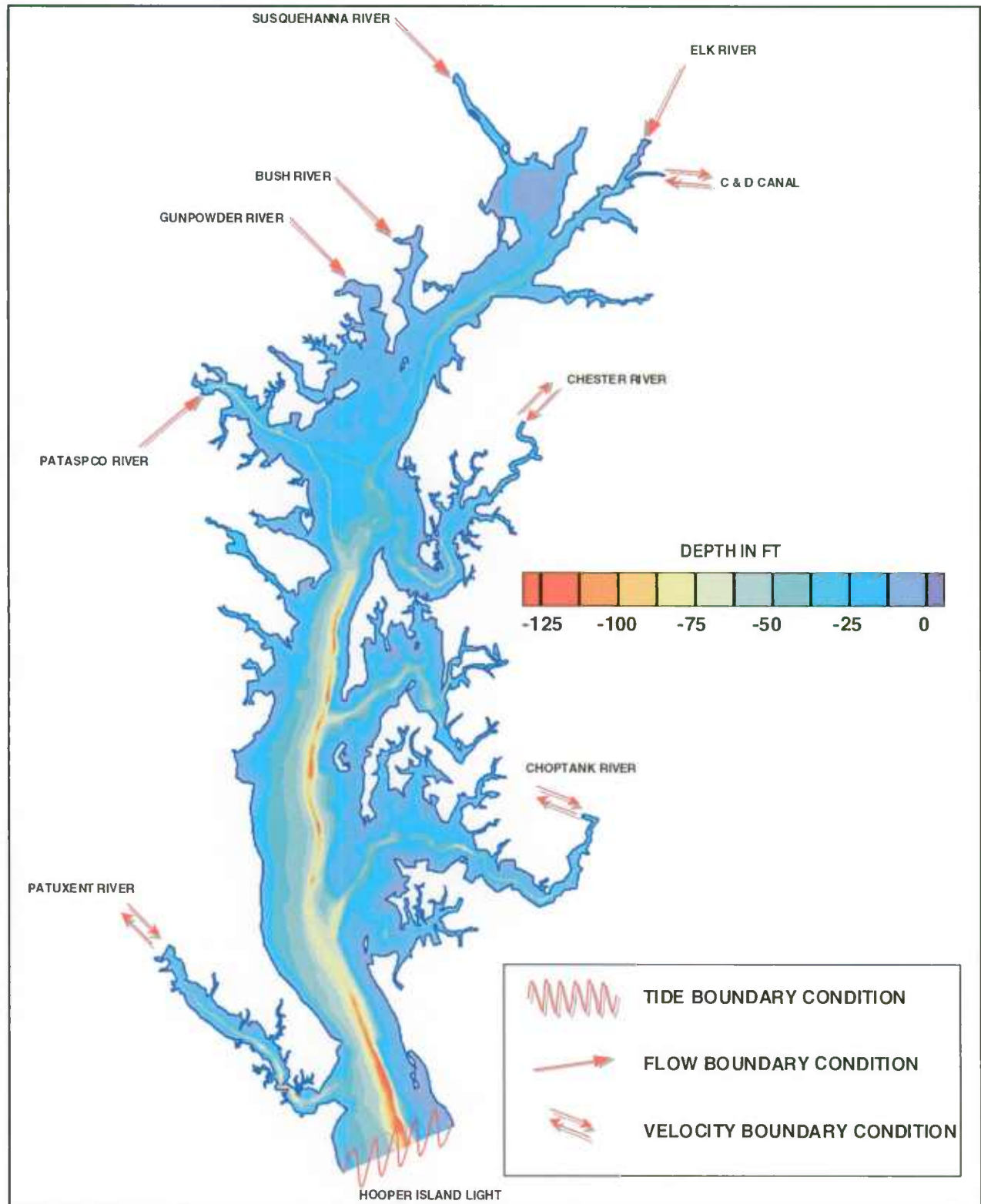


Figure 5-1: UCB-FEM Boundary Condition Locations

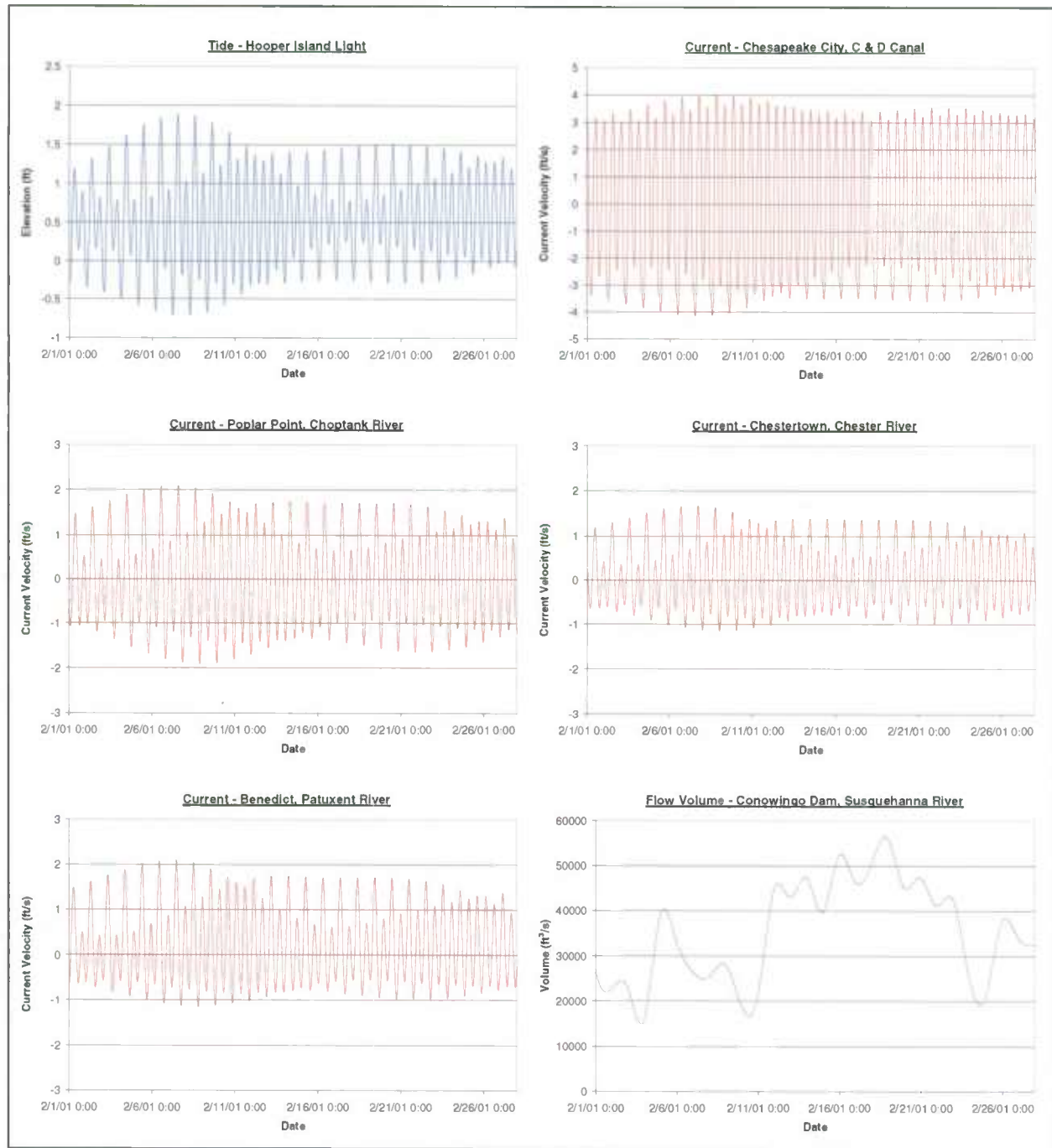


Figure 5-2: UCB-FEM Boundary Conditions

1  
2  
3  
4  
5  
6  
7  
8  
9  
10  
11  
12  
13  
14  
15  
16  
17  
18  
19  
20

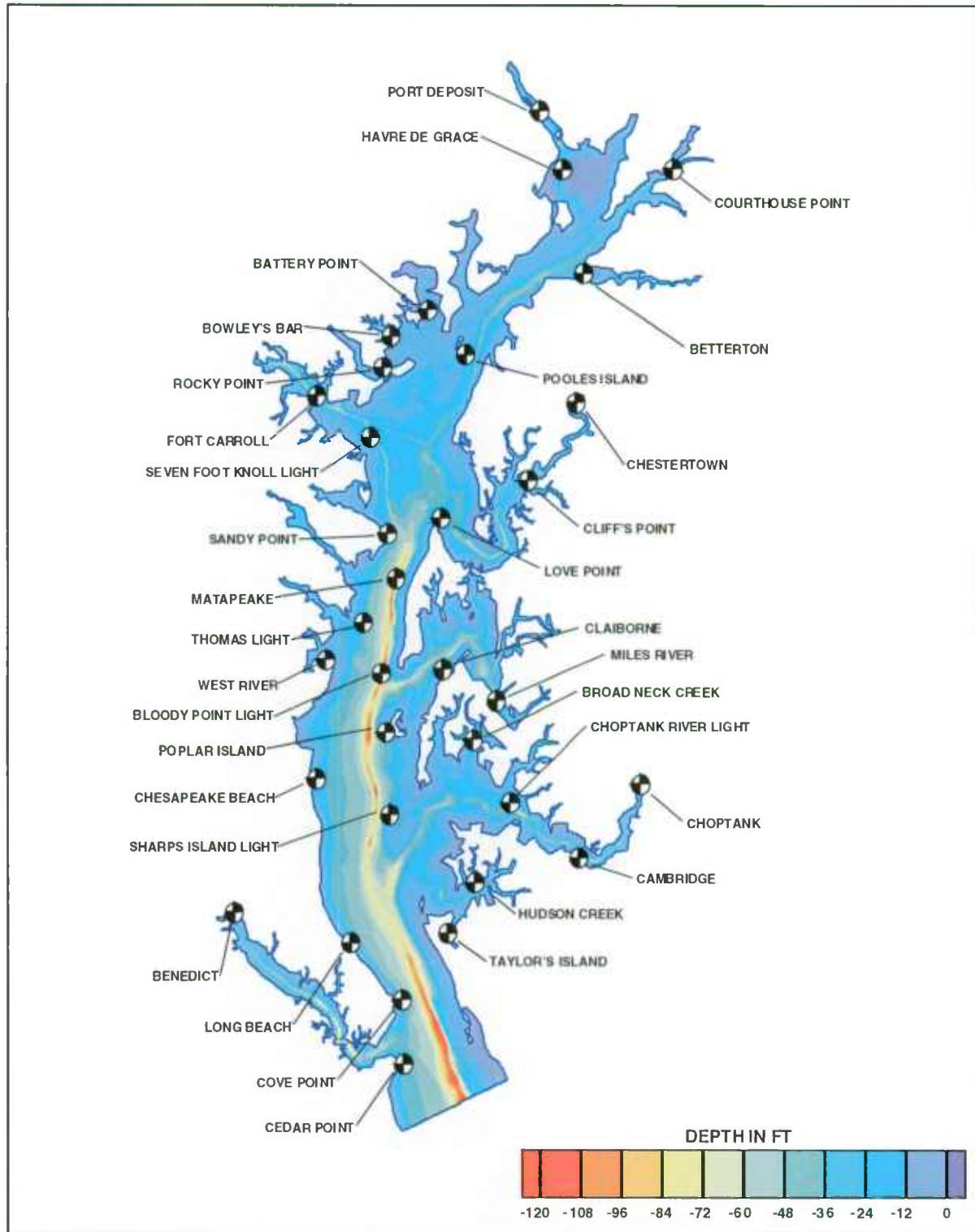


Figure 5-3: UCB-FEM Tidal Elevation Calibration Points

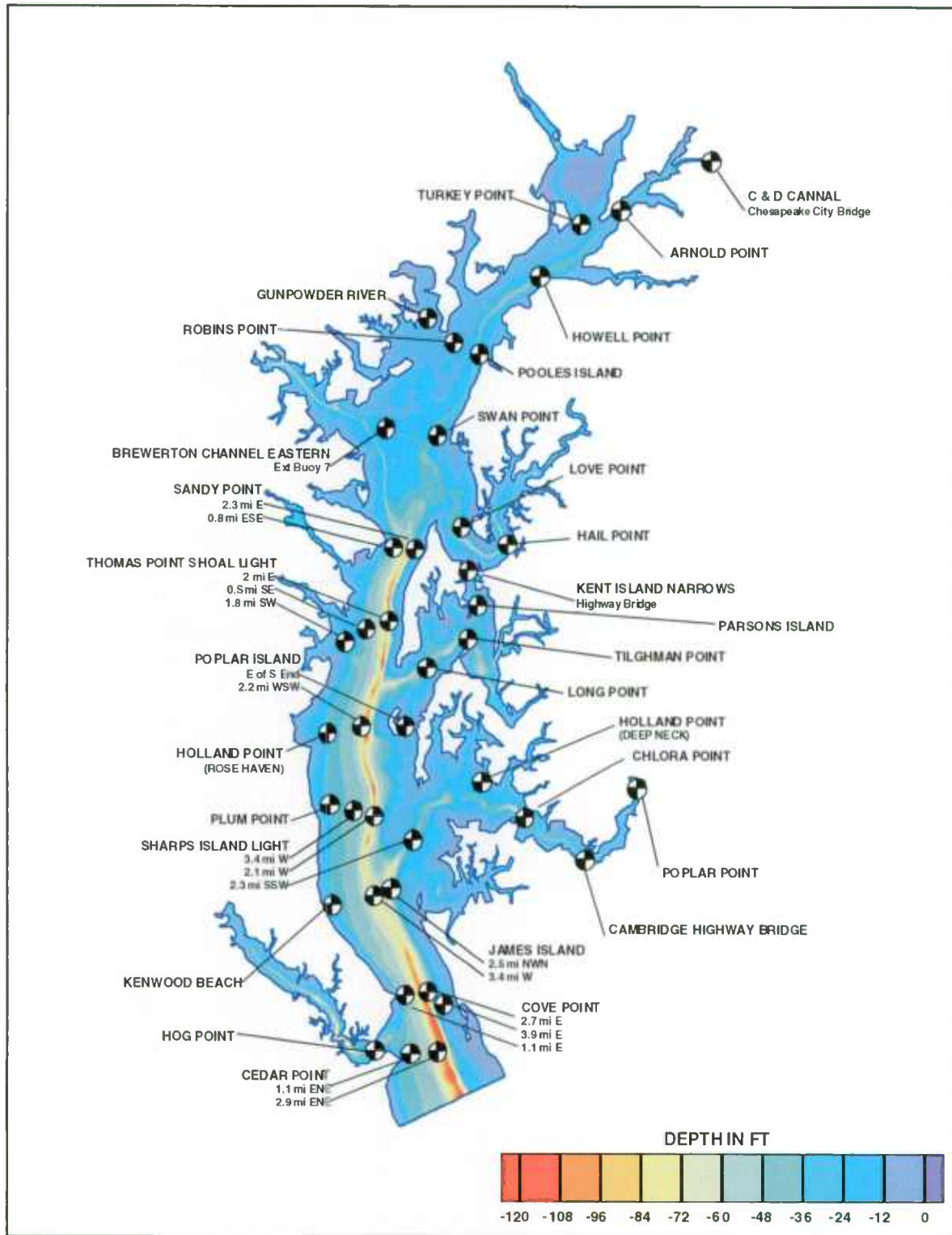


Figure 5-4: UCB-FEM Current Velocity Calibration Points

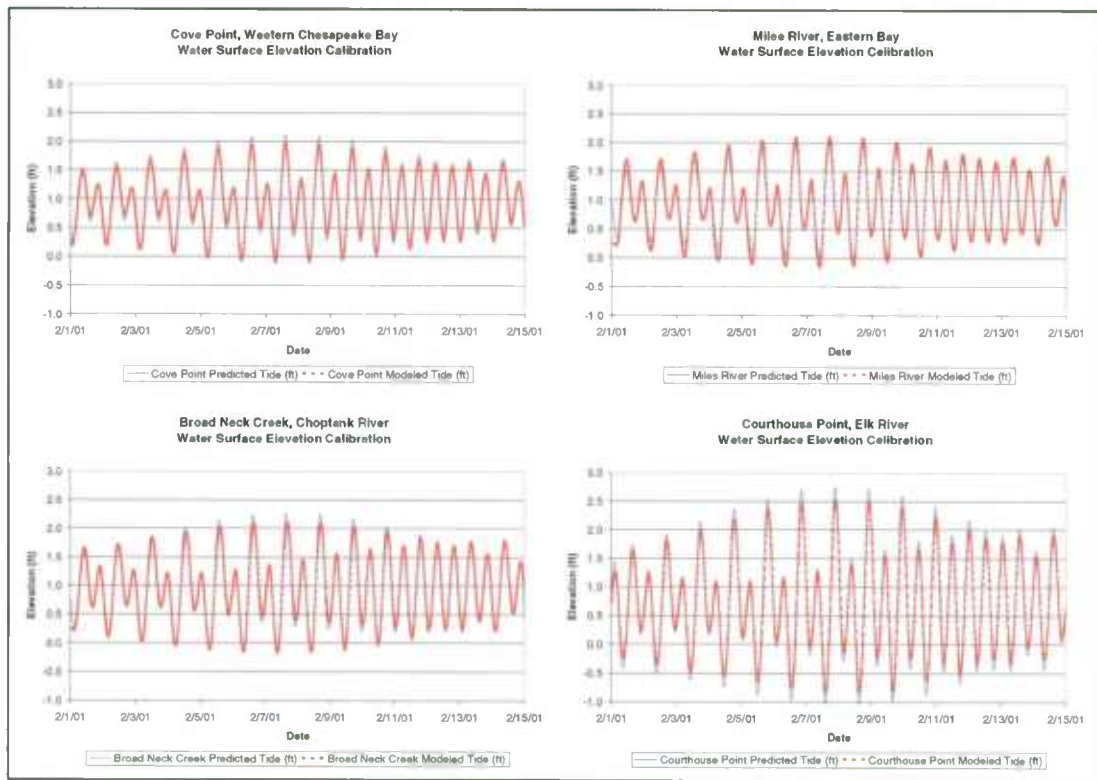


Figure 5-5: Tidal Elevation Calibration Results

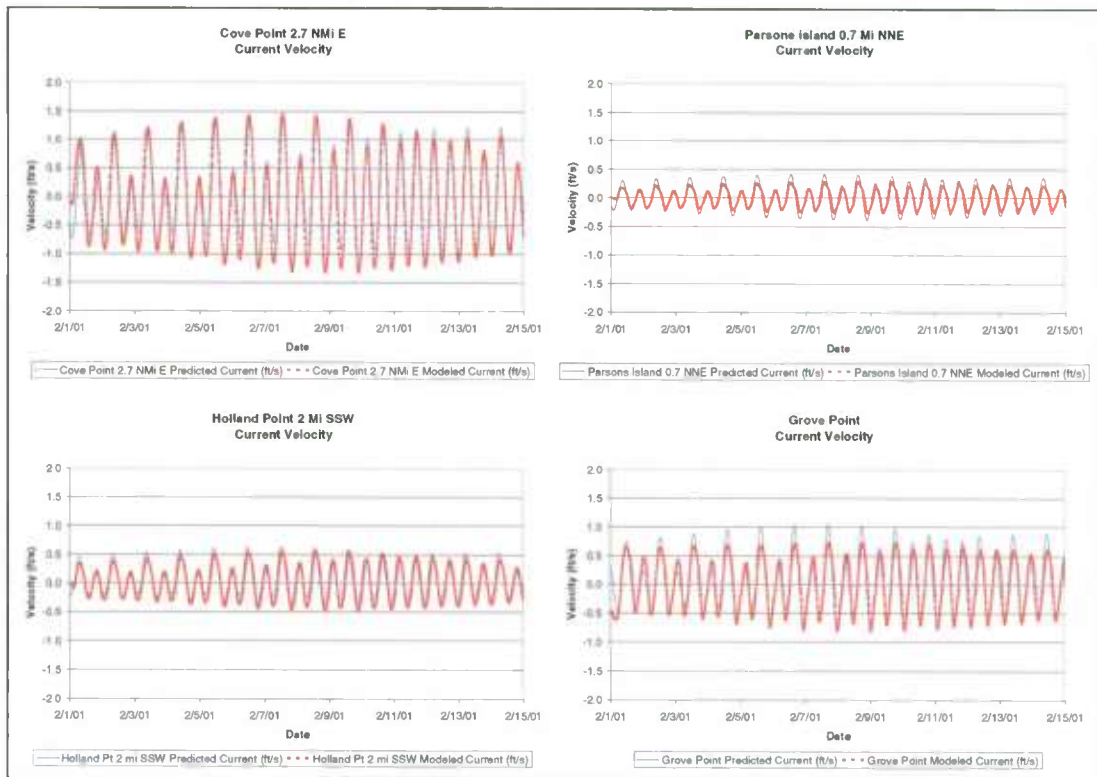


Figure 5-6: Current Velocity Calibration Results

1  
2  
3  
4  
5  
6  
7  
8  
9  
10  
11  
12  
13  
14  
15  
16  
17  
18  
19  
20  
21  
22  
23  
24  
25  
26  
27  
28  
29  
30  
31  
32  
33  
34  
35  
36  
37  
38  
39  
40  
41  
42  
43  
44

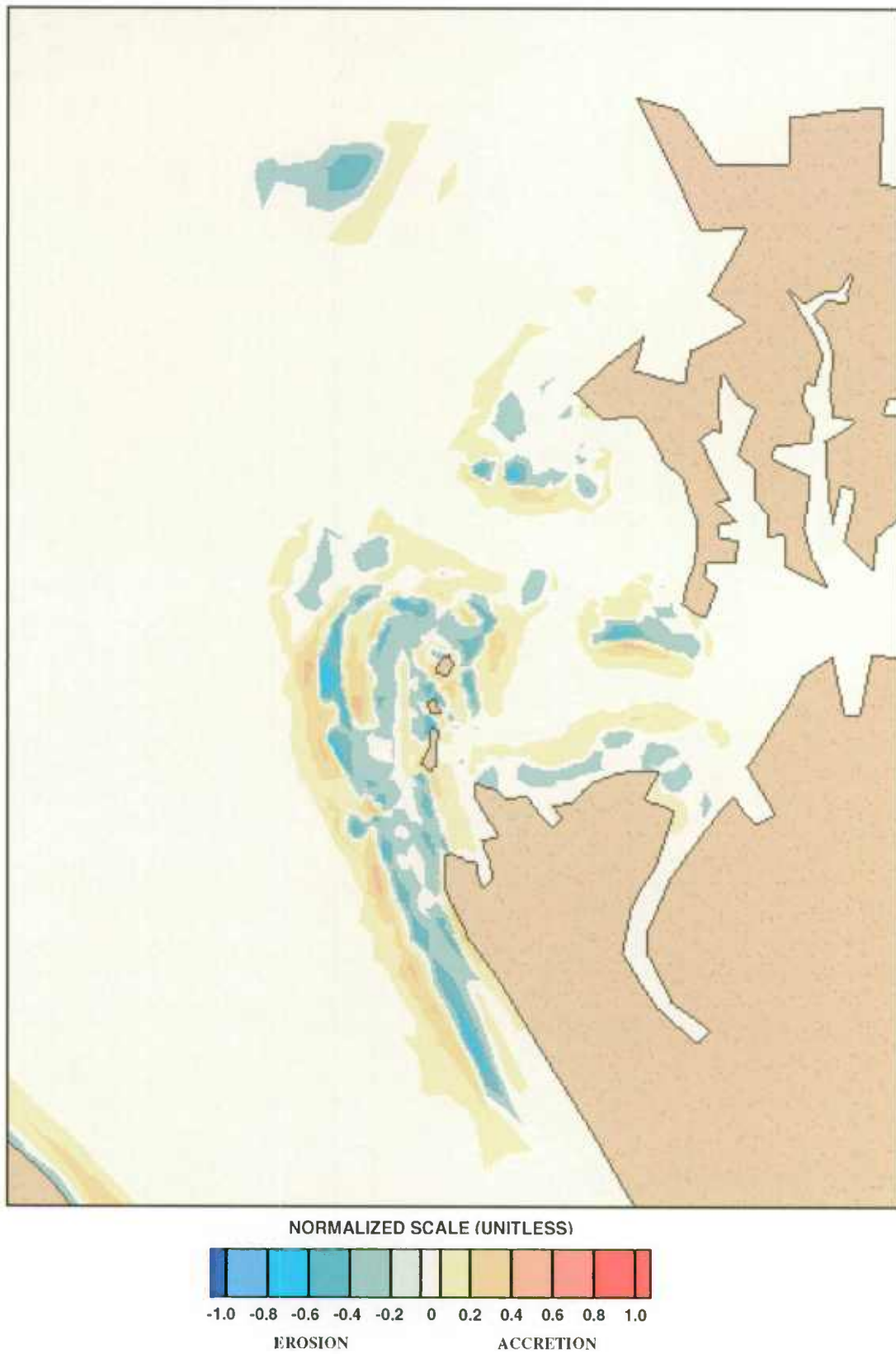


Figure 5-7: Non-Cohesive Sediment – NNW Wind 16 mph – Existing Conditions

1  
2  
3  
4  
5  
6  
7  
8  
9  
10  
11  
12  
13  
14  
15  
16  
17  
18  
19  
20  
21  
22  
23  
24  
25  
26  
27  
28  
29  
30  
31  
32  
33  
34  
35  
36  
37  
38  
39  
40  
41  
42  
43  
44

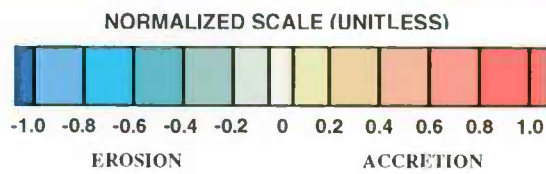
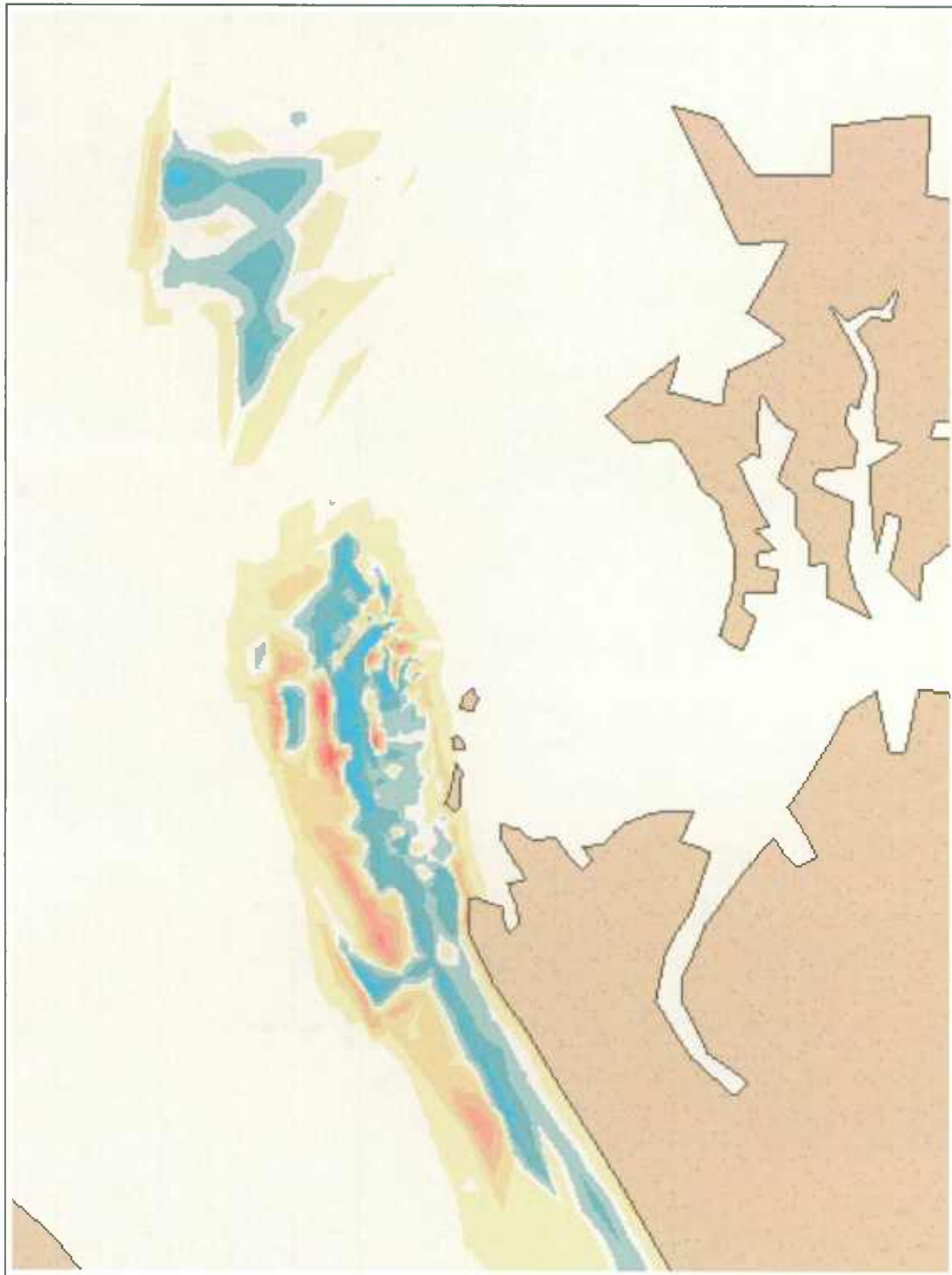


Figure 5-8: Non-Cohesive Sediment - SSE Wind 16 mph - Existing Conditions

1  
2  
3  
4  
5  
6  
7  
8  
9  
10  
11  
12  
13  
14  
15  
16  
17  
18  
19  
20  
21  
22  
23  
24  
25  
26  
27  
28  
29  
30  
31  
32  
33  
34  
35  
36  
37  
38  
39  
40  
41

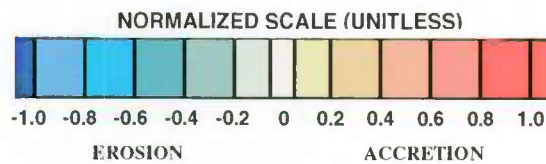
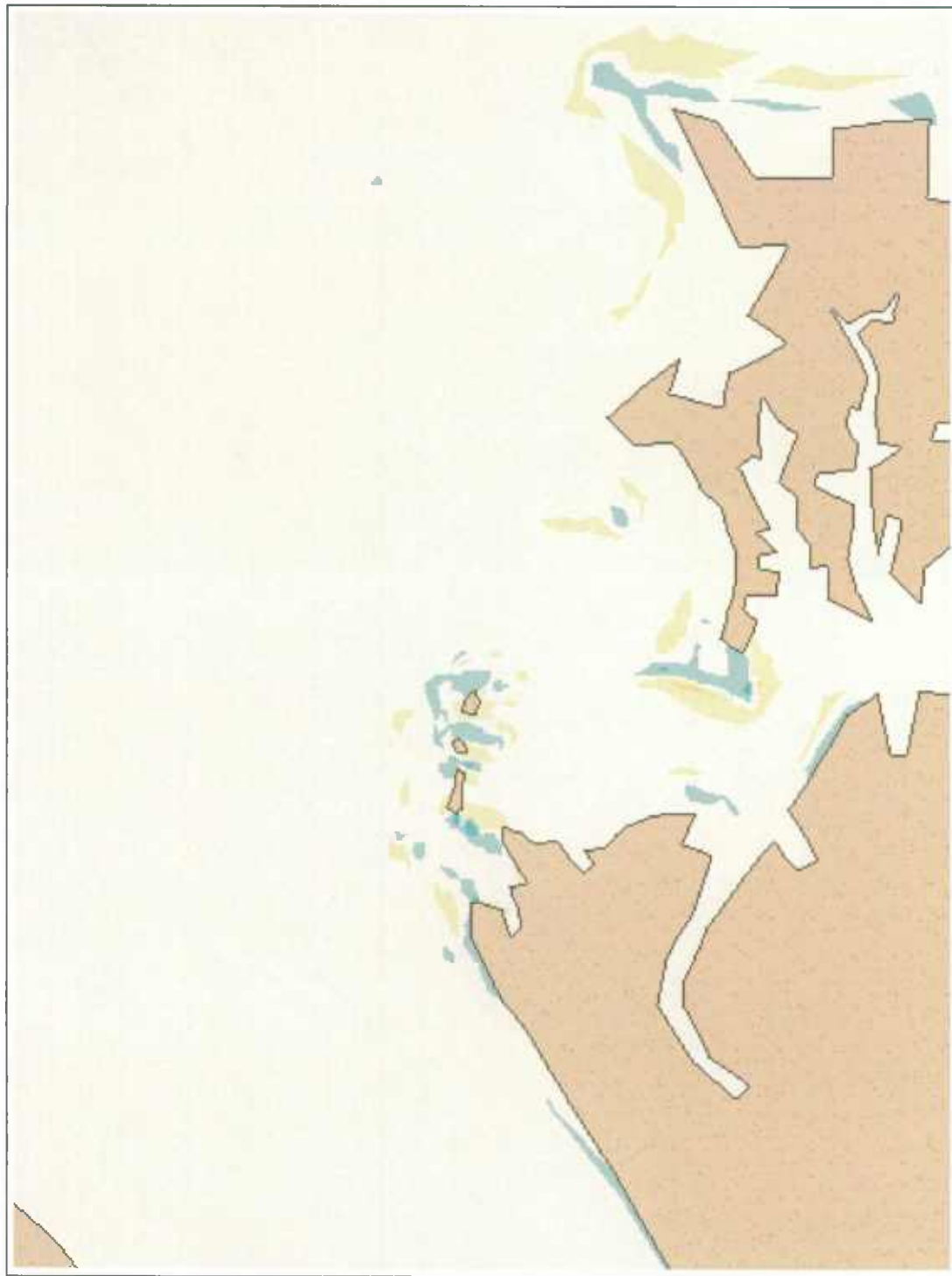


Figure 5-9: Non-Cohesive Sediment – WNW Wind 16 mph - Existing Conditions

1  
2  
3  
4  
5  
6  
7  
8  
9  
10  
11  
12  
13  
14  
15  
16  
17  
18  
19  
20  
21  
22  
23  
24  
25  
26  
27  
28  
29  
30  
31  
32  
33  
34  
35  
36  
37  
38  
39  
40  
41  
42  
43  
44  
45

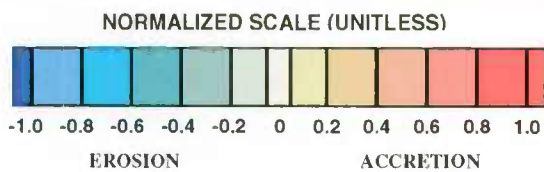


Figure 5-10: Cohesive Sediment – NNW Wind 13 mph - Existing Conditions

1  
2  
3  
4  
5  
6  
7  
8  
9  
10  
11  
12  
13  
14  
15  
16  
17  
18  
19  
20  
21  
22  
23  
24  
25  
26  
27  
28  
29  
30  
31  
32  
33  
34  
35  
36  
37  
38  
39  
40  
41  
42  
43  
44

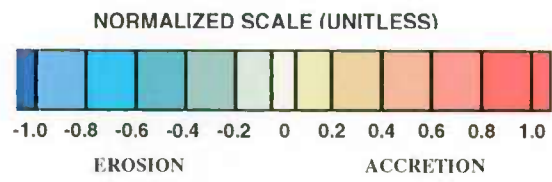


Figure 5-11: Cohesive Sediment – SSE Wind 13 mph - Existing Conditions

1  
2  
3  
4  
5  
6  
7  
8  
9  
10  
11  
12  
13  
14  
15  
16  
17  
18  
19  
20  
21  
22  
23  
24  
25  
26  
27  
28  
29  
30  
31  
32  
33  
34  
35  
36  
37  
38  
39  
40  
41  
42  
43  
44  
45

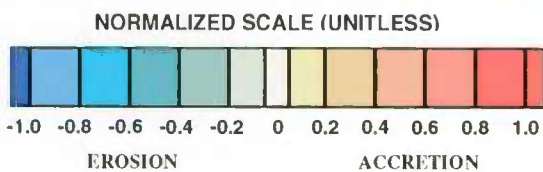


Figure 5-12: Cohesive Sediment – WNW Wind 13 mph - Existing Conditions

## 6. HYDRODYNAMIC MODELING RESULTS

### 6.1 GENERAL

Evaluation of the hydrodynamic impacts of the construction of the project at James Island has been conducted using the UCB-FEM model. The UCB-FEM model is used to assess impacts by applying identical hydrodynamic input boundary conditions to pre- and post- construction model bathymetry. Hydrodynamic results are then used as input into the sedimentation model which is also run using identical boundary conditions for pre- and post-construction conditions. The input conditions selected represent typical hydrodynamic conditions in the vicinity of James Island.

### 6.2 HABITAT ISLAND IMPACTS

Existing ebb and flood currents generally flow north and south in the main Bay west of James Island. In the gap between James Island and Taylors Island to the south, however, currents flow generally northeast on flood and southwest on ebb. The main flow into and out of the Little Choptank River generally follows the deeper natural channel around the north end of James Island. At peak flood tide, flow direction at this north end is towards the east, shifting southeast once past the mouth of the river. Ebb flow is reversed from flood; the magnitude of the flow velocities is about the same.

Results of the hydrodynamic simulations are compared numerically at locations north, east and south of the project site and visually for the entire project vicinity. The following sections describe the impacts of project construction on hydrodynamics.

#### 6.2.1 Alignment 1

Figure 6-1 shows the location of three comparison stations in the vicinity of James Island and Alignment 1. Plots summarizing water surface elevation and current velocity results for Alignment 1 are presented in Figure 6-2 for these locations. Hydrodynamic model results indicate that water surface elevations would be unaffected by construction of the project. This is not surprising considering that the area of the project is small compared to the Bay. Relatively

1 small impacts, however, do occur to current velocities. Figures 6-3 and 6-4 visually show the  
 2 differences in peak current velocity in the project area due to construction of the project. Peak  
 3 ebb and flood currents in the main Bay are not changed should Alignment 1 be constructed.  
 4 Following construction, flow would be displaced northward and southward, and current velocity  
 5 would increase both north and south of the project. Current velocity decreases primarily around  
 6 the existing James Island to the east where flow is blocked by the project. To a lesser extent,  
 7 velocity decreases would be observed west of the project. Maximum velocity increases would  
 8 be at the southeast dike, between the project and the existing southern James Island, and where  
 9 flow is trained along the northwest dike of the project as it enters the Little Choptank River.

10 Numerical comparisons of peak current velocity hydrodynamic modeling results between  
 11 existing conditions and Alternative 1 for the three locations are shown in Table 6-1. Maximum  
 12 change observed around existing James Island is about 0.44 ft/sec; a lesser change is observed in  
 13 the Little Choptank River.

14  
 15  
**Table 6-1: Hydrodynamic Modeling Results – Alternative 1**

	Existing Conditions		Alternative 1	
	<i>Peak Flood Current (ft/s)</i>	<i>Peak Ebb Current (ft/s)</i>	<i>Peak Flood Current (ft/s)</i>	<i>Peak Ebb Current (ft/s)</i>
North of Project	<b>0.54</b>	<b>0.46</b>	<b>0.55</b>	<b>0.61</b>
East of Project	<b>0.50</b>	<b>0.56</b>	<b>0.10</b>	<b>0.12</b>
South of Project	<b>0.32</b>	<b>0.32</b>	<b>0.74</b>	<b>0.72</b>

16 **6.2.2 Alignment 2**

17 Figure 6-5 shows the location of three comparison stations in the vicinity of James Island and  
 18 Alignment 2. Plots summarizing water surface elevation and current velocity results for  
 19 Alignment 2 are presented in Figure 6-6. As with Alignment 1, hydrodynamic model results  
 20 indicate that water surface elevations would be unaffected by construction of the project, with

1 relatively small impacts to current velocities. Figures 6-7 and 6-8 show the differences in peak  
 2 current velocity in the project area due to construction of the project. Peak ebb and flood  
 3 currents in the main Bay are not changed should Alignment 2 be constructed. Following  
 4 construction, flow would be displaced northward and southward, and current velocity would  
 5 increase both north and south of the project. Current velocity decreases primarily around the  
 6 existing James Island to the east where flow is blocked by the project, but the area where  
 7 velocities are reduced is larger for this alternative than Alternative 1 as the larger project area  
 8 affords more protection. Smaller velocity decreases would be observed west of the project.  
 9 Similar to Alternative 1, maximum velocity increases would be at the southeast dike between the  
 10 project and the existing southern James Island, and where flow is trained along the northwest  
 11 dike of the project as it enters the Little Choptank River.

12 Numerical comparisons of peak current velocity hydrodynamic modeling results for the three  
 13 locations shown in Figure 6-5 are shown in Table 6-2. Areas of change are similar to Alternative  
 14 1, with maximum change of about 0.46 ft/sec east of the project near the existing islands.

15  
 Table 6-2: Hydrodynamic Modeling Results – Alternative 2

	Existing Conditions		Alternative 2	
	<i>Peak Flood Current (ft/s)</i>	<i>Peak Ebb Current (ft/s)</i>	<i>Peak Flood Current (ft/s)</i>	<i>Peak Ebb Current (ft/s)</i>
North of Project	<b>0.54</b>	<b>0.46</b>	<b>0.66</b>	<b>0.61</b>
East of Project	<b>0.50</b>	<b>0.56</b>	<b>0.08</b>	<b>0.10</b>
South of Project	<b>0.49</b>	<b>0.47</b>	<b>0.74</b>	<b>0.75</b>

16  
 17 **6.2.3 Alignment 3**

18 Figure 6-9 shows the location of three comparison stations in the vicinity of James Island and  
 19 Alignment 3, with plots summarizing water surface elevation and current velocity results  
 20 presented in Figure 6-10. As before, results indicate that water surface elevations would be

1 unaffected by construction of the project and relatively small impacts occur to current velocities.  
 2 Figures 6-11 and 6-12 visually show the differences in peak current velocity in the project area  
 3 due to construction of the project. Peak ebb and flood currents in the main Bay are not changed  
 4 should Alignment 3 be constructed. Following construction, flow would be displaced northward  
 5 and southward, and current velocity would increase both north and south of the project. Current  
 6 velocity decreases around the existing James Island to the east similarly to Alternative 2, and  
 7 smaller velocity decreases would also be observed west of the project. Maximum velocity  
 8 increases would be at the southeast dike between the project and the existing southern James  
 9 Island, however, as this alignment extends further south, the increase in velocity is concentrated  
 10 at the tip of the dike and extends to Taylors Island. Increase in velocity is also observed where  
 11 flow is trained along the northwest dike of the project as it enters the Little Choptank River.

12 Numerical comparisons of peak current velocity hydrodynamic modeling results for the three  
 13 selected locations for Alternative 3 are shown in Table 6-3. Maximum change is about 0.49  
 14 ft/sec east of the project between it and James Island.

15  
**Table 6-3: Hydrodynamic Modeling Results – Alternative 3**

	Existing Conditions		Alternative 3	
	<i>Peak Flood Current (ft/s)</i>	<i>Peak Ebb Current (ft/s)</i>	<i>Peak Flood Current (ft/s)</i>	<i>Peak Ebb Current (ft/s)</i>
North of Project	<b>0.54</b>	<b>0.46</b>	<b>0.67</b>	<b>0.63</b>
East of Project	<b>0.50</b>	<b>0.56</b>	<b>0.05</b>	<b>0.07</b>
South of Project	<b>0.53</b>	<b>0.52</b>	<b>0.81</b>	<b>0.82</b>

16

#### 17 6.2.4 Alignment 4

18 Figure 6-13 shows the location of three comparison stations in the vicinity of James Island and  
 19 Alignment 4, with plots summarizing water surface elevation and current velocity results  
 20 presented in Figure 6-14. As before, results indicate that water surface elevations would be

1 unaffected by construction of the project with relatively small impacts to current velocities.  
 2 Figures 6-15 and 6-16 visually show the differences in peak current velocity in the project area  
 3 due to construction of the project. Peak ebb and flood currents in the main Bay are not changed  
 4 should Alignment 4 be constructed. Following construction, flow would be displaced northward  
 5 and southward, and current velocity would increase both north and south of the project. Current  
 6 velocity decreases primarily around the existing James Island to the east where flow is blocked  
 7 by the project. This alignment provides the most protection to James Island and thus provides  
 8 the greatest decrease in velocity. To a lesser extent, velocity decreases would be observed west  
 9 of the project. This alignment also extends furthest south towards Taylors Island, and maximum  
 10 velocity increases at the southeast dike between the project and extending completely to Taylors  
 11 Island. This increase in velocity is greatest among all alignments. Velocity also increases where  
 12 flow is trained along the northwest dike of the project as it enters the Little Choptank River.

13 Numerical comparisons of peak current velocity hydrodynamic modeling results for Alternative  
 14 4 are shown in Table 6-4. Maximum change is about 0.50 ft/sec, again east of the project.

15 **Table 6-4: Hydrodynamic Modeling Results – Alternative 4**

	Existing Conditions		Alternative 4	
	<i>Peak Flood Current (ft/s)</i>	<i>Peak Ebb Current (ft/s)</i>	<i>Peak Flood Current (ft/s)</i>	<i>Peak Ebb Current (ft/s)</i>
North of Project	<b>0.54</b>	<b>0.46</b>	<b>0.69</b>	<b>0.65</b>
East of Project	<b>0.50</b>	<b>0.56</b>	<b>0.05</b>	<b>0.06</b>
South of Project	<b>0.54</b>	<b>0.59</b>	<b>0.92</b>	<b>1.00</b>

16

### 17 6.2.5 Alignment 5

18 Figure 6-17 shows the location of three comparison stations in the vicinity of James Island and  
 19 Alignment 5, with plots summarizing water surface elevation and current velocity results  
 20 presented in Figure 6-18. As for all cases, results indicate that water surface elevations would be

1 unaffected by construction of the project and small impacts occur to current velocities. Figures  
 2 6-19 and 6-20 visually show the differences in peak current velocity in the project area due to  
 3 construction of the project. Peak ebb and flood currents in the main Bay are not changed should  
 4 Alignment 5 be constructed. Following construction, flow would be displaced northward and  
 5 southward, and current velocity would increase both north and south of the project. Current  
 6 velocity decreases primarily around the existing James Island to the east where flow is blocked  
 7 by the project; the reduction in velocity is similar to Alignments 2 and 3. To a lesser extent,  
 8 velocity decreases would be observed west of the project. Maximum velocity increases would  
 9 be at the southeast dike between the project and the existing southern James Island, similar to  
 10 Alignment 2 as these both have southern boundaries about the same location. Velocity increases  
 11 also occur where flow is trained along the northwest dike of the project as it enters the Little  
 12 Choptank River.

13 Numerical comparisons of peak current velocity hydrodynamic modeling results for Alternative  
 14 5 are shown in Table 6-5. Maximum change is east of the project at about 0.48 ft/sec.

15  
**Table 6-5: Hydrodynamic Modeling Results – Alternative 5**

	Existing Conditions		Alternative 5	
	<i>Peak Flood Current (ft/s)</i>	<i>Peak Ebb Current (ft/s)</i>	<i>Peak Flood Current (ft/s)</i>	<i>Peak Ebb Current (ft/s)</i>
North of Project	<b>0.54</b>	<b>0.46</b>	<b>0.66</b>	<b>0.62</b>
East of Project	<b>0.50</b>	<b>0.56</b>	<b>0.06</b>	<b>0.08</b>
South of Project	<b>0.50</b>	<b>0.52</b>	<b>0.84</b>	<b>0.92</b>

1  
2  
3  
4  
5  
6  
7  
8  
9  
10  
11  
12  
13  
14  
15  
16  
17  
18

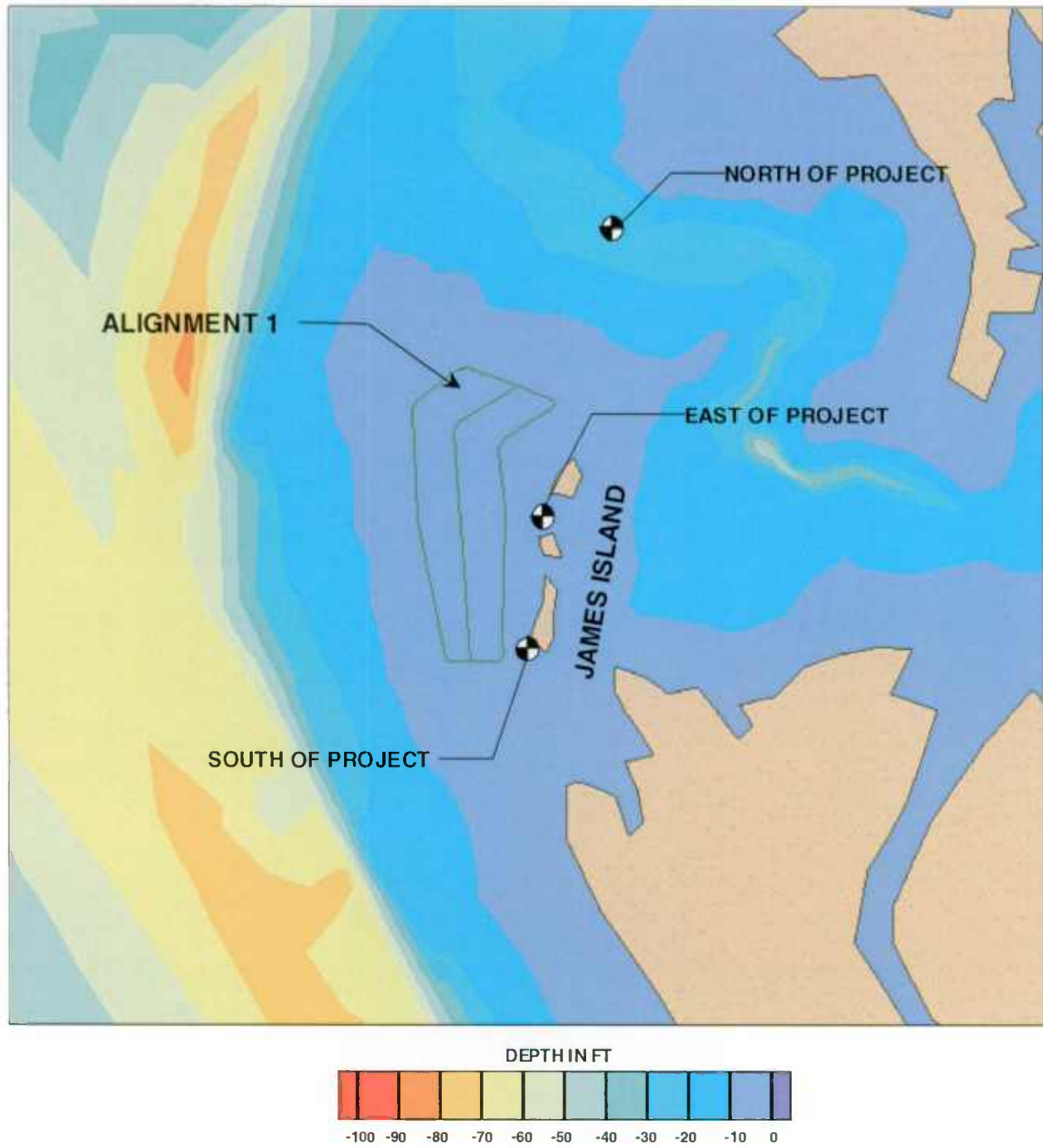


Figure 6-1: Results Comparison Locations for Alignment 1

1  
2  
3  
4  
5  
6  
7  
8  
9  
10  
11  
12  
13  
14  
15  
16  
17  
18  
19  
20  
21  
22  
23  
24  
25  
26  
27  
28  
29  
30  
31  
32  
33  
34  
35  
36  
37  
38  
39  
40  
41  
42  
43  
44  
45

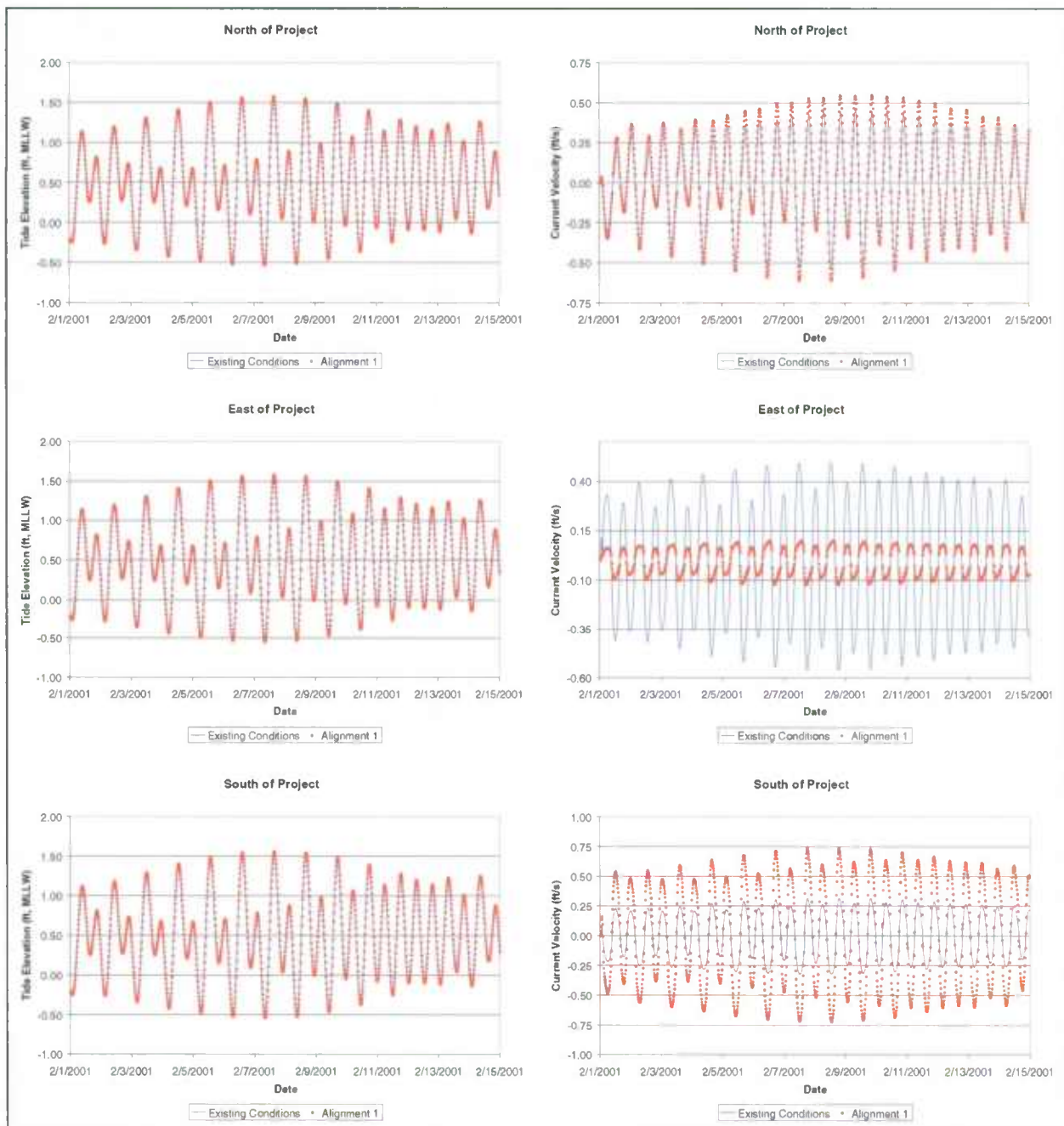


Figure 6-2: James Island Tidal Results Comparison for Alignment 1

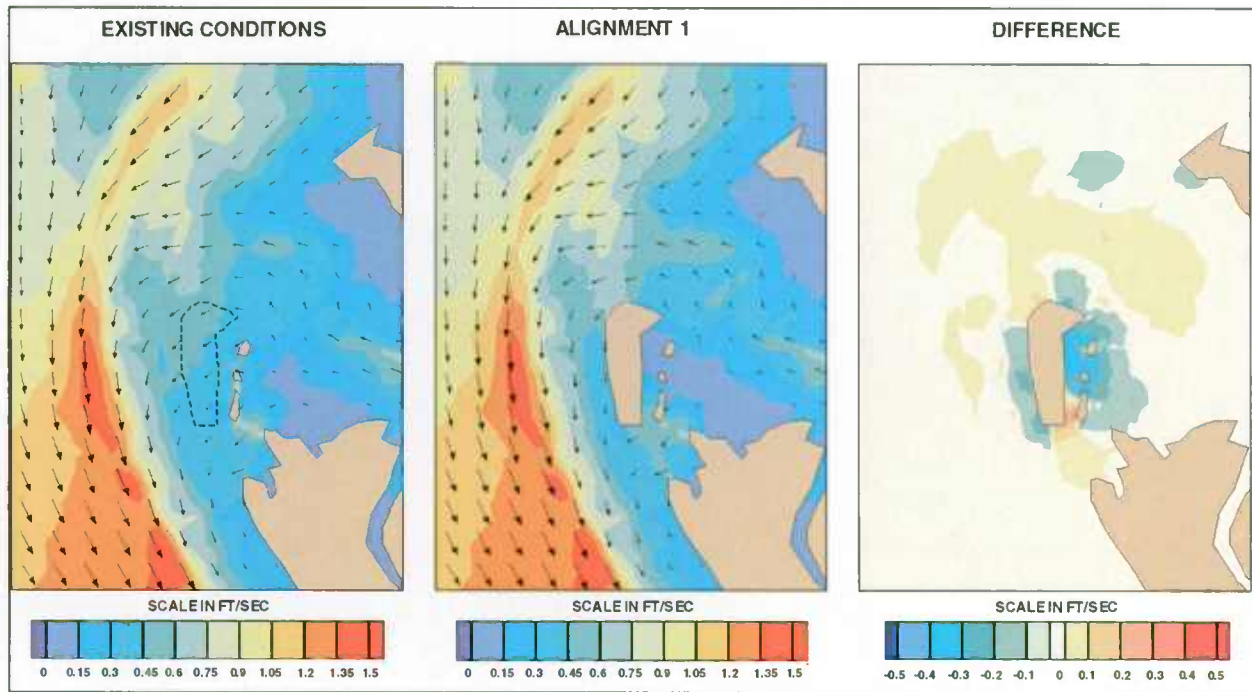


Figure 6-3: Peak Ebb Current Velocity – Alignment 1 vs. Existing Conditions

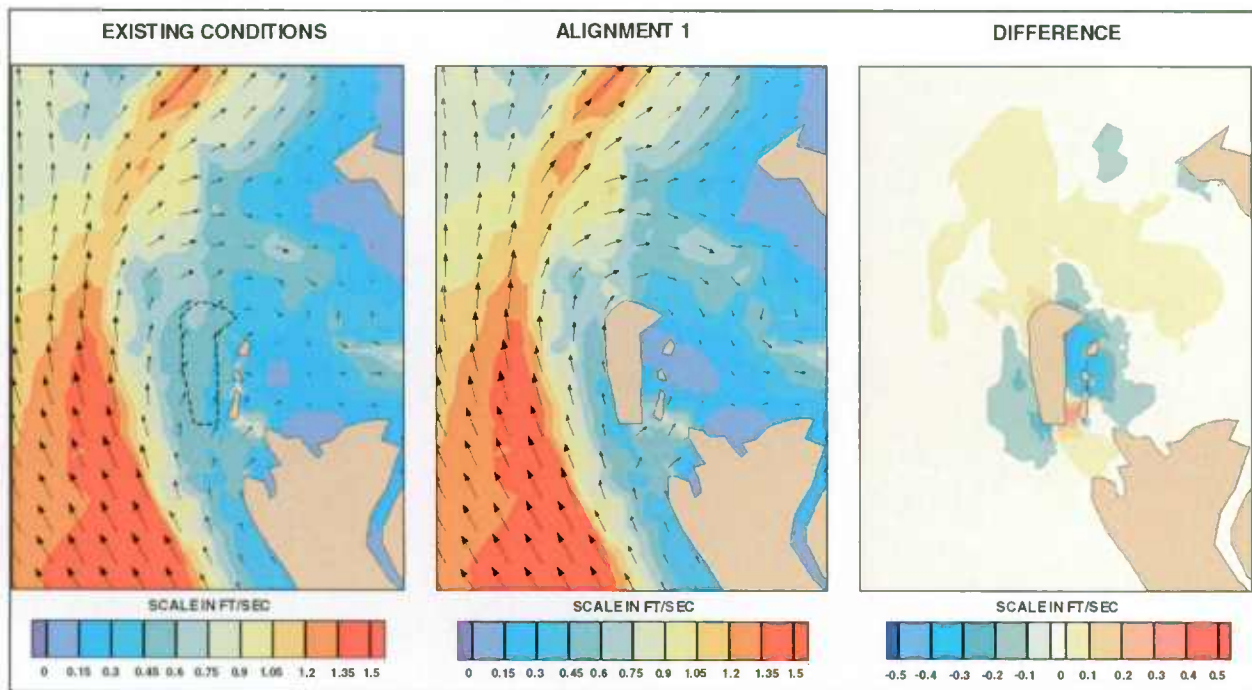


Figure 6-4: Peak Flood Current Velocity – Alignment 1 vs. Existing Conditions

1  
2  
3  
4  
5  
6  
7  
8  
9  
10  
11  
12  
13  
14  
15  
16  
17  
18

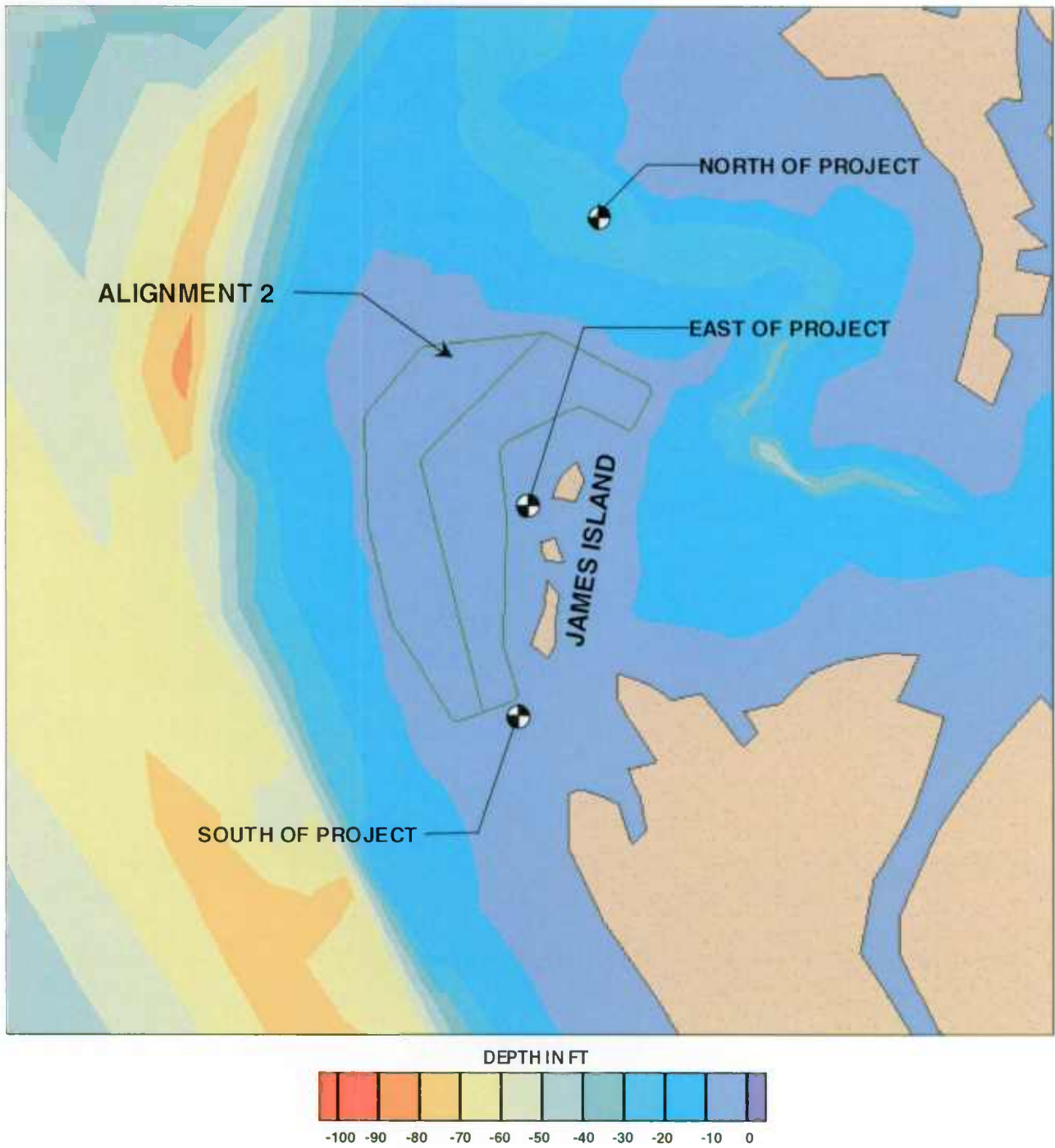


Figure 6-5: Results Comparison Locations for Alignment 2

1  
2  
3  
4  
5  
6  
7  
8  
9  
10  
11  
12  
13  
14  
15  
16  
17  
18  
19  
20  
21  
22  
23  
24  
25  
26  
27  
28  
29  
30  
31  
32  
33  
34  
35  
36  
37  
38  
39  
40  
41  
42  
43  
44

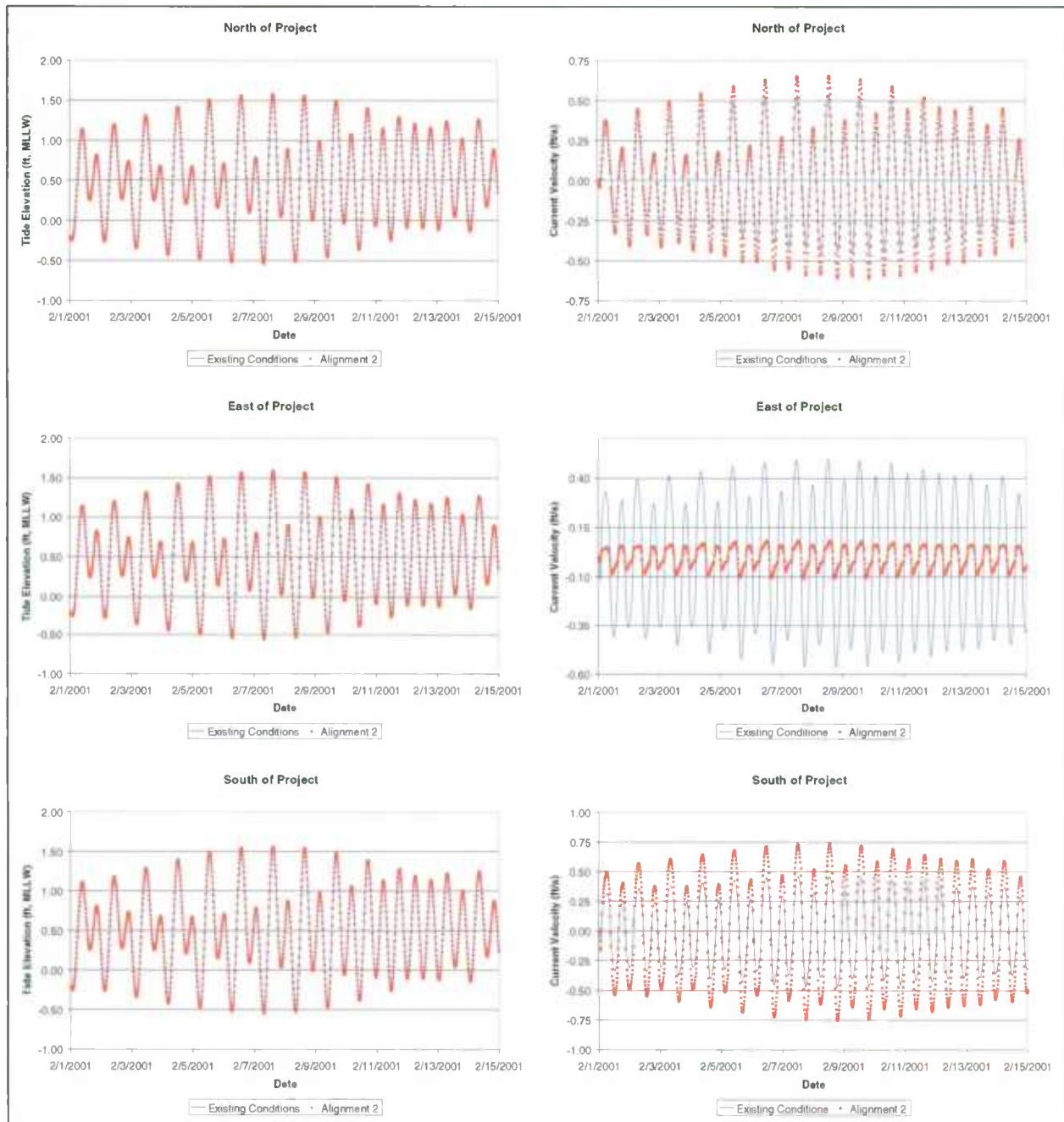


Figure 6-6: James Island Tidal Results Comparison for Alignment 2

1  
2  
3  
4  
5  
6  
7  
8  
9  
10  
11  
12  
13  
14  
15  
16  
17  
18  
19

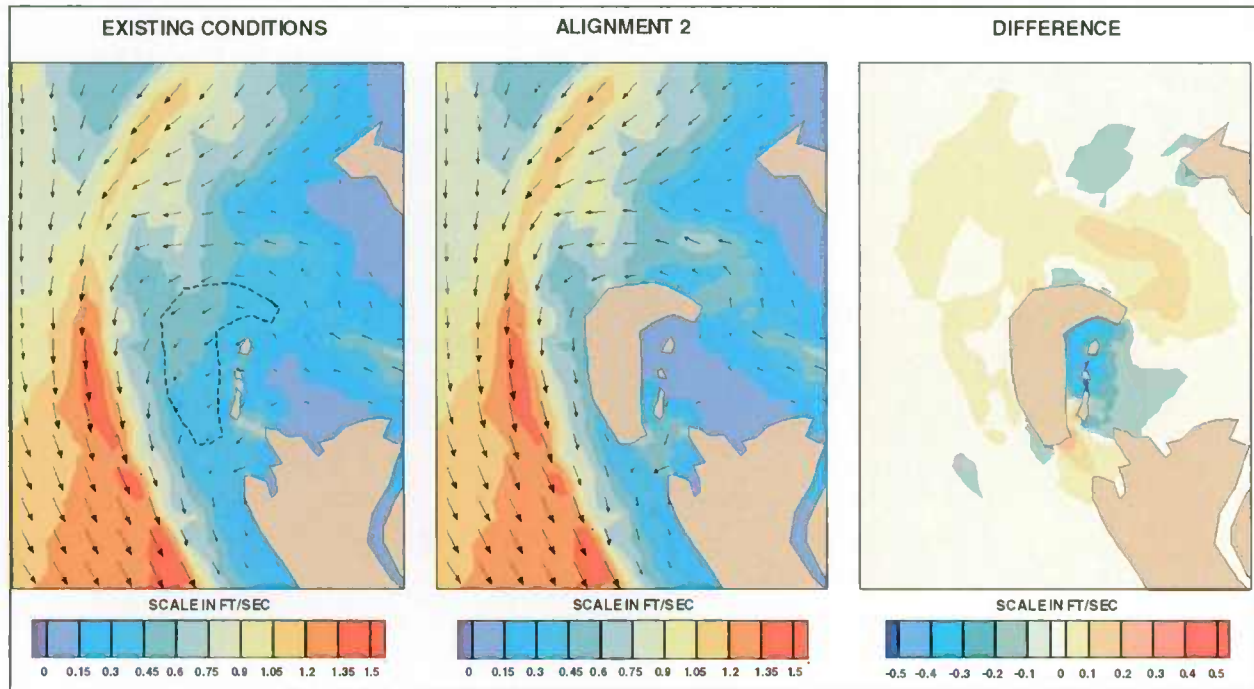


Figure 6-7: Peak Ebb Current Velocity – Alignment 2 vs. Existing Conditions

20  
21  
22  
23  
24  
25  
26  
27  
28  
29  
30  
31  
32  
33  
34  
35  
36  
37  
38  
39  
40  
41  
42  
43

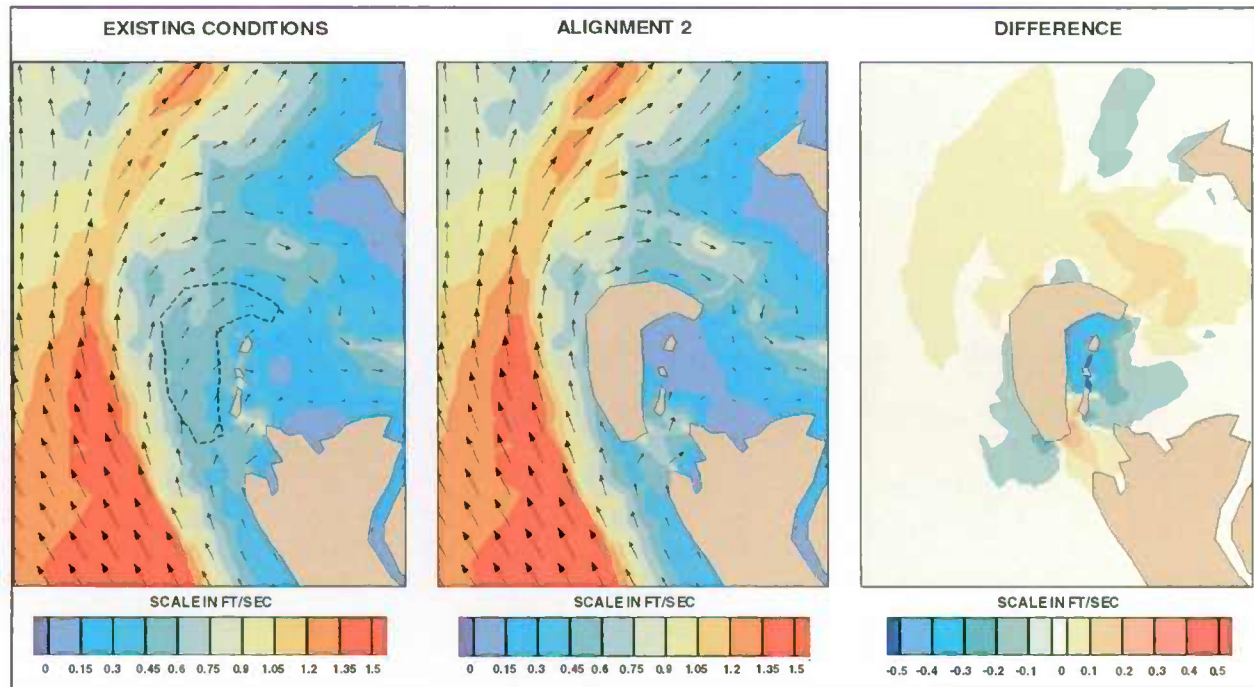


Figure 6-8: Peak Flood Current Velocity – Alignment 2 vs. Existing Conditions

1  
2  
3  
4  
5  
6  
7  
8  
9  
10  
11  
12  
13  
14  
15  
16  
17  
18  
19  
20  
21  
22  
23

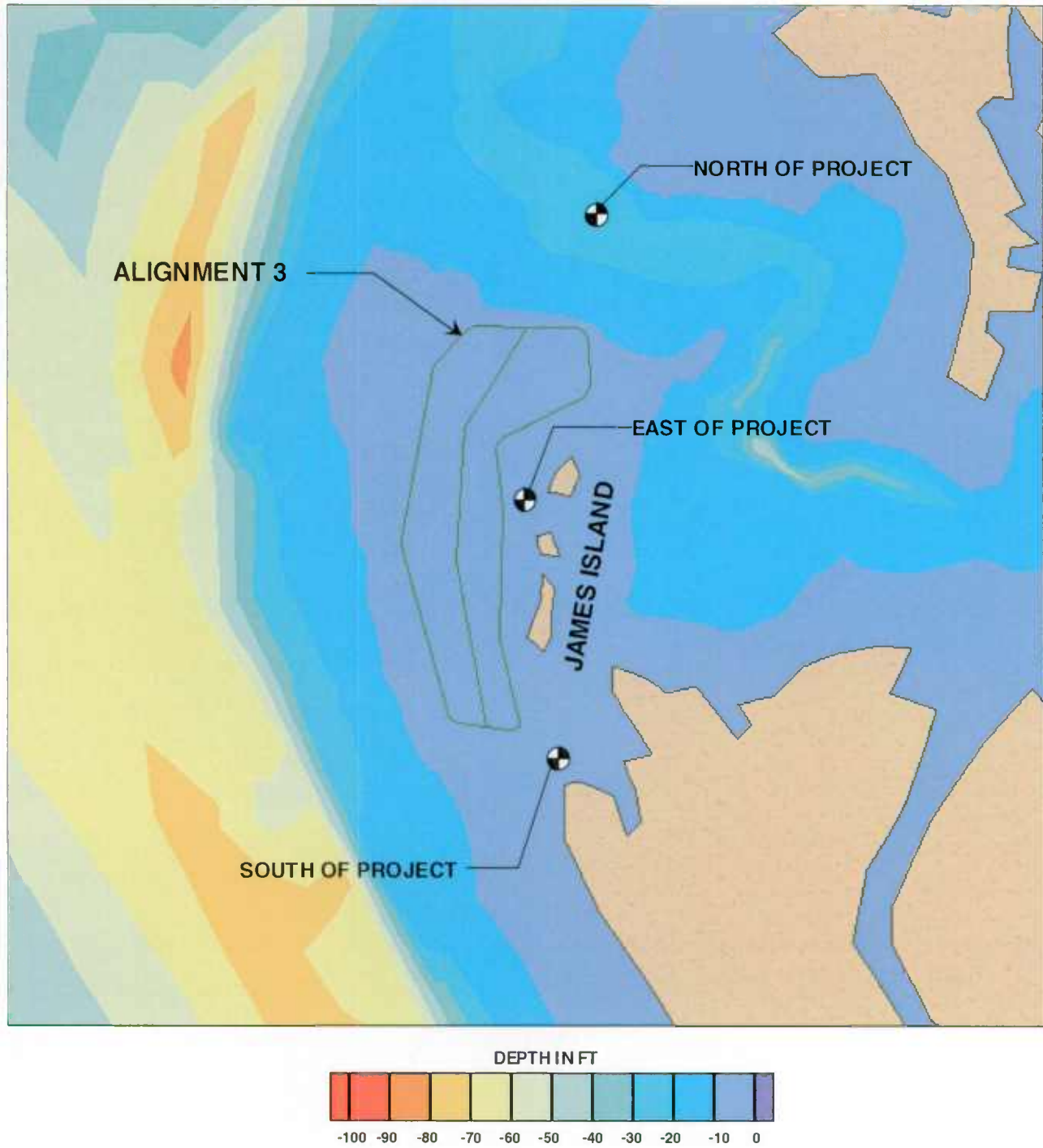


Figure 6-9: Results Comparison Locations for Alignment 3

1  
2  
3  
4  
5  
6  
7  
8  
9  
10  
11  
12  
13  
14  
15  
16  
17  
18  
19  
20  
21  
22  
23  
24  
25  
26  
27  
28  
29  
30  
31  
32  
33  
34  
35  
36  
37  
38  
39  
40  
41  
42

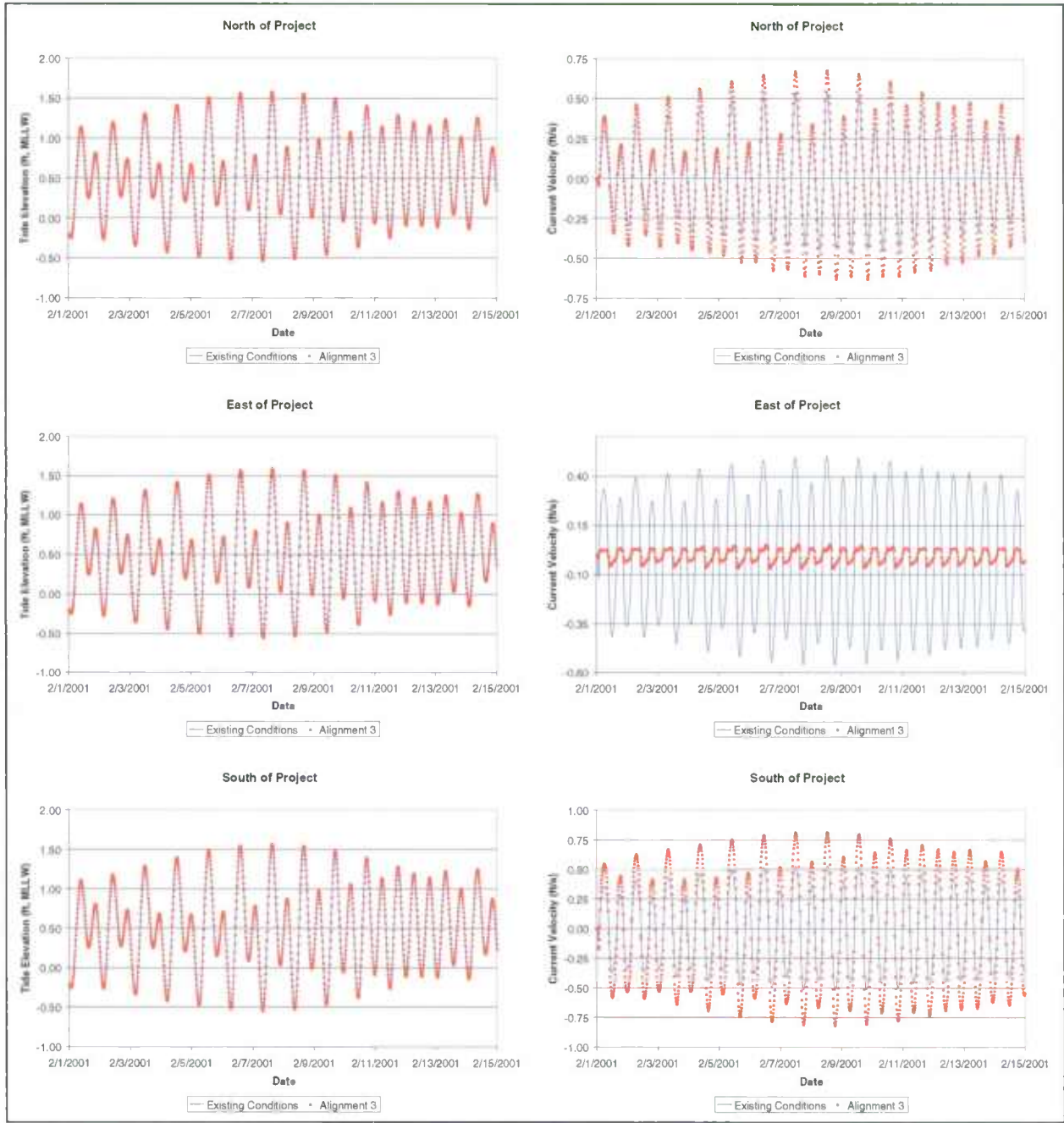


Figure 6-10: James Island Tidal Results Comparison for Alignment 3

1  
2  
3  
4  
5  
6  
7  
8  
9  
10  
11  
12  
13  
14  
15  
16  
17  
18  
19  
20  
21  
22  
23  
24  
25  
26  
27  
28  
29  
30  
31  
32  
33  
34  
35  
36  
37  
38  
39  
40  
41  
42  
43

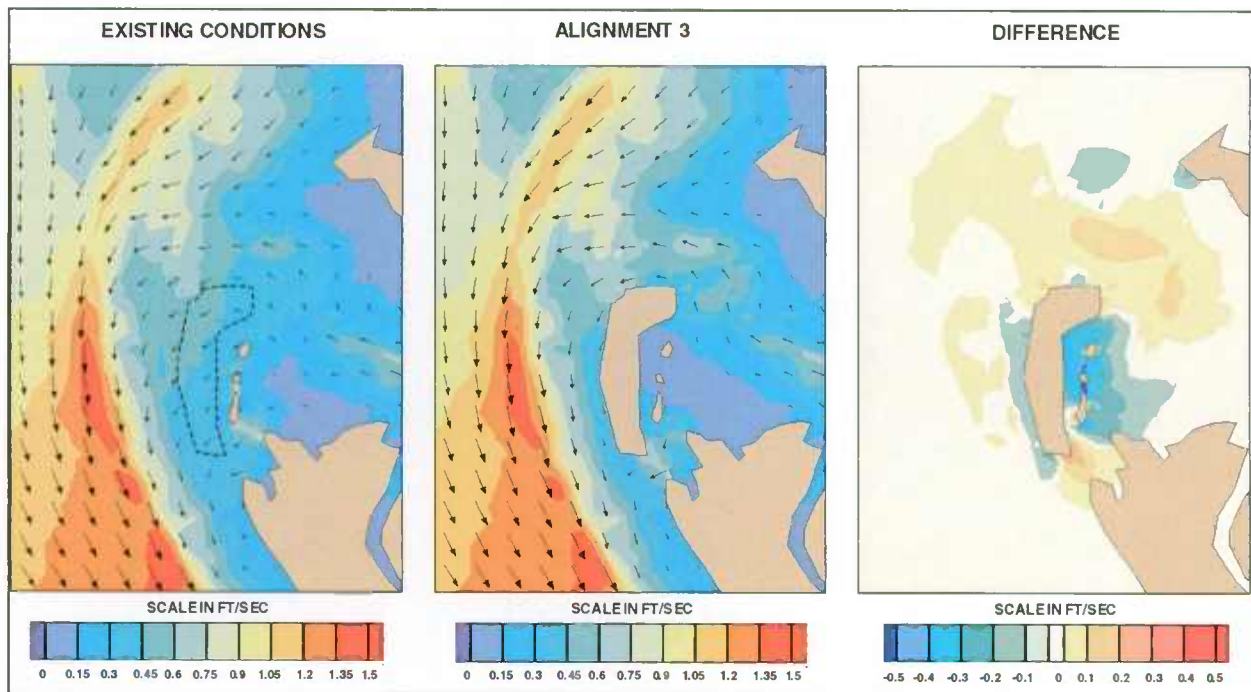


Figure 6-11: Peak Ebb Current Velocity – Alignment 3 vs. Existing Conditions

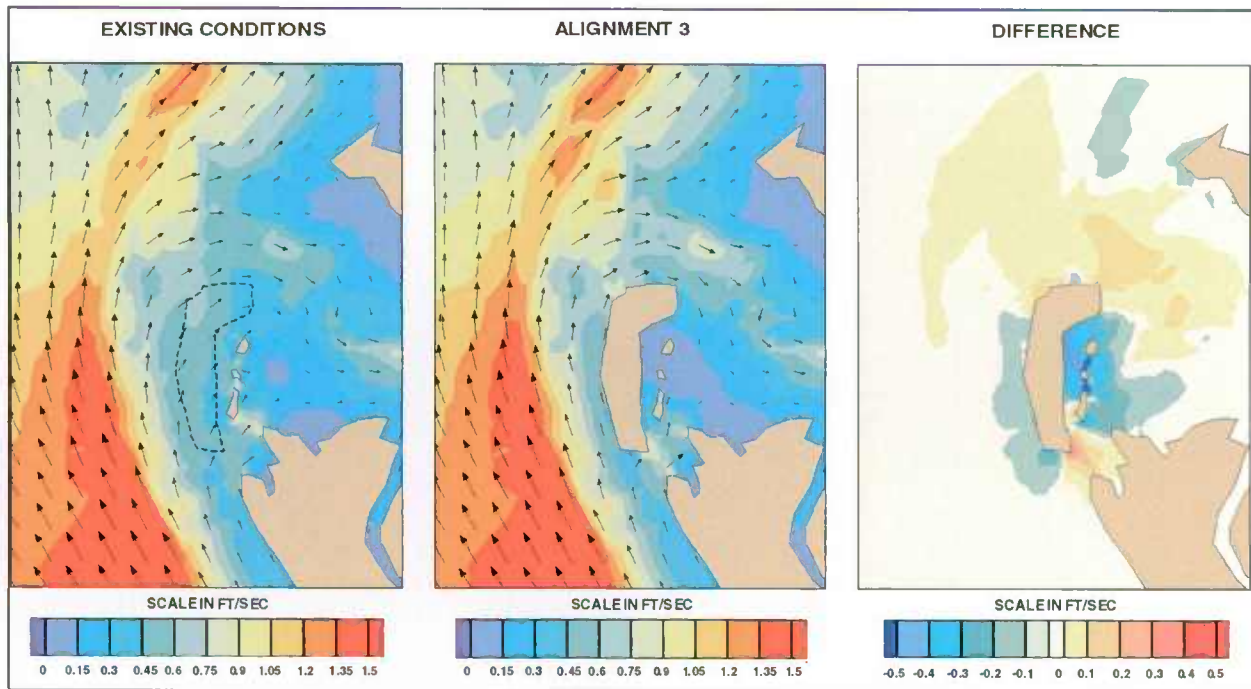
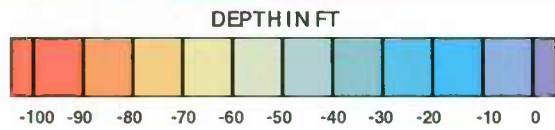
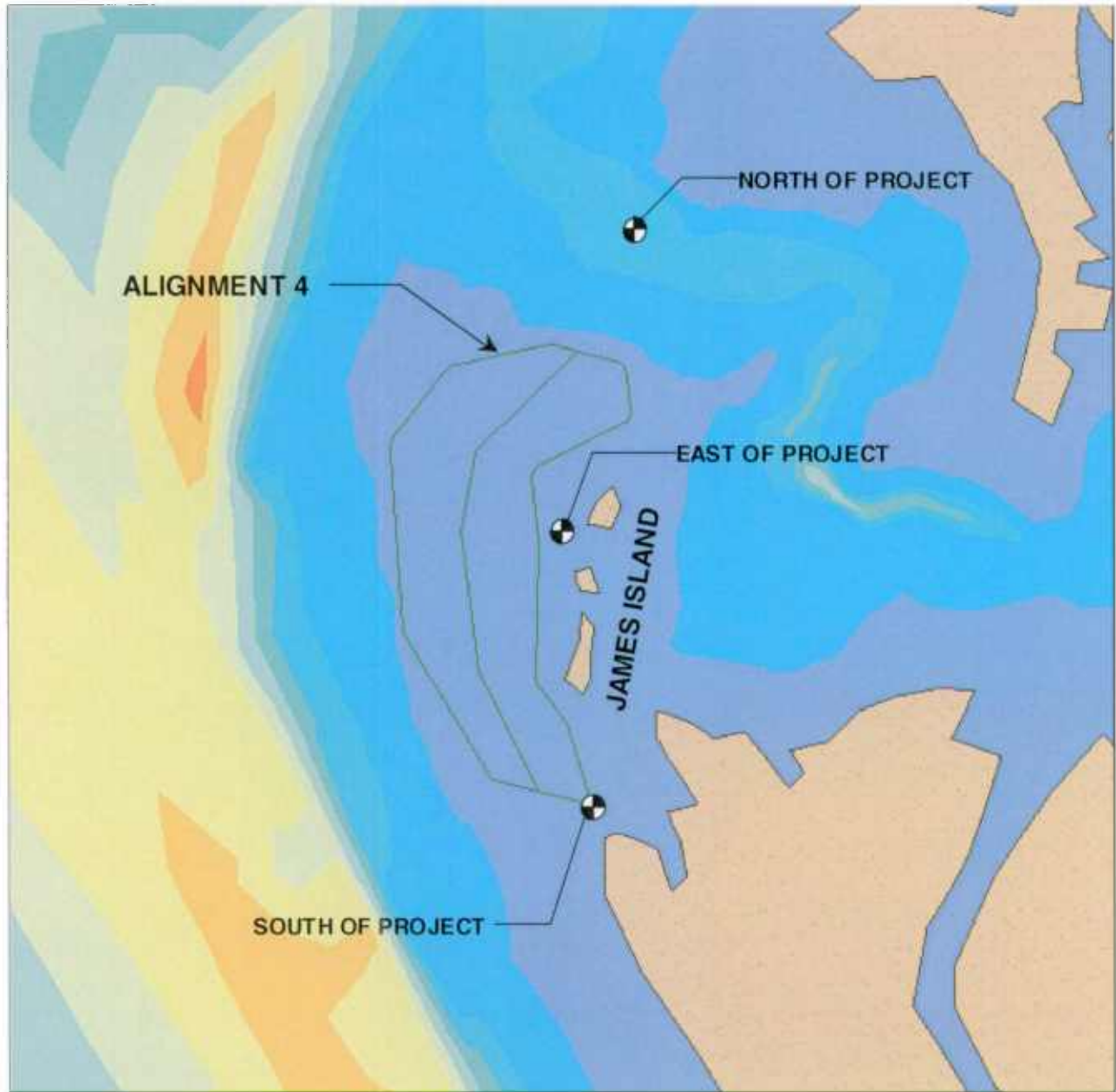


Figure 6-12: Peak Flood Current Velocity – Alignment 3 vs. Existing Conditions

1  
2  
3  
4  
5  
6  
7  
8  
9  
10  
11  
12  
13  
14  
15



16  
17  
18  
19  
20  
21  
22  
23

Figure 6-13: Results Comparison Locations for Alignment 4

1  
2  
3  
4  
5  
6  
7  
8  
9  
10  
11  
12  
13  
14  
15  
16  
17  
18  
19  
20  
21  
22  
23  
24  
25  
26  
27  
28  
29  
30  
31  
32  
33  
34  
35  
36  
37  
38

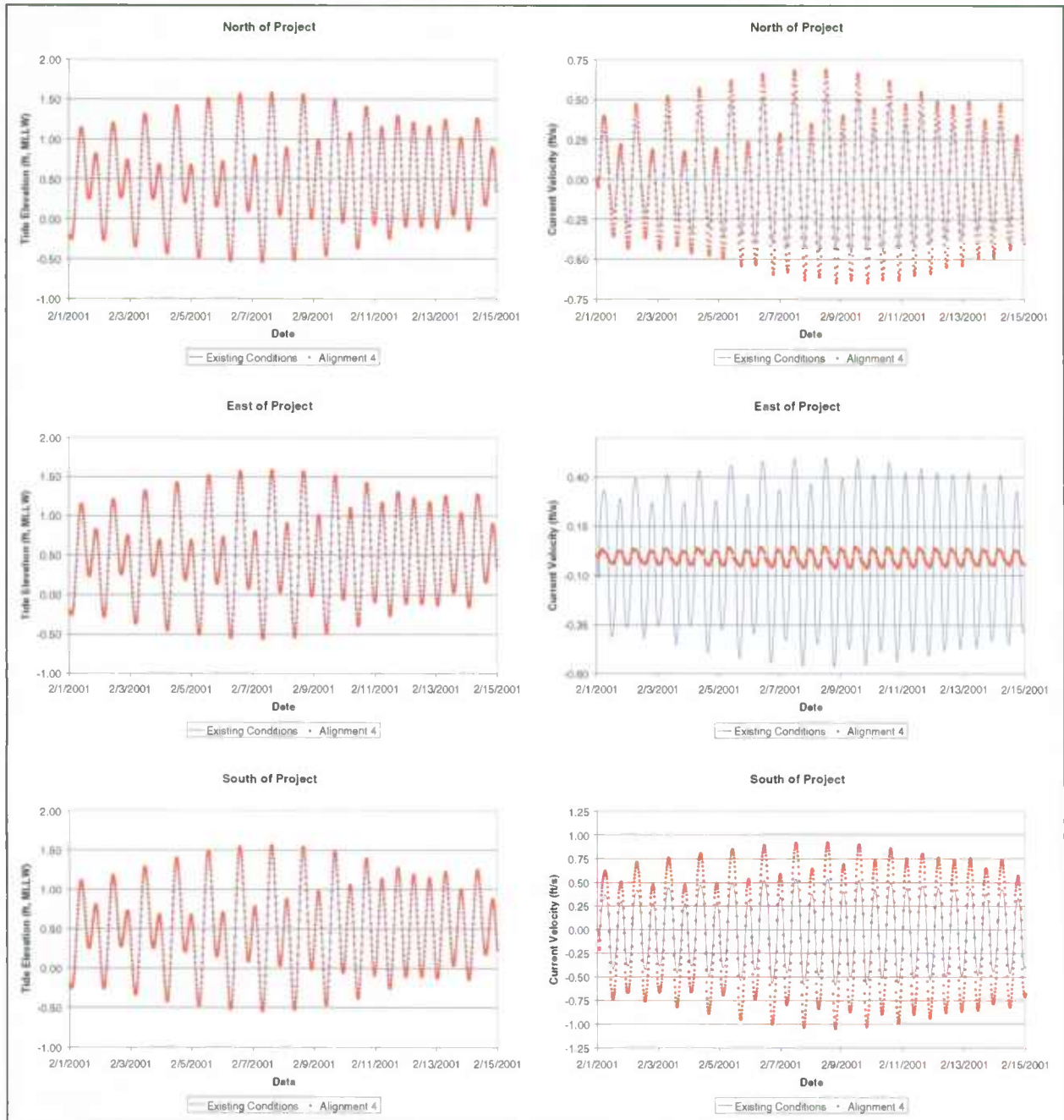


Figure 6-14: James Island Tidal Results Comparison for Alignment 4

1  
2  
3  
4  
5  
6  
7  
8  
9  
10  
11  
12  
13  
14  
15  
16  
17  
18  
19  
20  
21  
22  
23  
24  
25  
26  
27  
28  
29  
30  
31  
32  
33  
34  
35  
36  
37  
38  
39  
40  
41  
42  
43

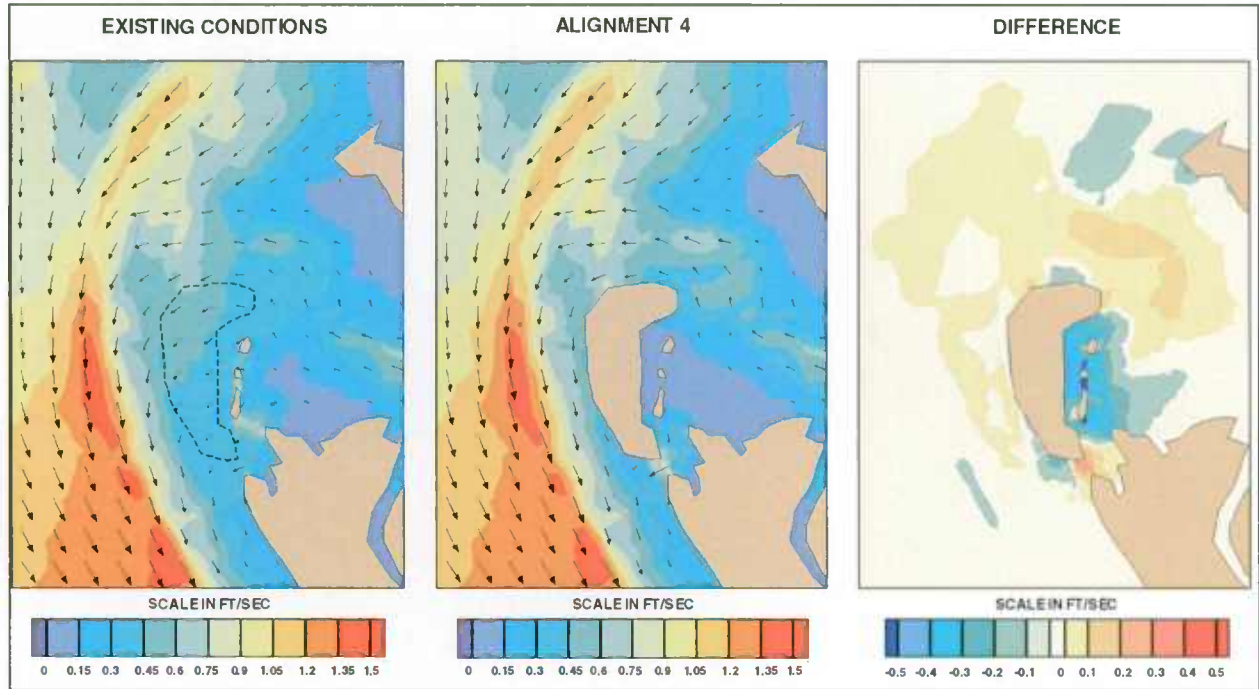


Figure 6-15: Peak Ebb Current Velocity – Alignment 4 vs. Existing Conditions

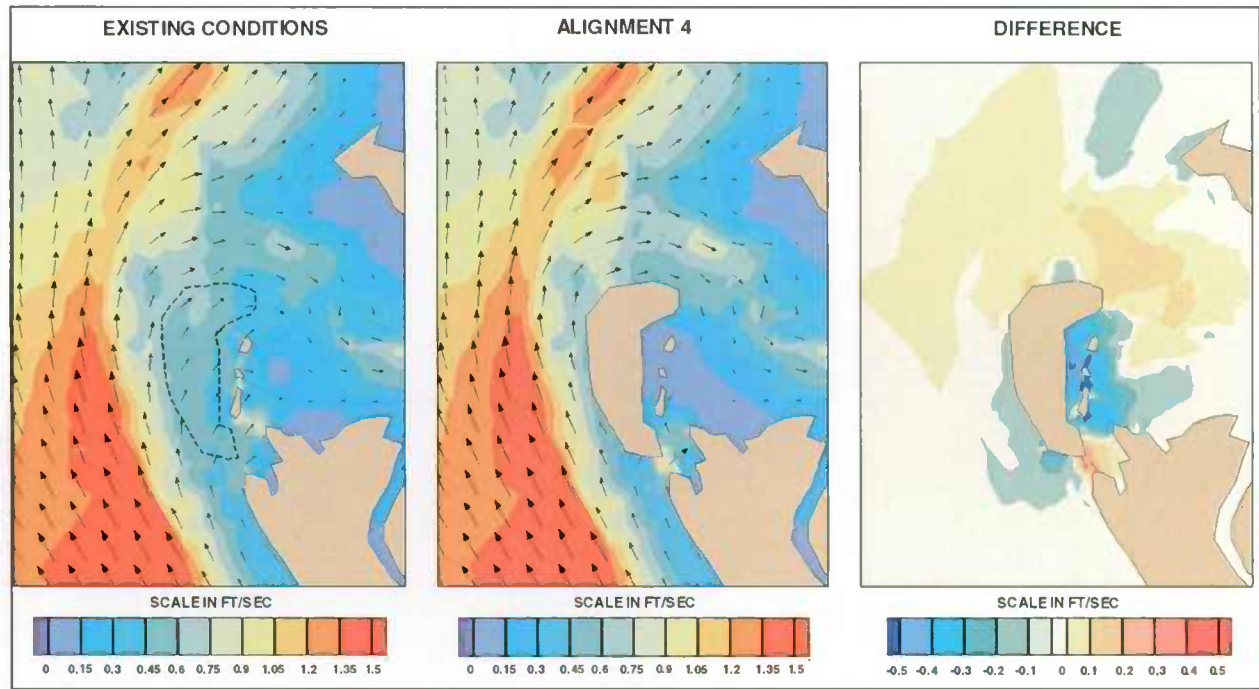


Figure 6-16: Peak Flood Current Velocity – Alignment 4 vs. Existing Conditions

1  
2  
3  
4  
5  
6  
7  
8  
9  
10  
11  
12  
13  
14  
15  
16  
17  
18  
19  
20  
21  
22  
23

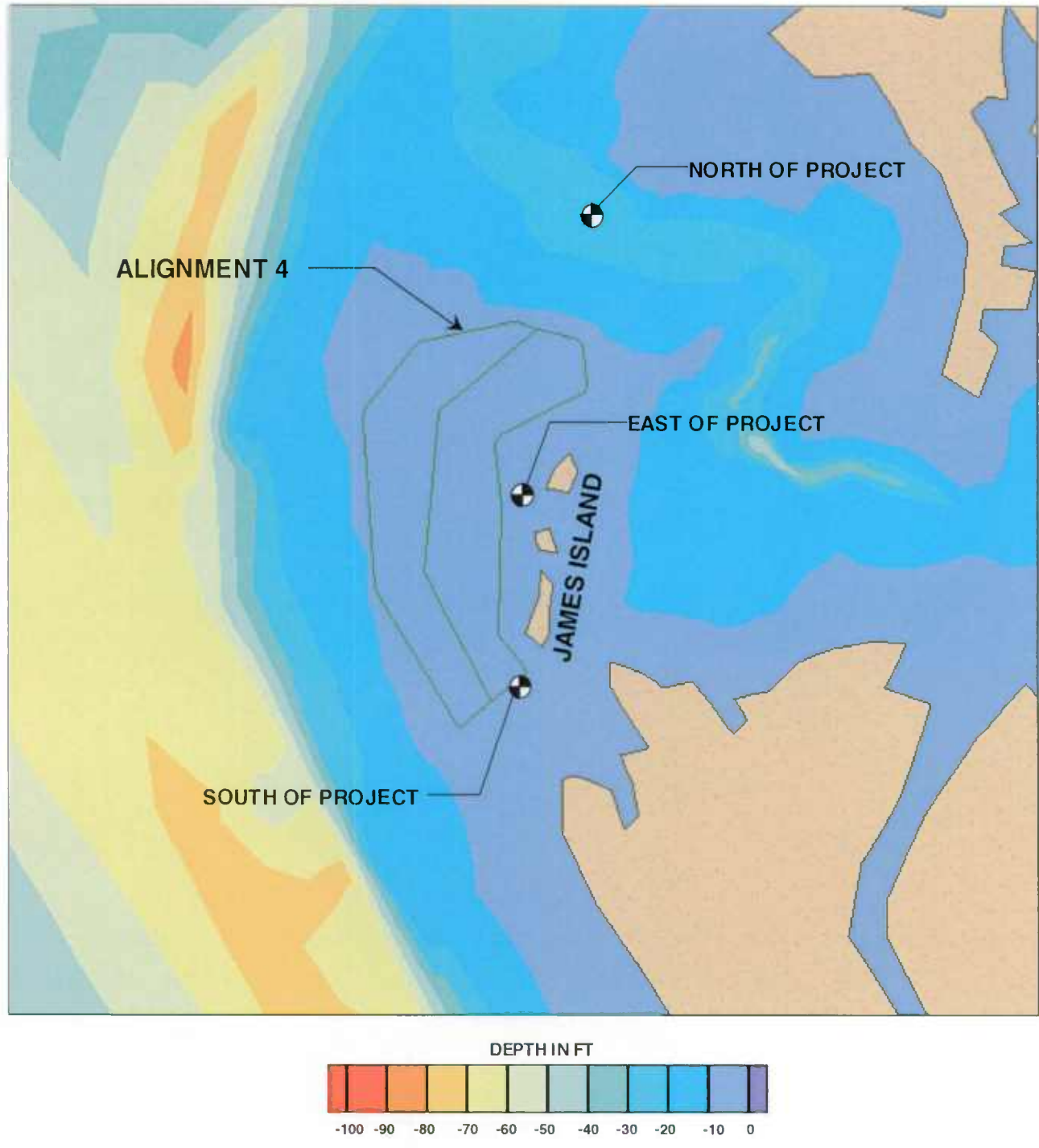


Figure 6-17: Results Comparison Locations for Alignment 5

1  
2  
3  
4  
5  
6  
7  
8  
9  
10  
11  
12  
13  
14  
15  
16  
17  
18  
19  
20  
21  
22  
23  
24  
25  
26  
27  
28  
29  
30  
31  
32  
33  
34  
35  
36  
37  
38  
39  
40  
41  
42

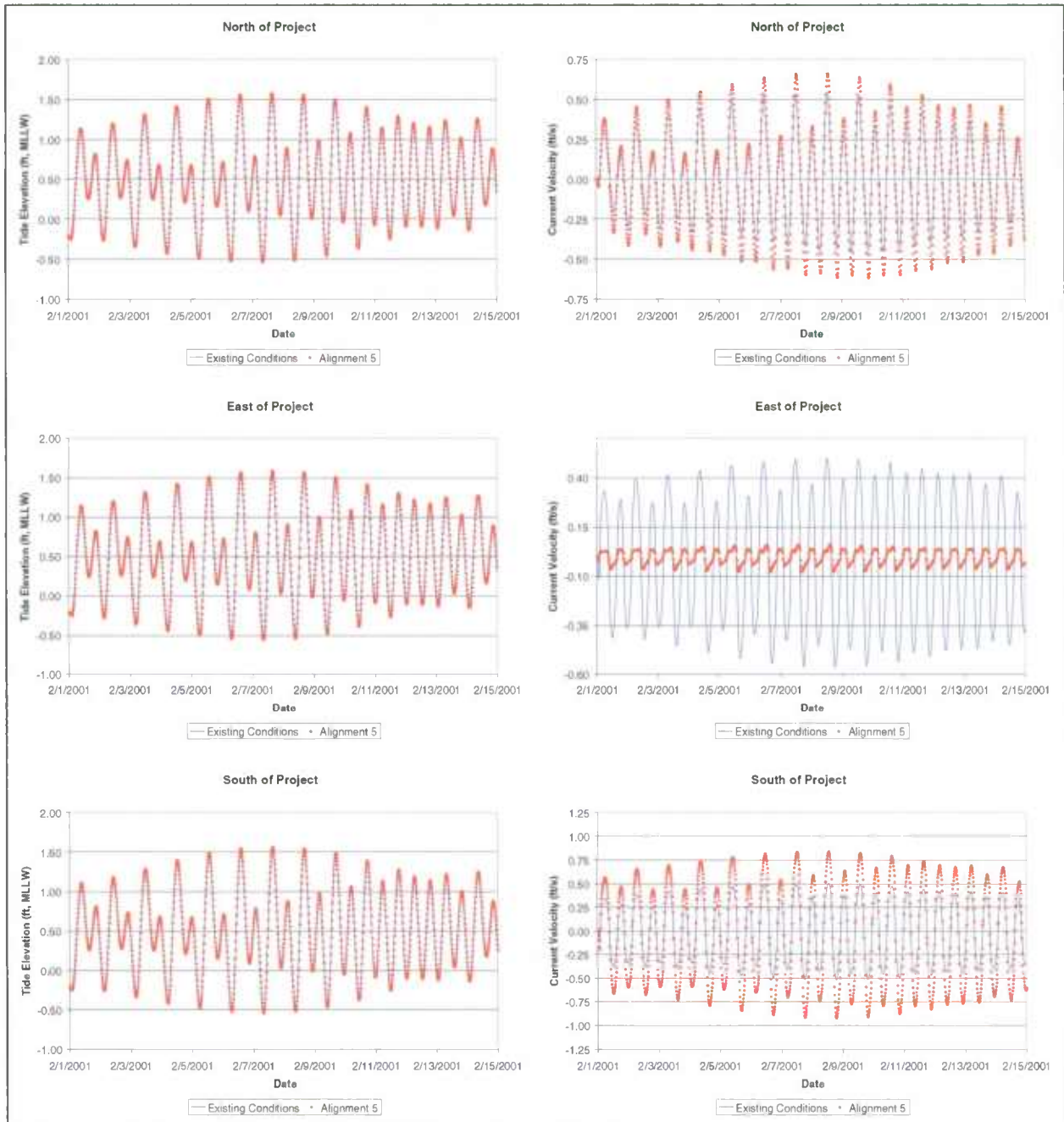


Figure 6-18: James Island Tidal Results Comparison for Alignment 5

1  
2  
3  
4  
5  
6  
7  
8  
9  
10  
11  
12  
13  
14  
15  
16  
17  
18  
19  
20  
21  
22  
23  
24  
25  
26  
27  
28  
29  
30  
31  
32  
33  
34  
35  
36  
37  
38  
39  
40  
41

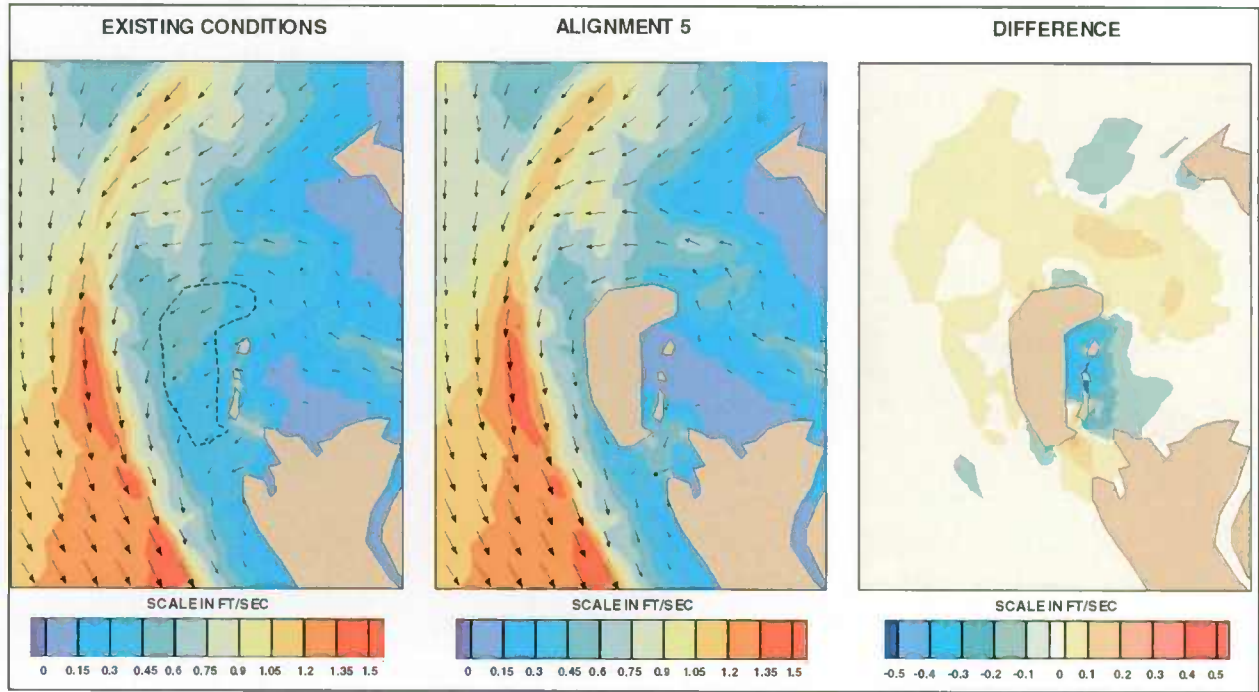


Figure 6-19: Peak Ebb Current Velocity – Alignment 5 vs. Existing Conditions

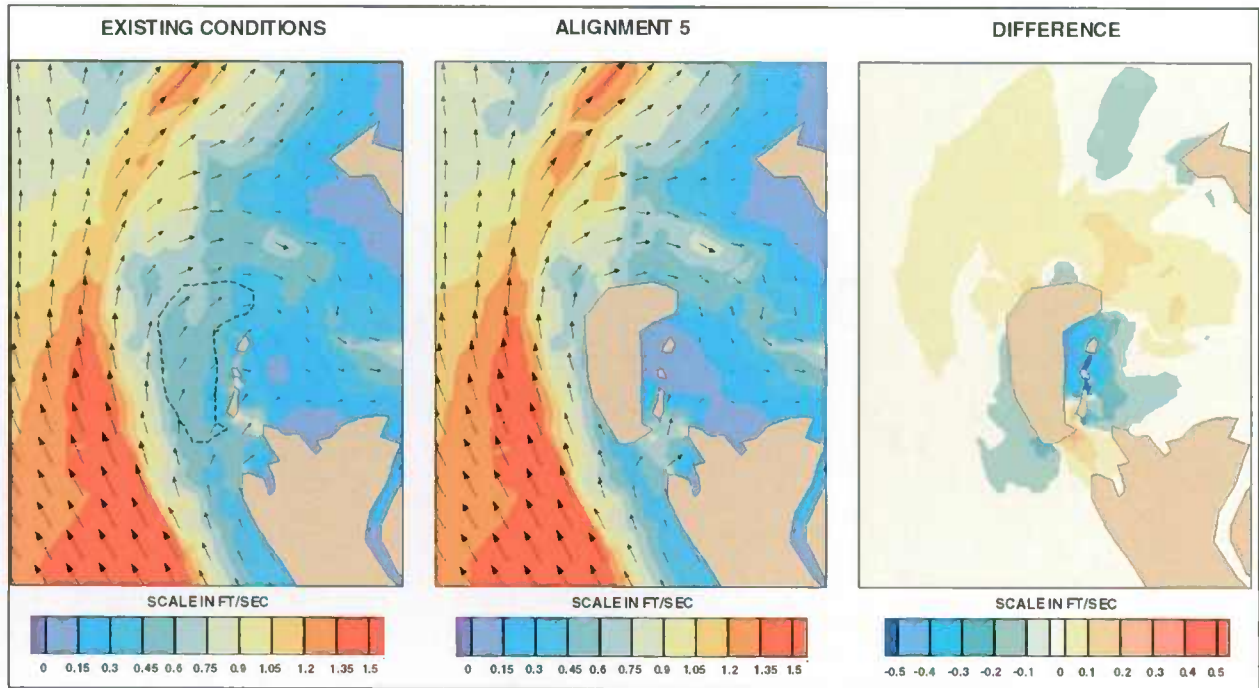


Figure 6-20: Peak Flood Current Velocity – Alignment 5 vs. Existing Conditions

## 7. SEDIMENTATION MODELING RESULTS

### 7.1 GENERAL

The UCB-FEM sedimentation model was used to examine transport of non-cohesive and cohesive materials (i.e. sand and clay) which characterize sediment in the vicinity of the project site. Detailed sediment data for the vicinity of James Island were not available so the model was used empirically by running the model to dynamic equilibrium as discussed in Section 5.3 and interpreting the results with a normalized unit scale. Examination of model results for both non-cohesive and cohesive sediments indicates that normal tidal currents are insufficient to directly cause sediment suspension and transport. Wind generated waves increase bottom shear stresses significantly and can cause sediment suspension. Various wind speeds were modeled and 16-mph winds were determined to be the minimum necessary to cause sediment suspension and transport for non-cohesive sediments. Thirteen-mph winds were the minimum necessary to cause substantial sediment suspension and transport for cohesive sediments.

Numerical modeling analyses indicate that sedimentation in the vicinity of James Island is affected by the construction of the project. Results of the UCB-FEM sedimentation model simulations are compared visually for the entire project vicinity.

The UCB-FEM sedimentation model was run for each alignment as well as existing conditions starting each simulation with the same initial conditions. The following sections describe the impacts of each habitat construction alignment on sedimentation. Results have been normalized to a unitless scale due to the empirical use of the sedimentation model as a result of insufficient local calibration data. Cohesive sediments have properties (shape, plasticity, electric charge) that cause the particles to remain in suspension for relatively long periods of time before they settle out, resulting in a larger area affected by sedimentation and erosion than for non-cohesive sediments.

### 7.2 ALTERNATIVE 1 IMPACTS

Non-cohesive and cohesive sediment model results for Alternative 1 are presented in Figures 7-1

1 through 7-6.

### 2 7.2.1 Non-Cohesive Sediment

3 Figures 7-1 through 7-3 show sedimentation modeling results for 0.004 inch non-cohesive  
4 sediments for 16-mph NNW, SSE and WNW winds, respectively. Comparison of sedimentation  
5 patterns with bathymetry shows that the areas of erosion correspond to shallow water depths  
6 while deposition occurs in adjacent deep water areas.

7 Construction of Alternative 1 would interrupt the long NNW wind fetch from across the Bay,  
8 thereby reducing erosion in the project area as shown in Figure 7-1. Figure 7-1 shows a large  
9 area south of the project extending to and along the shoreline of Taylors Island where erosion of  
10 the shallow water is reduced. The difference plot of Figure 7-1 shows a yellow to orange area  
11 (labeled more sediment on the scale) that represents areas that are eroding under existing  
12 conditions would have reduced or no erosion for the with-project conditions.

13 For winds from the SSE, construction of Alternative 1 would also interrupt a large portion of the  
14 long wind fetch, reducing the rates of erosion and accretion James Island as shown in the  
15 difference plot of Figure 7-2. The orange to red region along the west dike labeled as more  
16 sediment represents an area that is currently eroding would become an accretion area. The  
17 difference plot also shows areas labeled less sediment (green) where accretion is reduced that is  
18 due to the reduced erosion of the shallow areas, and subsequently less sediment in the water  
19 column.

20 Figure 7-3 shows results from construction of Alternative 1 for winds from the WNW. This  
21 figure shows that less erosion occurs for these winds, as the fetch length is much less. The with-  
22 project plot and difference plot in Figure 7-3 shows reduced erosion of areas around James  
23 Island and near the northern tip of Taylors Island.

### 24 7.2.2 Cohesive Sediment

25 Figures 7-4 through 7-6 show sedimentation modeling results for cohesive sediments for 13-mph  
26 NNW, SSE, and WNW winds, respectively. Figure 7-4 shows a significant reduction in erosion  
27 in the project area following construction, plus significantly more sediment accretion in the lee

1 of the project, extending south to Taylors Island. Of interest to note in the difference plot is a  
2 bluish area labeled less sediment southeast James Island, which is actually a reduction in  
3 accretion. Figure 7-5 shows modeling results for 13-mph SSE winds. The difference plot in this  
4 figure shows less erosion in addition to accretion north of the project, plus reduced accretion east  
5 of the project. Figure 7-6 shows modeling results for 13-mph WNW winds. This figure shows  
6 that current erosion around James Island would essentially be eliminated.

### 7 7.3 ALTERNATIVE 2 IMPACTS

8 Figures 7-7 through 7-9 show sedimentation modeling results for 0.004 inch non-cohesive  
9 sediments for 16-mph NNW, SSE and WNW winds, respectively. Comparison of sedimentation  
10 patterns with bathymetry shows that the areas of erosion correspond to shallow water depths  
11 while deposition occurs in adjacent deep water areas.

12 Construction of Alternative 2 provides the most protection to James Island from the long NNW  
13 wind fetch from across the Bay, preventing erosion in the lee of the project as shown in Figure 7-  
14 7. Figure 7-7 shows that the large area south of the project extending to and along the shoreline  
15 of Taylors Island where erosion would be reduced upon construction of Alternative 1 is  
16 completely eliminated upon construction of Alternative 2. This is because Alignment 2 extends  
17 further to the west. The difference plot of Figure 7-7 shows that areas that are accreting under  
18 existing conditions would either erode or accrete less along the dikes exposed to the N, NW and  
19 W.

20 For winds from the SSE, construction of Alternative 2 would also interrupt a large portion of the  
21 long wind fetch, reducing the rates of erosion in the shallows around James Island. This results  
22 in reduced accretion, as indicated by the less sediment area as shown in the difference plot of  
23 Figure 7-8. Figure 7-9 shows results from construction of Alternative 2 for winds from the  
24 WNW. As for Alignment 1, this figure shows that less erosion occurs for these winds, as the  
25 fetch length is much less. The with-project plot and difference plot in Figure 7-9 shows reduced  
26 erosion of areas around James Island and near the northern tip of Taylors Island.

### 1 7.3.1 Cohesive Sediment

2 Figures 7-10 through 7-12 show sedimentation modeling results for cohesive sediments for 13-  
3 mph NNW, SSE, and WNW winds, respectively. Figure 7-10 shows a significant reduction in  
4 erosion in the project area following construction, plus significantly more sediment accretion in  
5 the lee of the project, extending south to Taylors Island. This area is greater than for Alternative  
6 1 as shown by the difference plot. Similarly to Alternative 1, in the difference plot is a bluish  
7 area labeled less sediment southeast James Island, which is actually a reduction in accretion.  
8 Figure 7-11 shows modeling results for 13-mph SSE winds. The difference plot in this figure  
9 shows less erosion in addition to accretion north of the project, plus reduced accretion east of the  
10 project. Once again, the area of impact is greater than for Alternative 1, although not to the same  
11 extent as for NNW winds. Figure 7-12 shows modeling results for 13-mph WNW winds. This  
12 figure shows that current erosion around James Island would essentially be eliminated.

## 13 7.4 ALTERNATIVE 3 IMPACTS

14 Non-cohesive and cohesive sediment model results for Alternative 3 are presented in Figures 7-  
15 13 through 7-18.

### 16 7.4.1 Non-Cohesive Sediment

17 Figures 7-13 through 7-15 show sedimentation modeling results for 0.004 inch non-cohesive  
18 sediments for 16-mph NNW, SSE and WNW winds, respectively. Comparison of sedimentation  
19 patterns with bathymetry shows that the areas of erosion correspond to shallow water depths  
20 while deposition occurs in adjacent deep water areas.

21 Construction of Alternative 3 would interrupt the long NNW wind fetch from across the Bay,  
22 thereby reducing erosion in the project area as shown in Figure 7-13. Figure 7-13 shows a large  
23 area south of the project extending to and along the shoreline of Taylors Island where erosion of  
24 the shallow water is reduced. Erosion would still occur along the west dikes of the project.

25 For winds from the SSE, construction of Alternative 3 would also interrupt a large portion of the  
26 long wind fetch, reducing the rates of erosion and accretion around James Island as shown in the  
27 difference plot of Figure 7-14. The orange to red region along the west dike labeled as more

1 sediment represents an area that is currently eroding would become an accretion area. The  
2 difference plot also shows areas labeled less sediment (green) where accretion is reduced that is  
3 due to the reduced erosion of the shallow areas, and subsequently less sediment in the water  
4 column.

5 Figure 7-15 shows results from construction of Alternative 3 for winds from the WNW. This  
6 figure shows that less erosion occurs for these winds, as the fetch length is much less. Similar to  
7 the other two alignments, the with-project plot and difference plot in Figure 7-15 shows reduced  
8 erosion of areas around James Island and near the northern tip of Taylors Island.

#### 9 **7.4.2 Cohesive Sediment**

10 Figures 7-16 through 7-18 show sedimentation modeling results for cohesive sediments for 13-  
11 mph NNW, SSE, and WNW winds, respectively. Figure 7-16 shows a significant reduction in  
12 erosion in the project area following construction, plus significantly more sediment accretion in  
13 the lee of the project, extending south to Taylors Island. This is similar to Alternative 1, where  
14 in the difference plot the bluish area labeled less sediment southeast James Island, which is  
15 actually a reduction in accretion. Figure 7-17 shows modeling results for 13-mph SSE winds.  
16 The difference plot in this figure shows less erosion in addition to accretion north of the project,  
17 plus reduced accretion east of the project. Figure 7-18 shows modeling results for 13-mph  
18 WNW winds. As for the other two alignments, erosion around James Island due to WNW winds  
19 would essentially be eliminated.

### 20 **7.5 ALTERNATIVE 4 IMPACTS**

21 Non-cohesive and cohesive sediment model results for Alternative 4 are presented in Figures 7-  
22 19 through 7-24.

#### 23 **7.5.1 Non-Cohesive Sediment**

24 Figures 7-19 through 7-21 show sedimentation modeling results for 0.004 inch non-cohesive  
25 sediments for 16-mph NNW, SSE and WNW winds, respectively. Comparison of sedimentation  
26 patterns with bathymetry shows that the areas of erosion correspond to shallow water depths

1 while deposition occurs in adjacent deep water areas. Sedimentation changes due to construction  
2 of this alignment are similar to that for Alignment 2 and 5.

3 Construction of Alternative 4 would interrupt the long NNW wind fetch from across the Bay,  
4 thereby reducing erosion in the project area as shown in Figure 7-19. Figure 7-19 shows a large  
5 area south of the project extending to and along the shoreline of Taylors Island where erosion of  
6 the shallow water is reduced. The difference plot of Figure 7-19 shows a yellow to orange area  
7 (labeled more sediment on the scale) that represents areas that are eroding under existing  
8 conditions would have reduced or no erosion for the with-project conditions.

9 For winds from the SSE, construction of Alternative 4 would also interrupt a large portion of the  
10 long wind fetch, reducing the rates of erosion and accretion James Island as shown in the  
11 difference plot of Figure 7-20. The orange to red region along the west dike labeled as more  
12 sediment represents an area that is currently eroding would become an accretion area. The  
13 difference plot also shows areas labeled less sediment (green) where accretion is reduced that is  
14 due to the reduced erosion of the shallow areas, and subsequently less sediment in the water  
15 column.

16 Figure 7-21 shows results from construction of Alternative 4 for winds from the WNW.

### 17 **7.5.2 Cohesive Sediment**

18 Figures 7-22 through 7-24 show sedimentation modeling results for cohesive sediments for 13-  
19 mph NNW, SSE, and WNW winds, respectively. Figure 7-22 shows a significant reduction in  
20 erosion in the project area following construction, plus significantly more sediment accretion in  
21 the lee of the project, extending south to Taylors Island. Results are similar to Alignment 2, but  
22 over less area. The same bluish area southeast of James Island labeled less sediment is a  
23 reduction in accretion. Figure 7-23 shows modeling results for 13-mph SSE winds. The  
24 difference plot in this figure shows less erosion in addition to accretion north of the project, plus  
25 reduced accretion east of the project. Figure 7-24 shows modeling results for 13-mph WNW  
26 winds, which also show that current erosion around James Island would essentially be  
27 eliminated.

## 1 7.6 ALTERNATIVE 5 IMPACTS

2 Non-cohesive and cohesive sediment model results for Alternative 5 are presented in Figures 7-  
3 25 through 7-30.

### 4 7.6.1 Non-Cohesive Sediment

5 Figures 7-25 through 7-27 show sedimentation modeling results for 0.004 inch non-cohesive  
6 sediments for 16-mph NNW, SSE and WNW winds, respectively. Comparison of sedimentation  
7 patterns with bathymetry shows that the areas of erosion correspond to shallow water depths  
8 while deposition occurs in adjacent deep water areas. Sedimentation changes are similar to  
9 Alignment 2 and 4.

10 Construction of Alternative 5 would interrupt the long NNW wind fetch from across the Bay,  
11 thereby reducing erosion in the project area as shown in Figure 7-25. Figure 7-25 shows a large  
12 area south of the project extending to and along the shoreline of Taylors Island where erosion of  
13 the shallow water is reduced. The difference plot of Figure 7-25 shows a yellow to orange area  
14 (labeled more sediment on the scale) that represents areas that are eroding under existing  
15 conditions would have no erosion for the with-project conditions.

16 For winds from the SSE, construction of Alternative 5 would also interrupt a large portion of the  
17 long wind fetch, reducing the rates of erosion and accretion James Island as shown in the  
18 difference plot of Figure 7-26. The orange to red region along the west dike labeled as more  
19 sediment represents an area that is currently eroding would become an accretion area. The  
20 difference plot also shows areas labeled less sediment (green and blue) where accretion is  
21 reduced that is due to the reduced erosion of the shallow areas, and subsequently less sediment in  
22 the water column.

23 Figure 7-27 shows results from construction of Alternative 5 for winds from the WNW. Results  
24 are similar to the previous alignments and show reduced erosion of areas around James Island  
25 and near the northern tip of Taylors Island.

1 **7.6.2 Cohesive Sediment**

2 Figures 7-28 through 7-30 show sedimentation modeling results for cohesive sediments for 13-  
3 mph NNW, SSE, and WNW winds, respectively. Figure 7-28 shows a significant reduction in  
4 erosion in the project area following construction, plus significantly more sediment accretion in  
5 the lee of the project, extending south to Taylors Island. Similar to all alignments, the difference  
6 plot shows a bluish area labeled less sediment southeast James Island that is a reduction in  
7 accretion. Figure 7-29 shows modeling results for 13-mph SSE winds. The difference plot in  
8 this figure shows less erosion in addition to accretion north of the project, plus reduced accretion  
9 east of the project. Figure 7-30 shows modeling results for 13-mph WNW winds that indicate  
10 erosion around James Island would essentially be eliminated.

11  
12  
13  
14

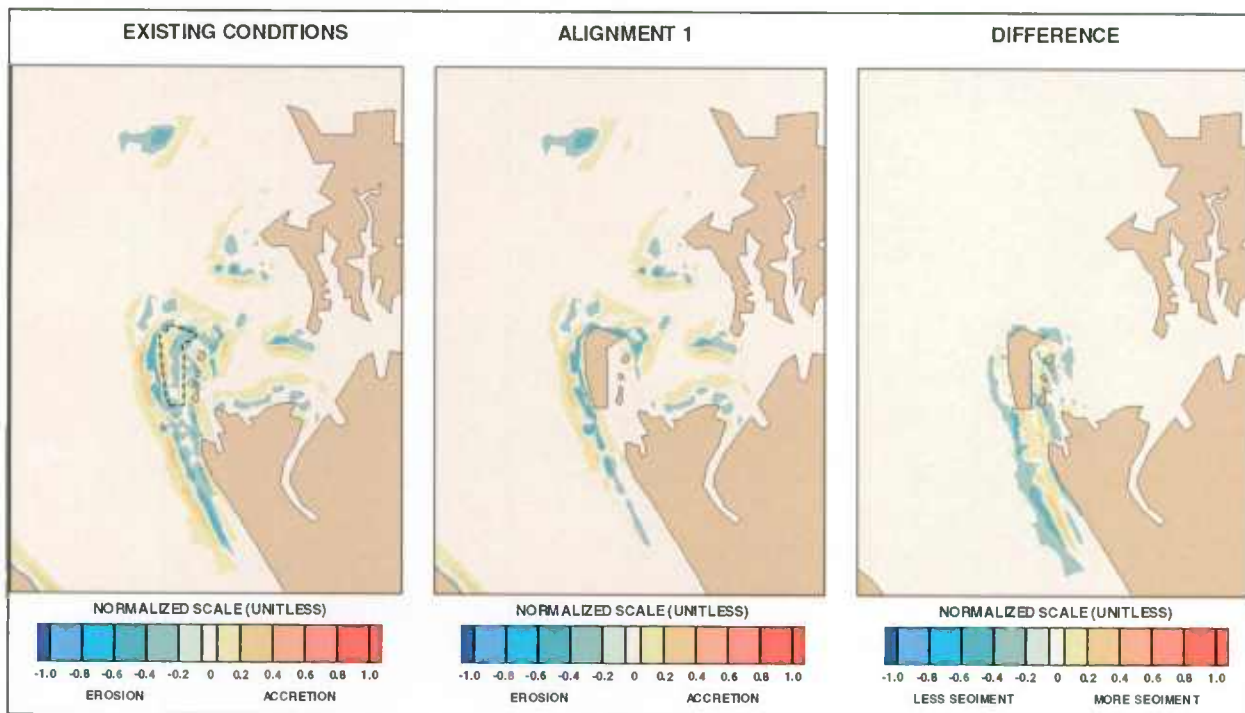


Figure 7-1: Non-Cohesive Sediment – North-Northwest Wind 16 mph – Alignment 1 vs. Existing Conditions

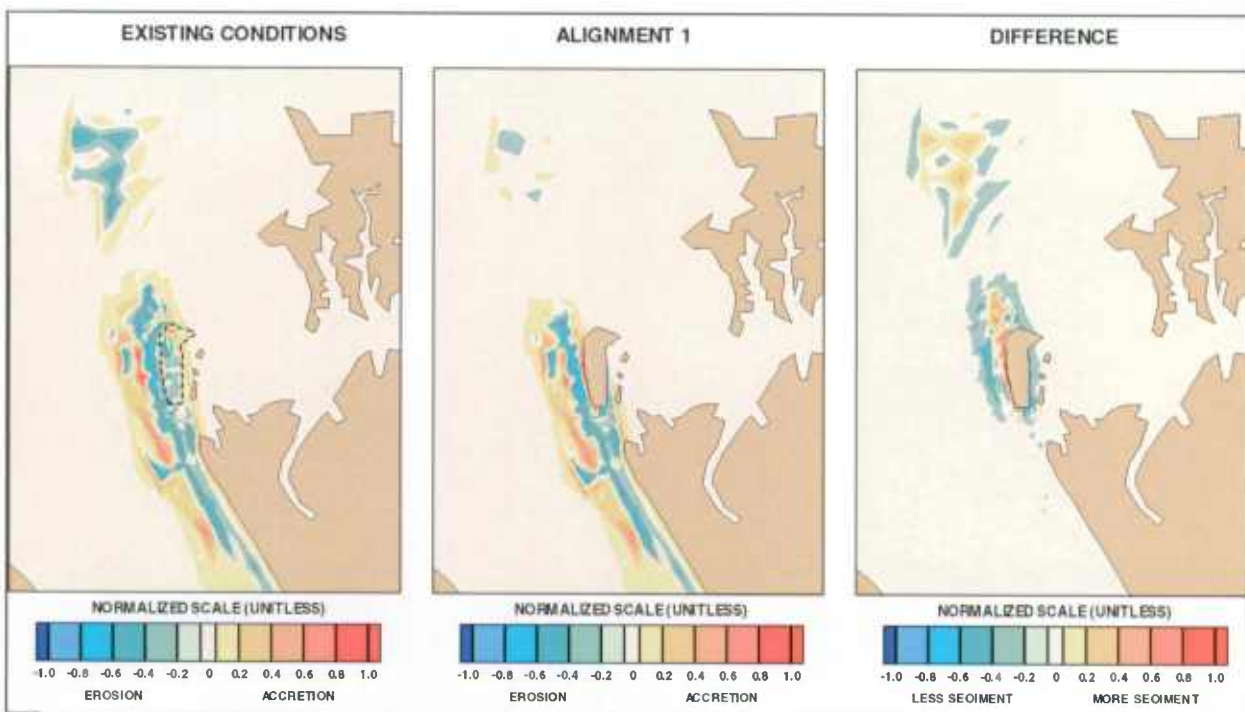


Figure 7-2: Non-Cohesive Sediment – South-Southeast Wind 16 mph – Alignment 1 vs. Existing Conditions

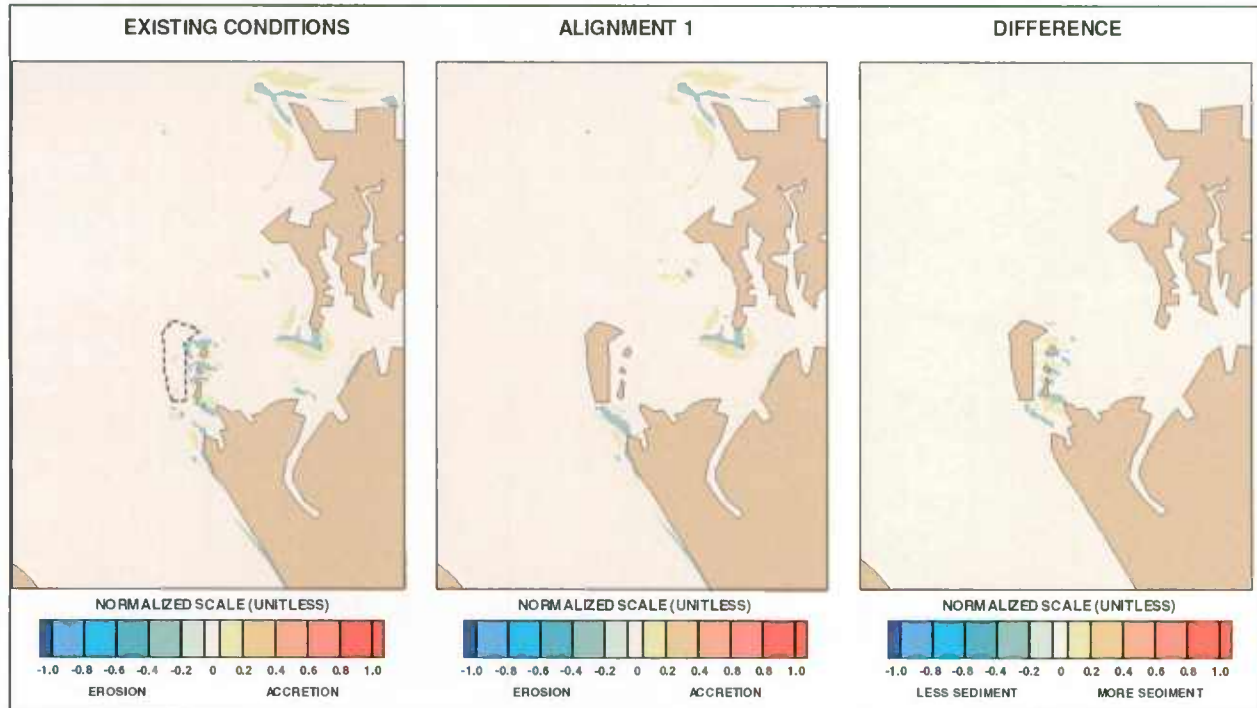


Figure 7-3: Non-Cohesive Sediment – West -Northwest Wind 16 mph – Alignment 1 vs. Existing Conditions

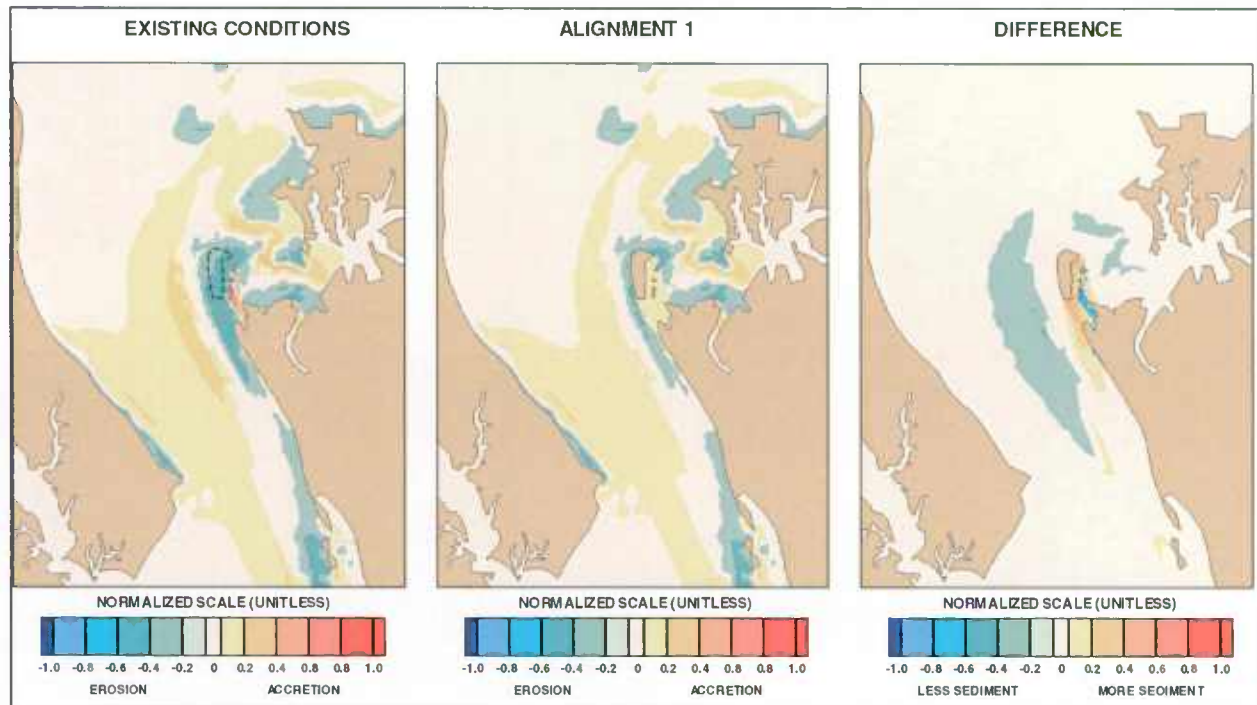


Figure 7-4: Cohesive Sediment – North-Northwest Wind 13 mph Alignment 1 vs. Existing Conditions

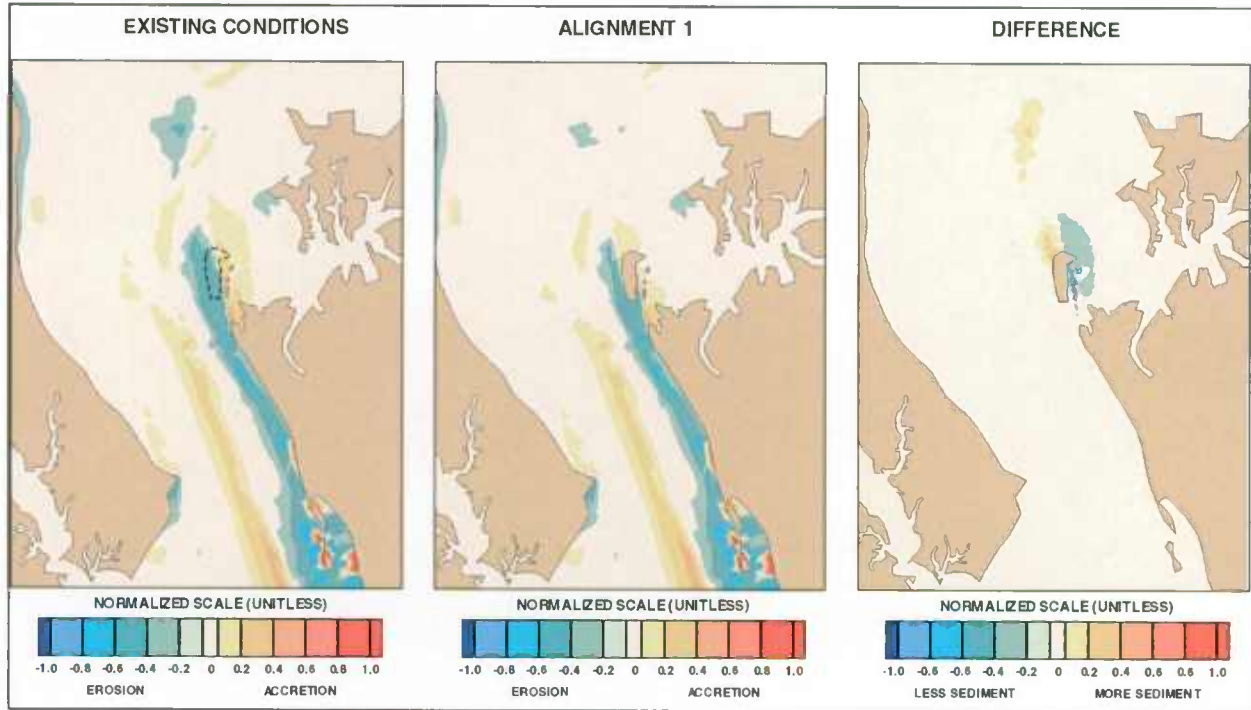


Figure 7-5: Cohesive Sediment – South-Southeast Wind 13 mph – Alignment 1 vs. Existing Conditions

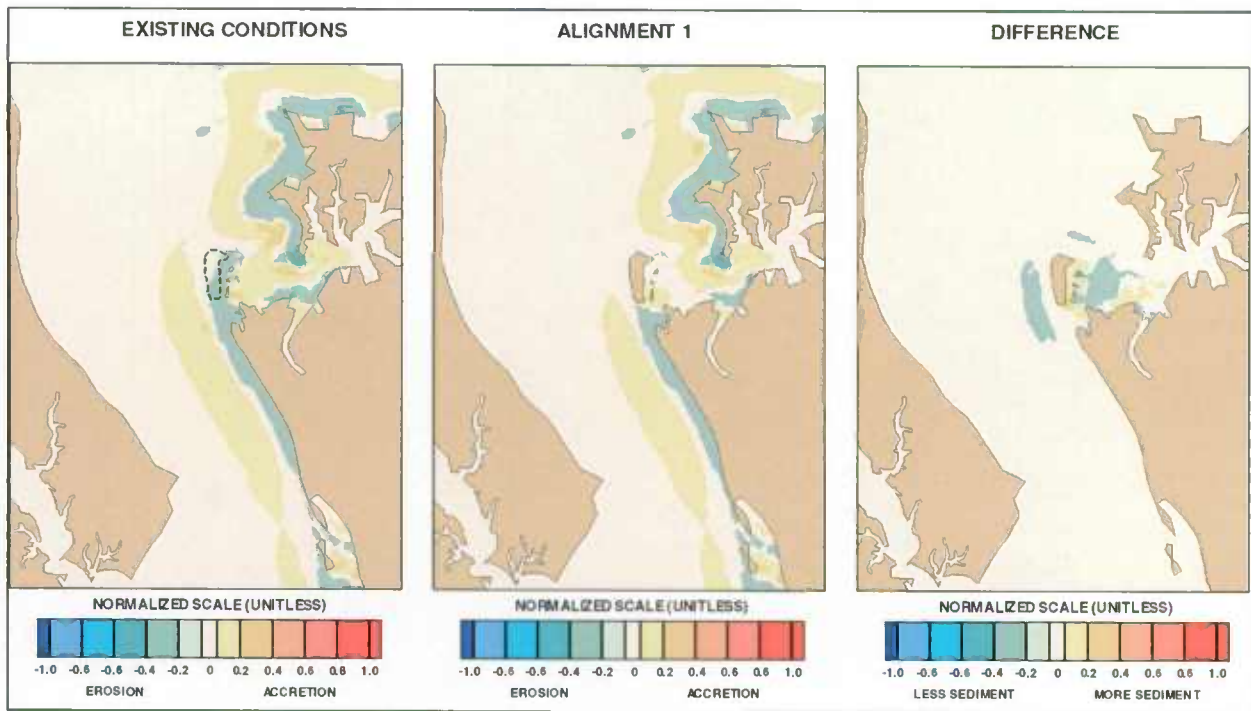


Figure 7-6: Cohesive Sediment – West-Northwest Wind 13 mph – Alignment 1 vs. Existing Conditions

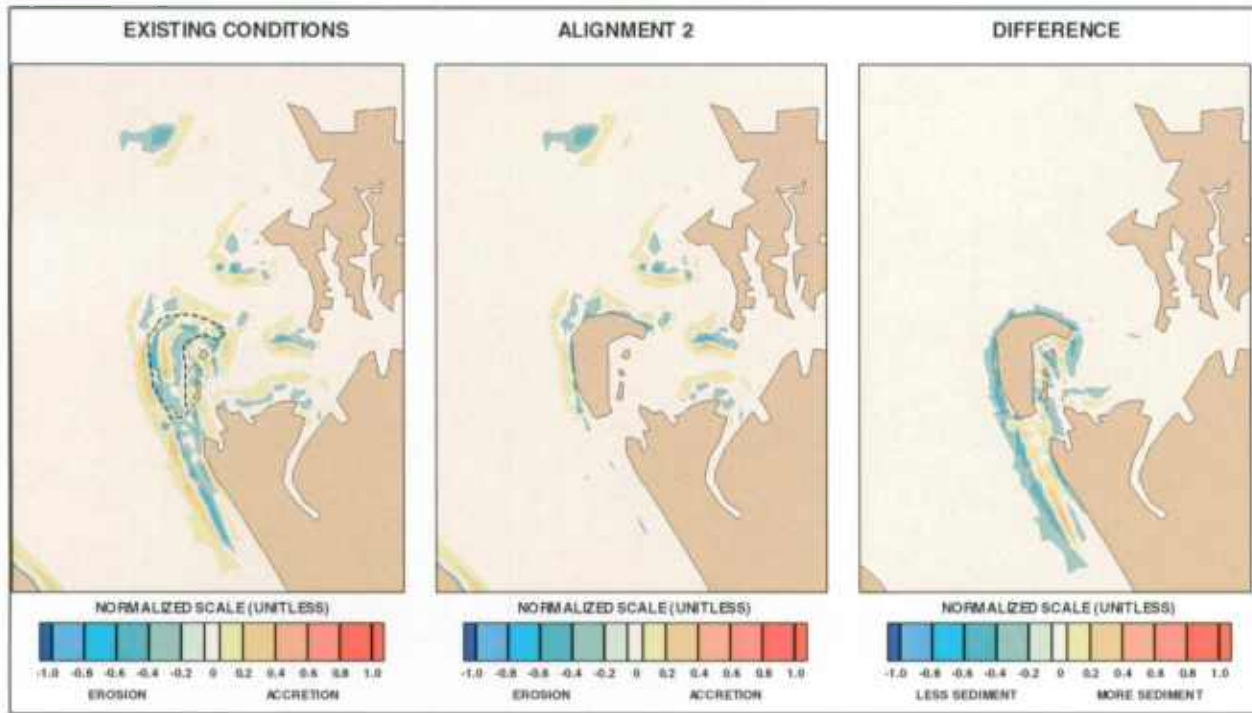


Figure 7-7: Non-Cohesive Sediment – North-Northwest Wind 16 mph – Alignment 2 vs. Existing Conditions

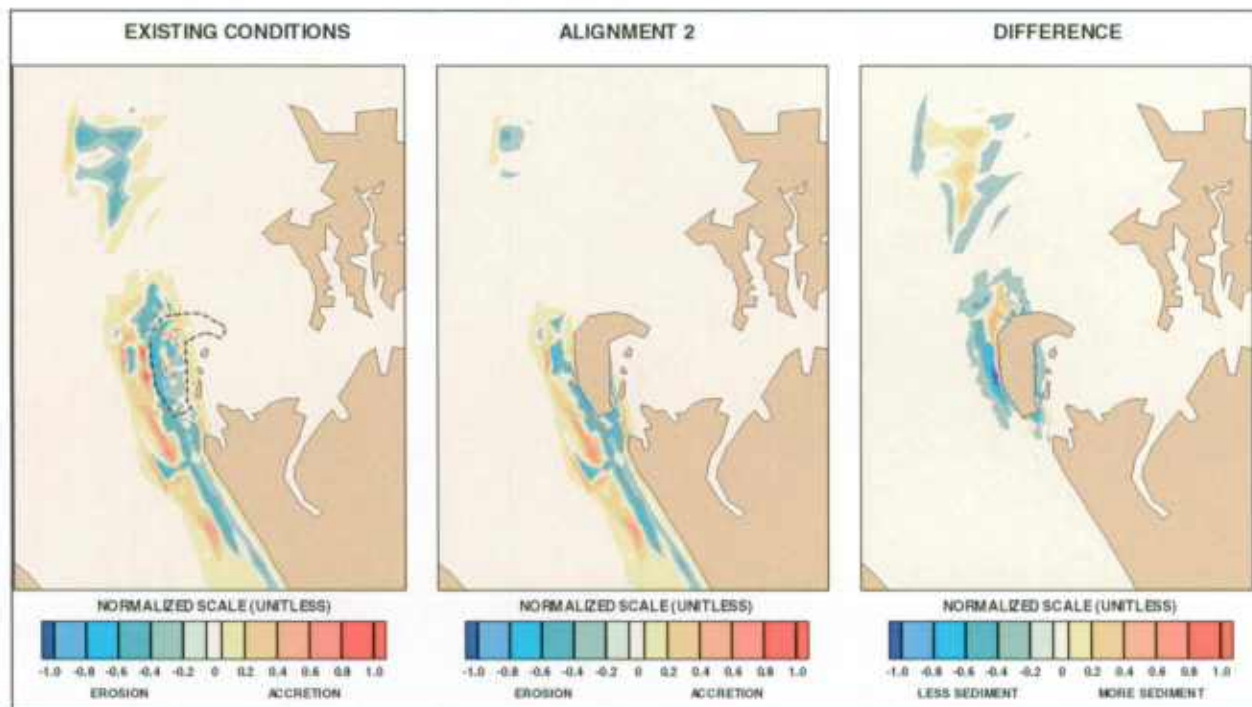


Figure 7-8: Non-Cohesive Sediment – South-Southeast Wind 16 mph – Alignment 2 vs. Existing Conditions

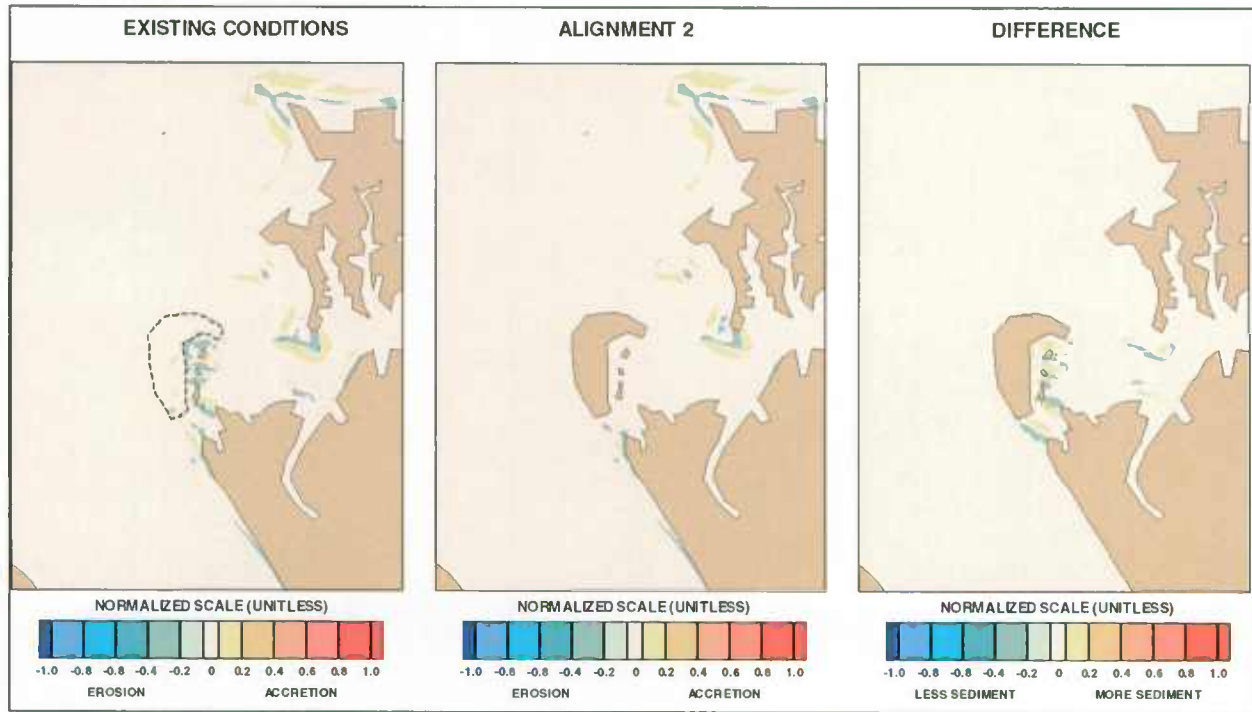


Figure 7-9: Non-Cohesive Sediment – West -Northwest Wind 16 mph – Alignment 2 vs. Existing Conditions

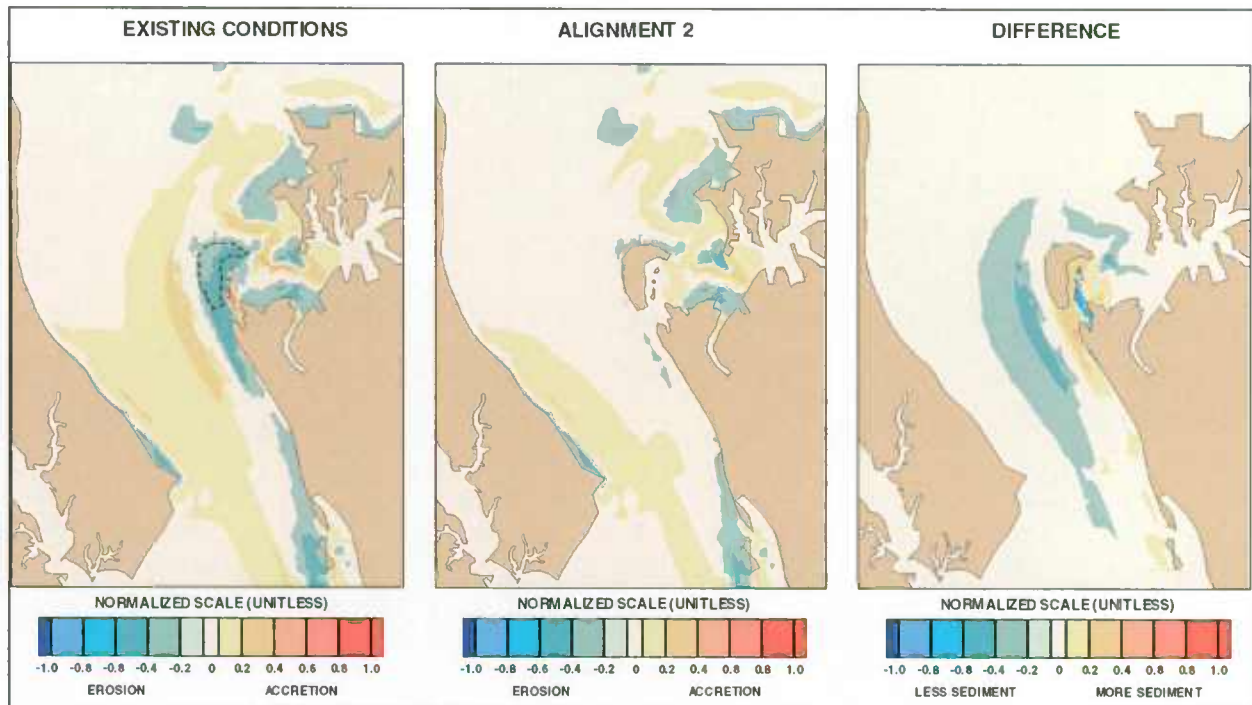


Figure 7-10: Cohesive Sediment – North-Northwest Wind 13 mph Alignment 2 vs. Existing Conditions

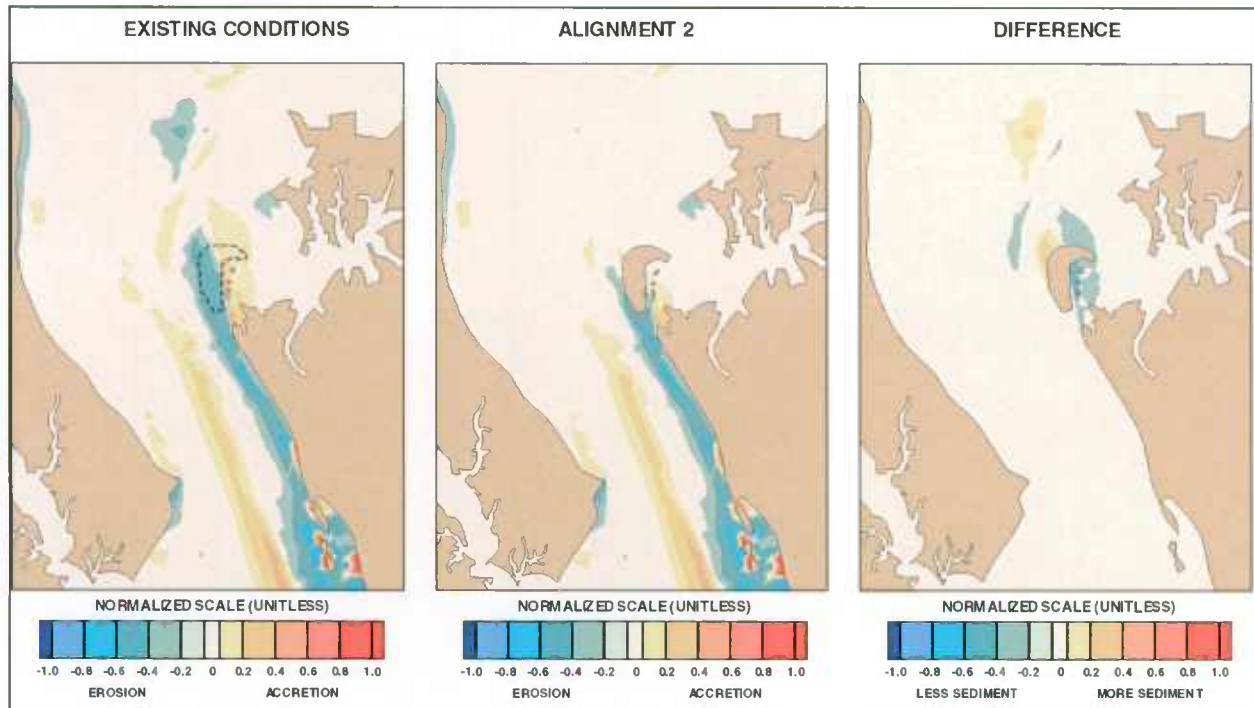


Figure 7-11: Cohesive Sediment – South-Southeast Wind 13 mph – Alignment 2 vs. Existing Conditions

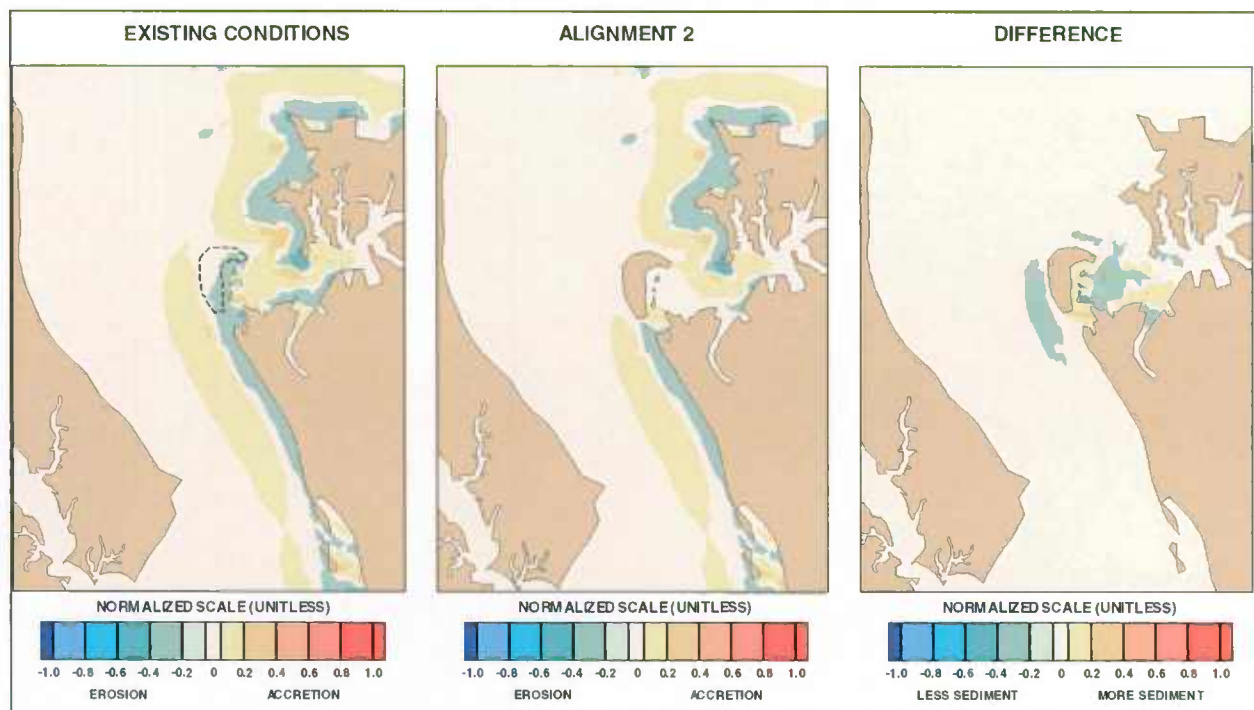


Figure 7-12: Cohesive Sediment – West-Northwest Wind 13 mph – Alignment 2 vs. Existing Conditions

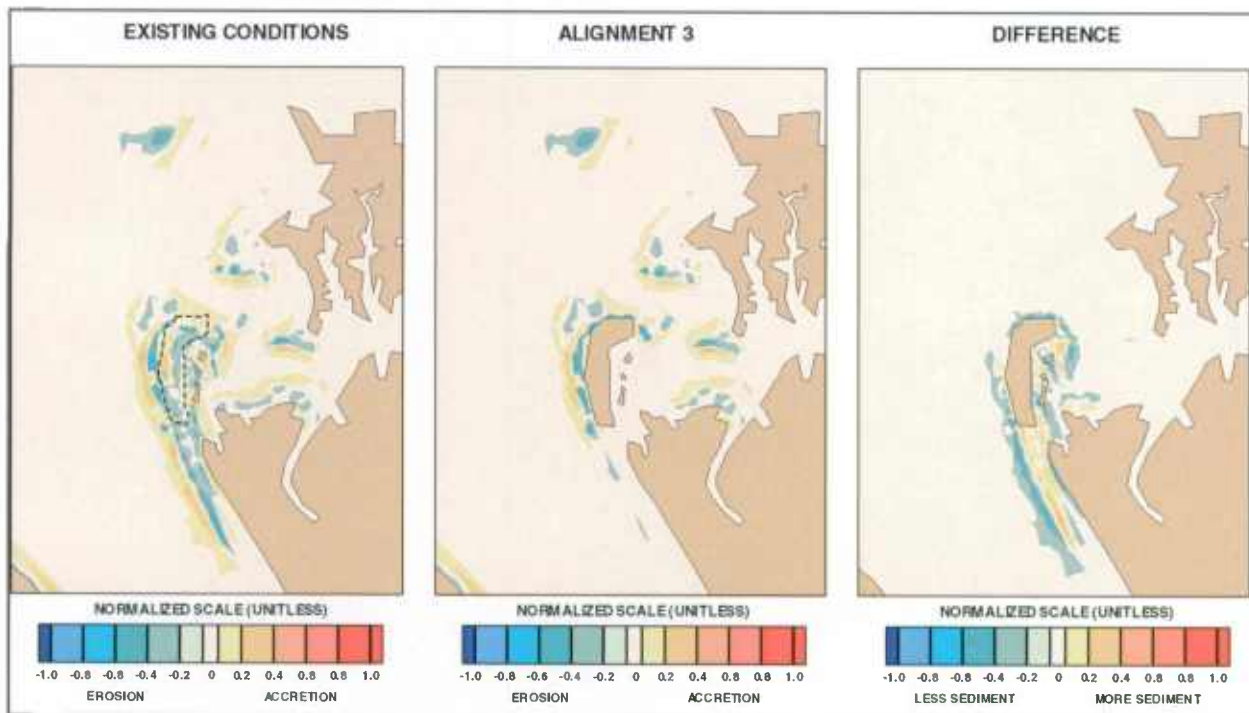


Figure 7-13: Non-Cohesive Sediment – North-Northwest Wind 16 mph – Alignment 3 vs. Existing Conditions

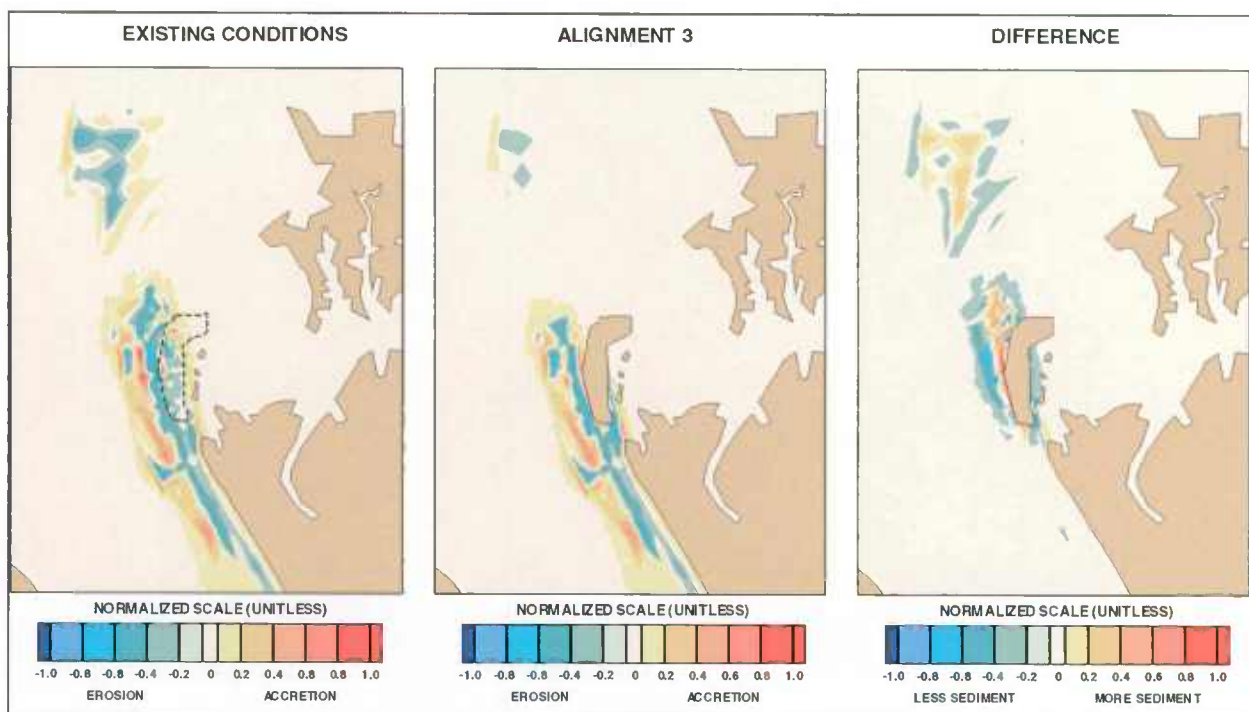


Figure 7-14: Non-Cohesive Sediment – South-Southeast Wind 16 mph – Alignment 3 vs. Existing Conditions

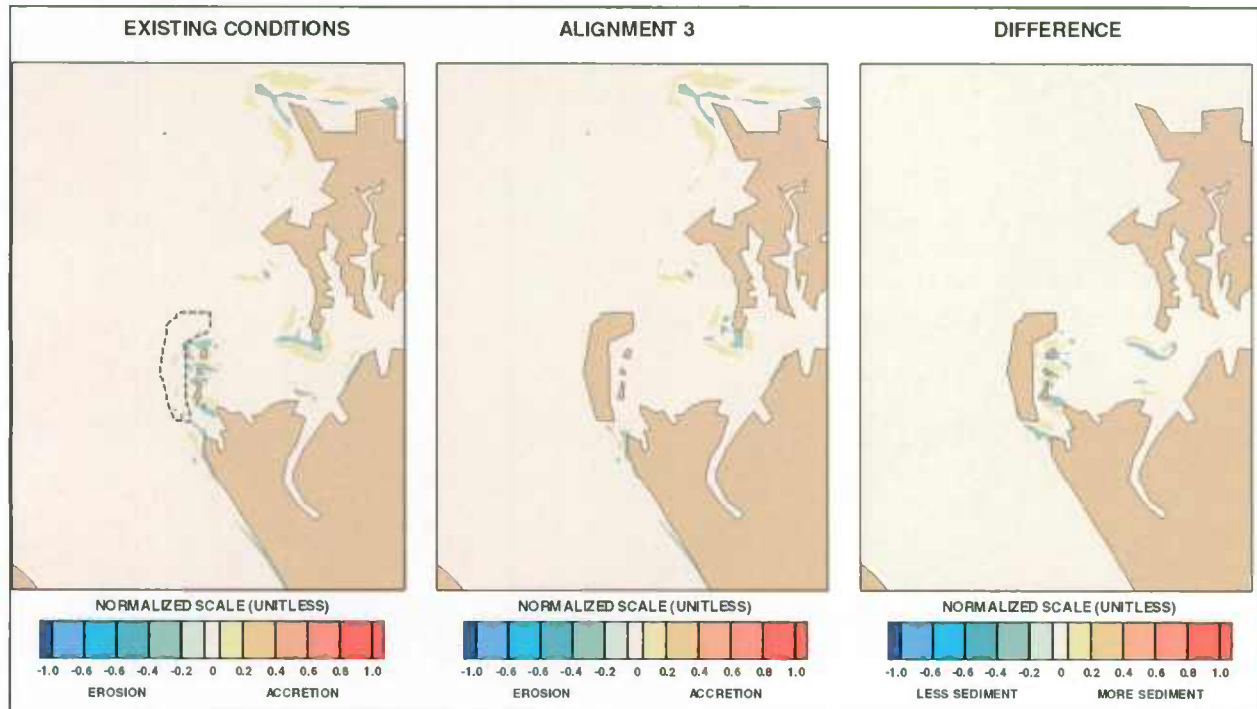


Figure 7-15: Non-Cohesive Sediment – West -Northwest Wind 16 mph – Alignment 3 vs. Existing Conditions

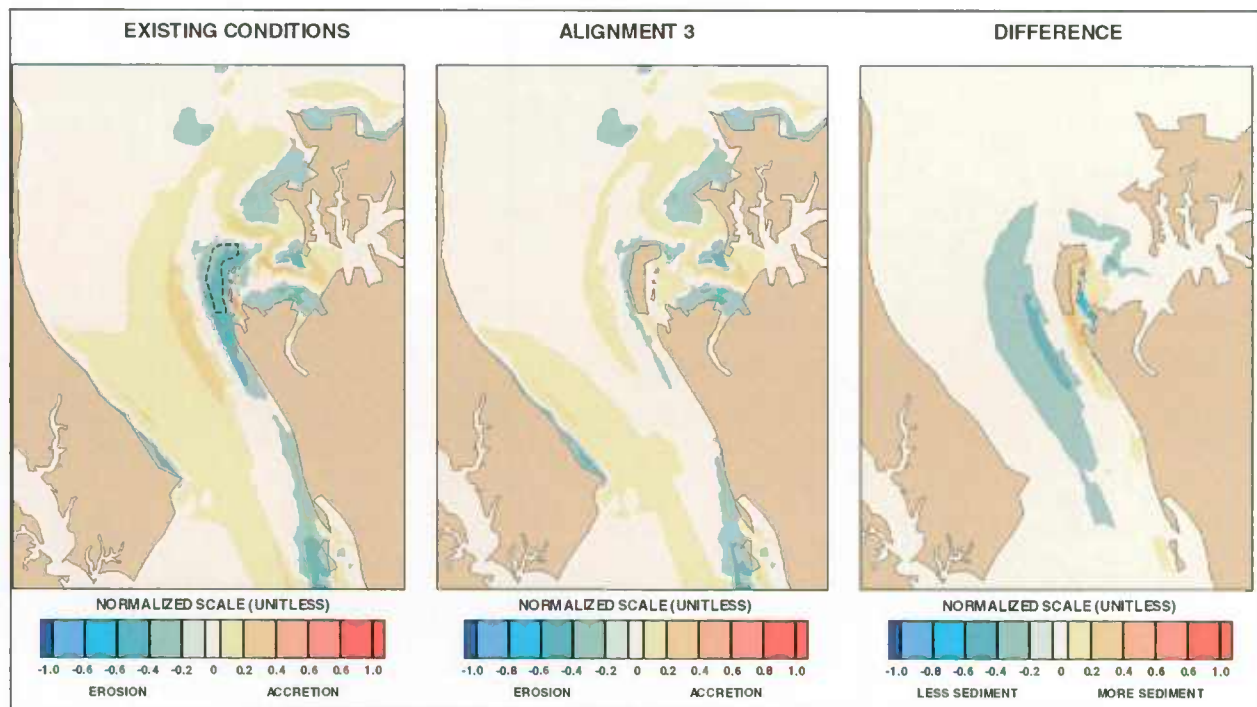


Figure 7-16: Cohesive Sediment – North-Northwest Wind 13 mph Alignment 3 vs. Existing Conditions

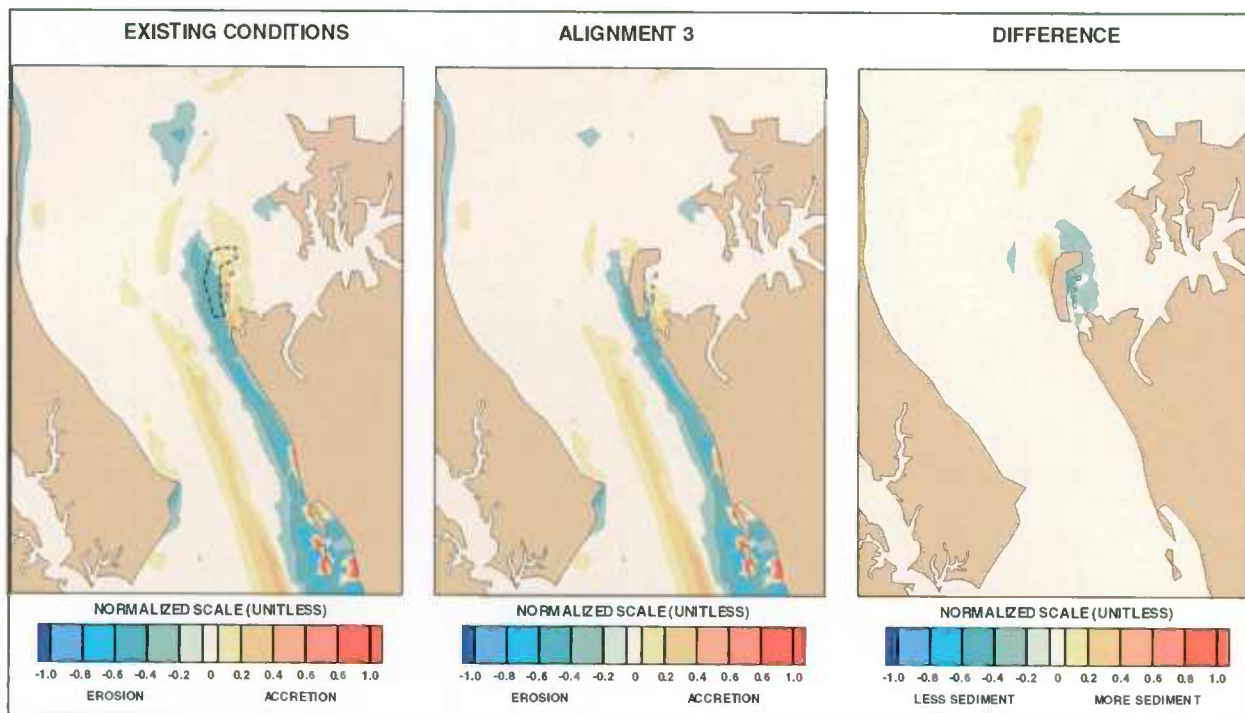


Figure 7-17: Cohesive Sediment – South-Southeast Wind 13 mph – Alignment 3 vs. Existing Conditions

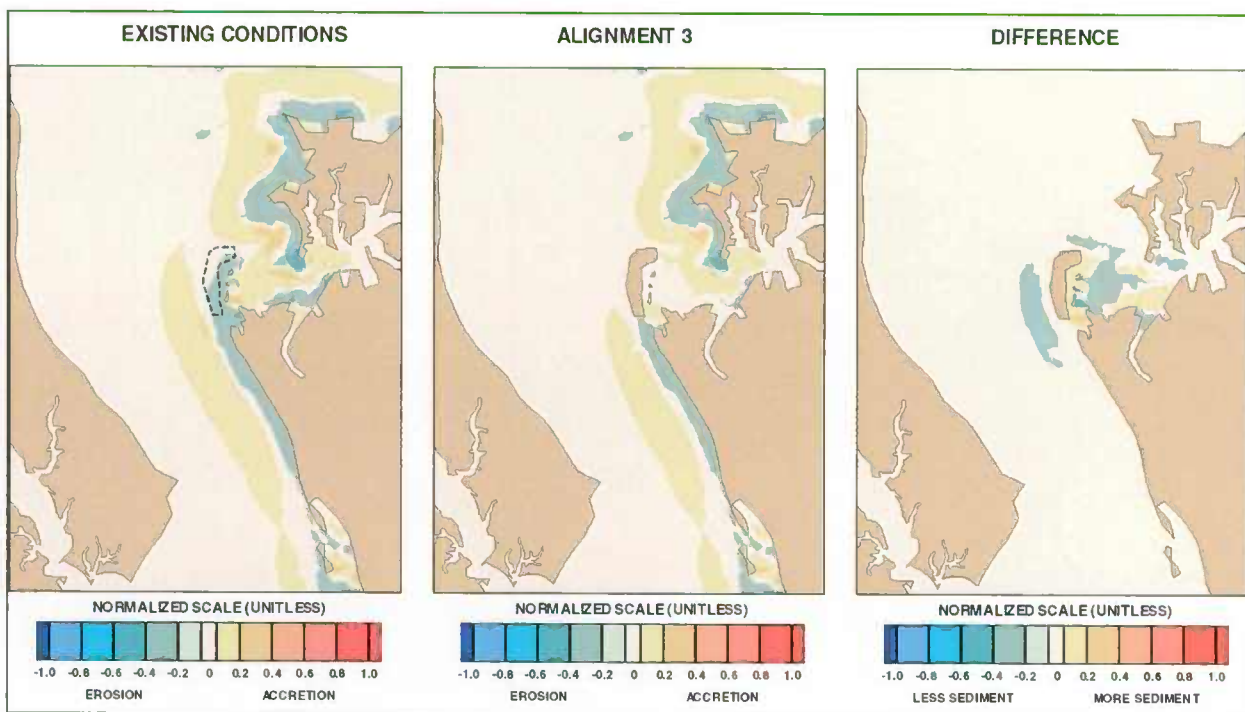
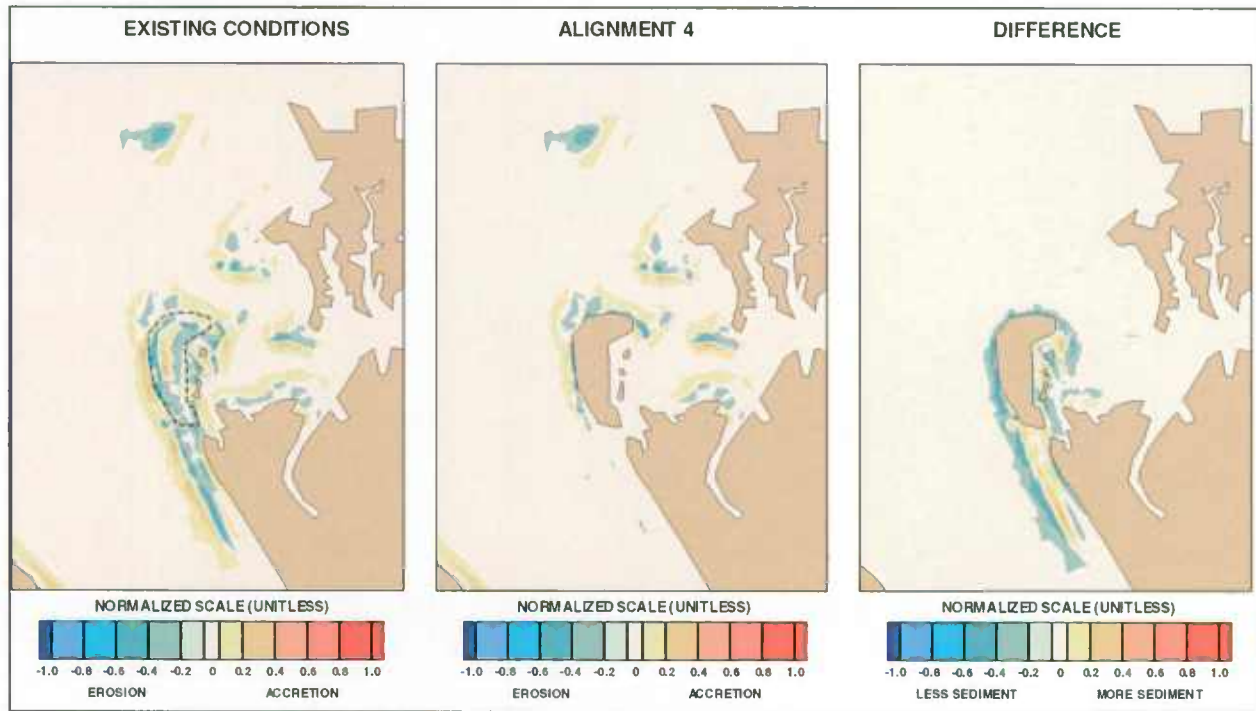
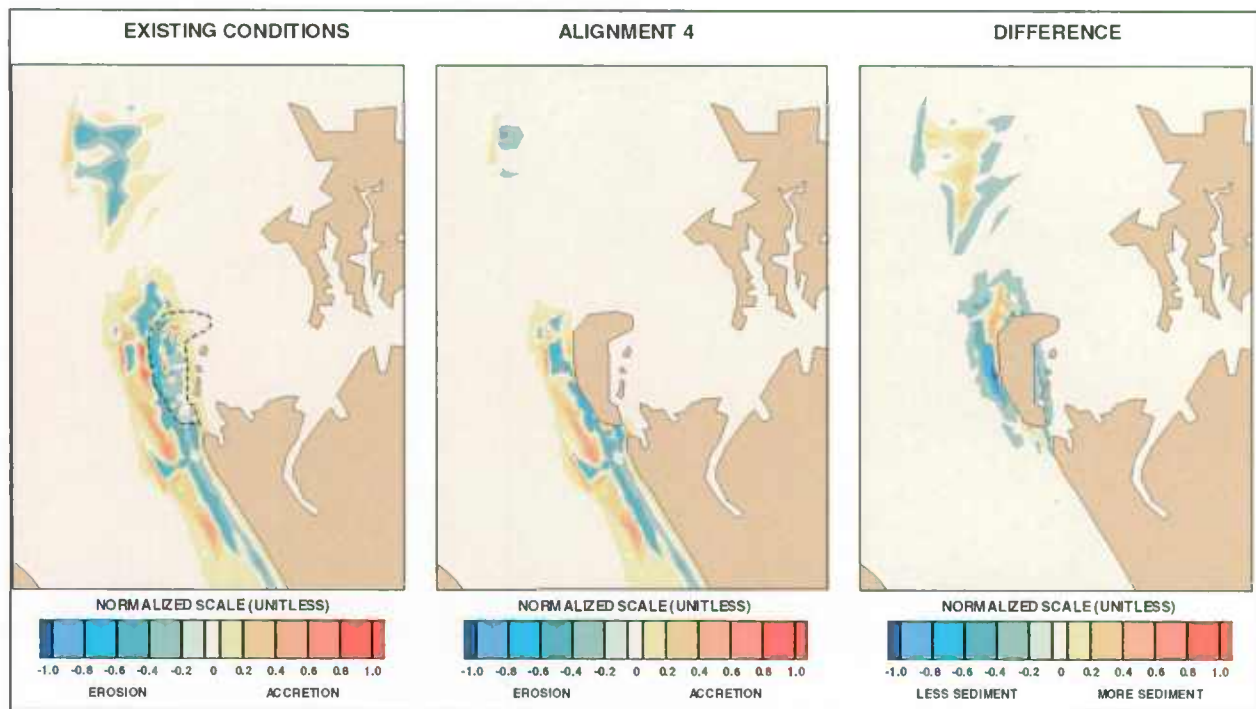


Figure 7-18: Cohesive Sediment – West-Northwest Wind 13 mph – Alignment 3 vs. Existing Conditions



20 **Figure 7-19: Non-Cohesive Sediment – North-Northwest Wind 16 mph – Alignment 4 vs.**  
21 **Existing Conditions**



42 **Figure 7-20: Non-Cohesive Sediment – South-Southeast Wind 16 mph – Alignment 4 vs.**  
43 **Existing Conditions**

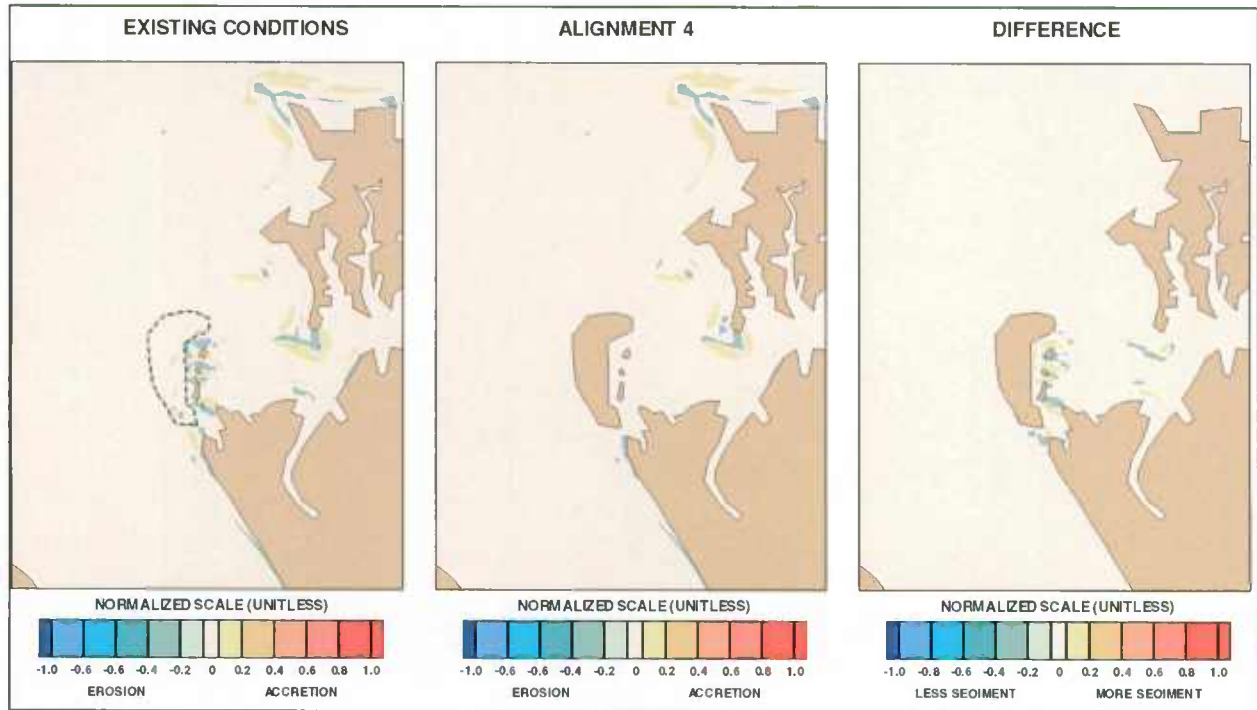


Figure 7-21: Non-Cohesive Sediment – West -Northwest Wind 16 mph – Alignment 4 vs. Existing Conditions

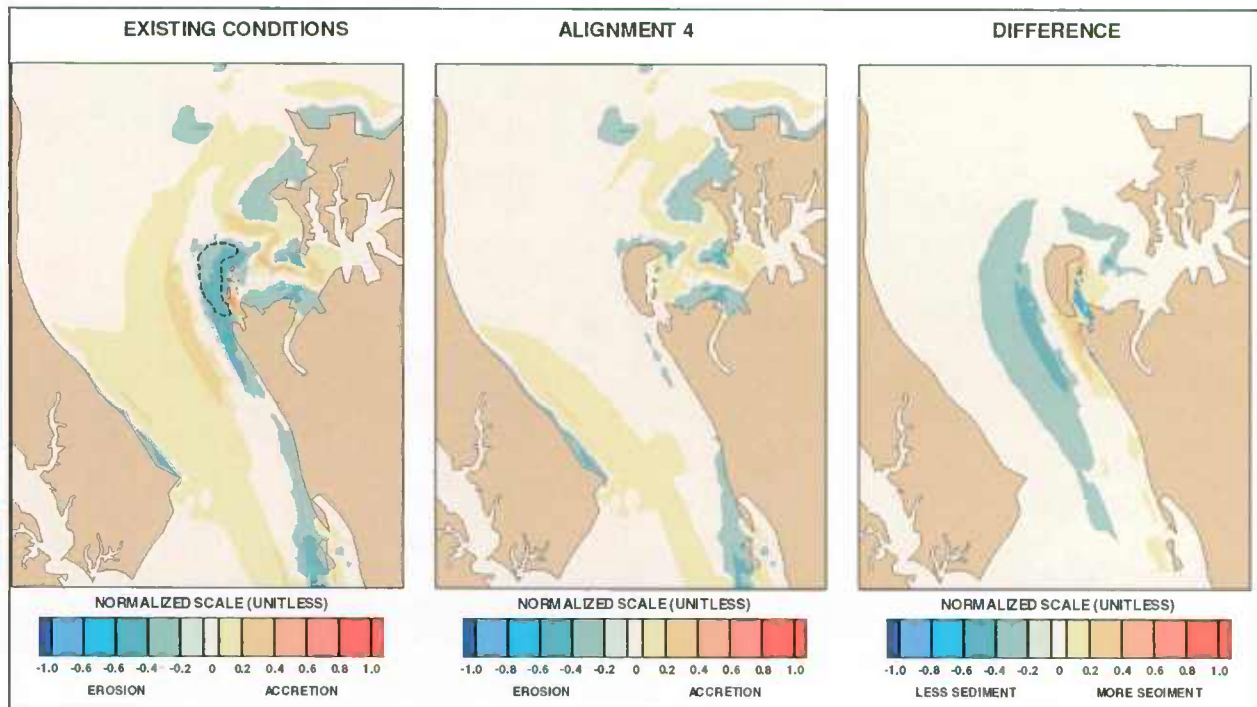


Figure 7-22: Cohesive Sediment – North-Northwest Wind 13 mph Alignment 4 vs. Existing Conditions

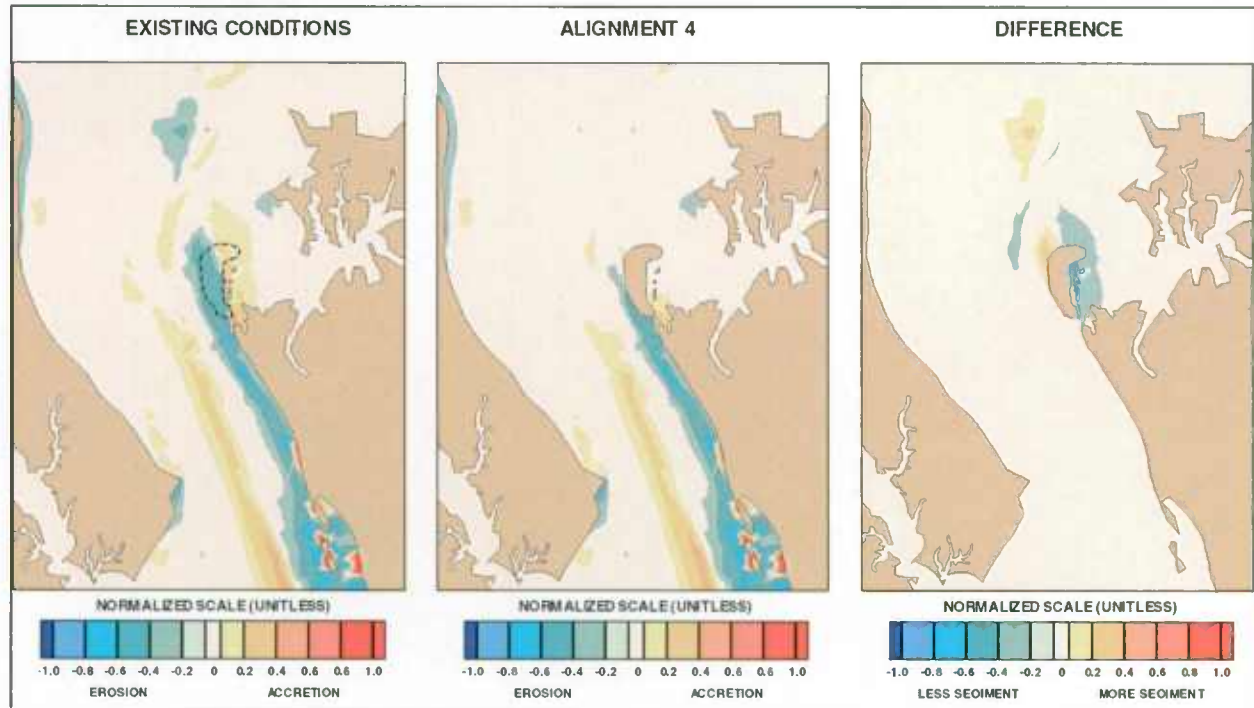


Figure 7-23: Cohesive Sediment – South-Southeast Wind 13 mph – Alignment 4 vs. Existing Conditions

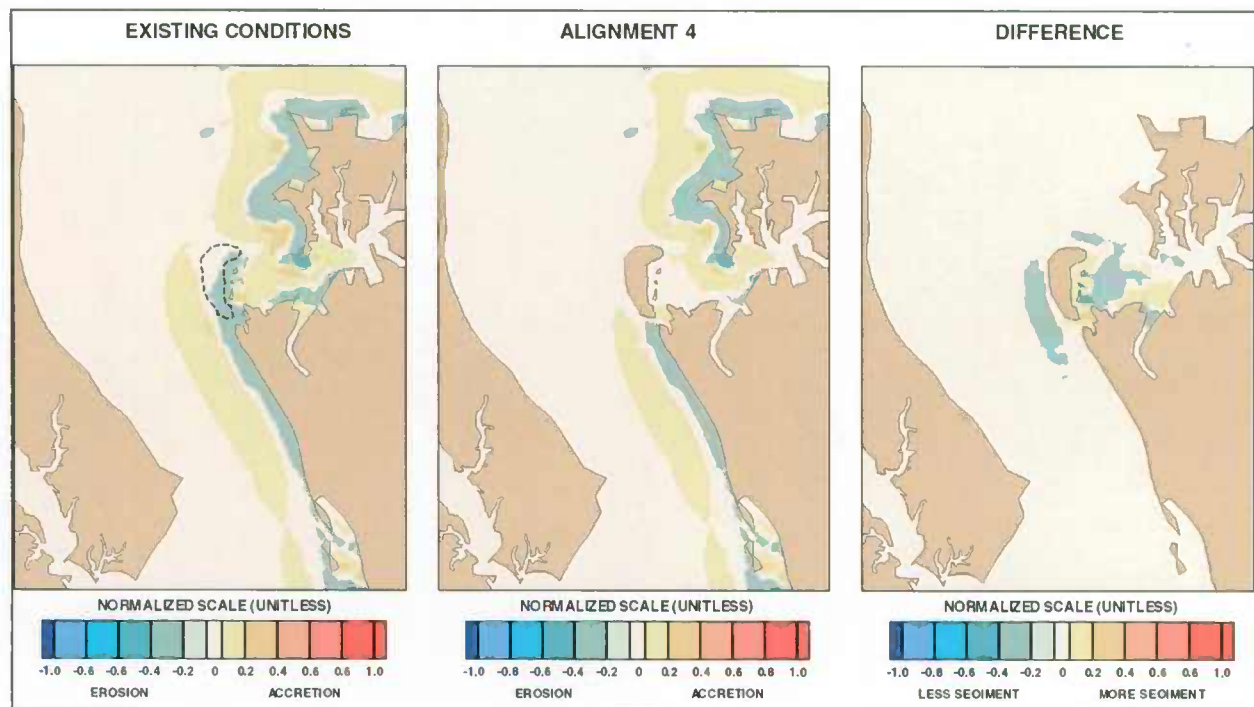


Figure 7-24: Cohesive Sediment – West-Northwest Wind 13 mph – Alignment 4 vs. Existing Conditions

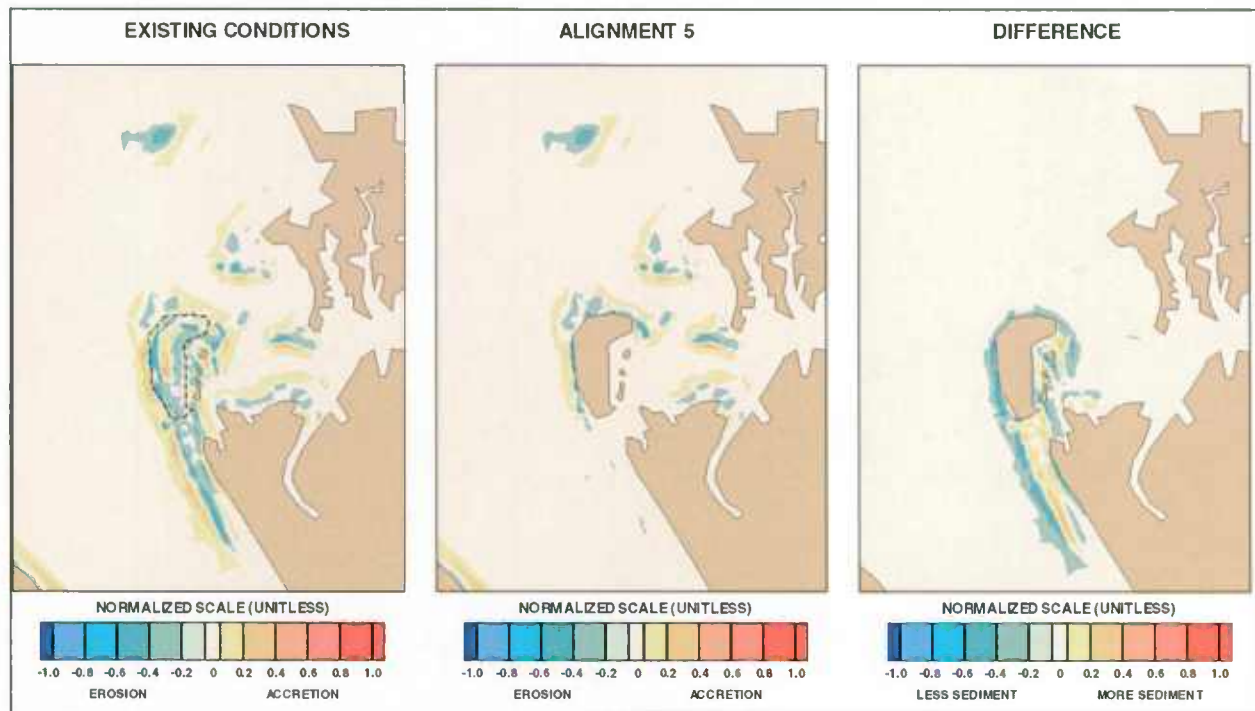


Figure 7-25: Non-Cohesive Sediment – North-Northwest Wind 16 mph – Alignment 5 vs. Existing Conditions

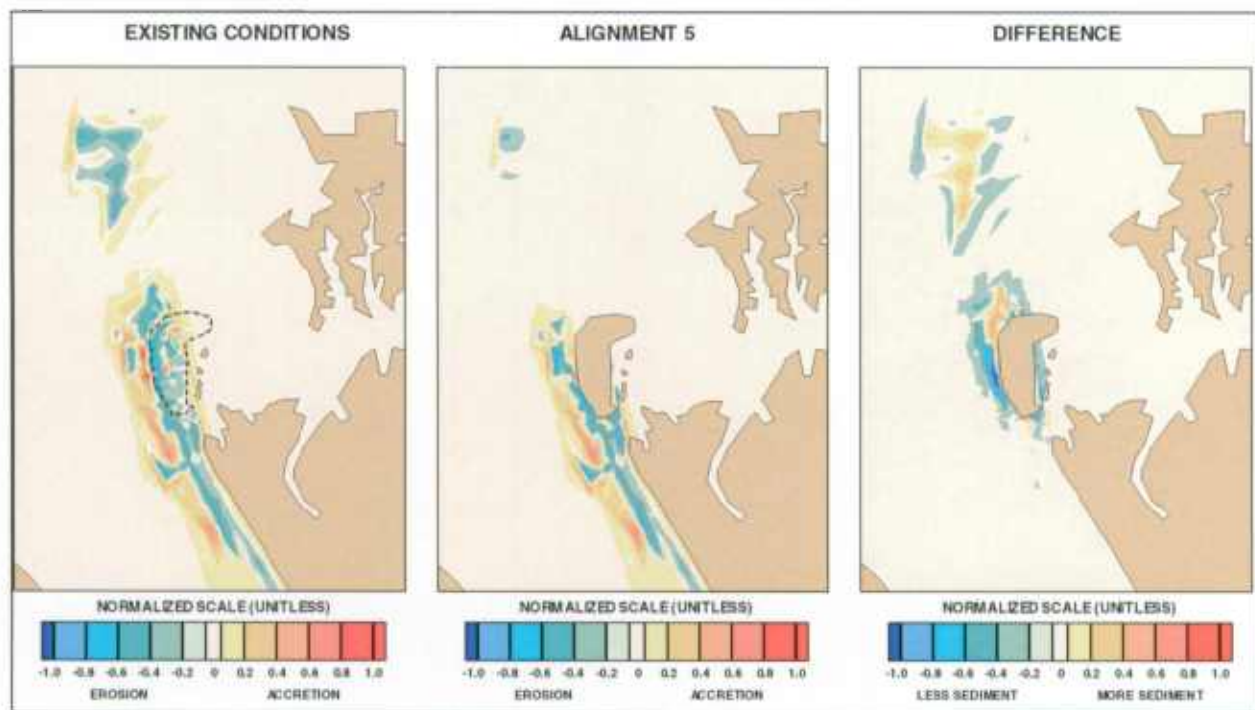


Figure 7-26: Non-Cohesive Sediment – South-Southeast Wind 16 mph – Alignment 5 vs. Existing Conditions

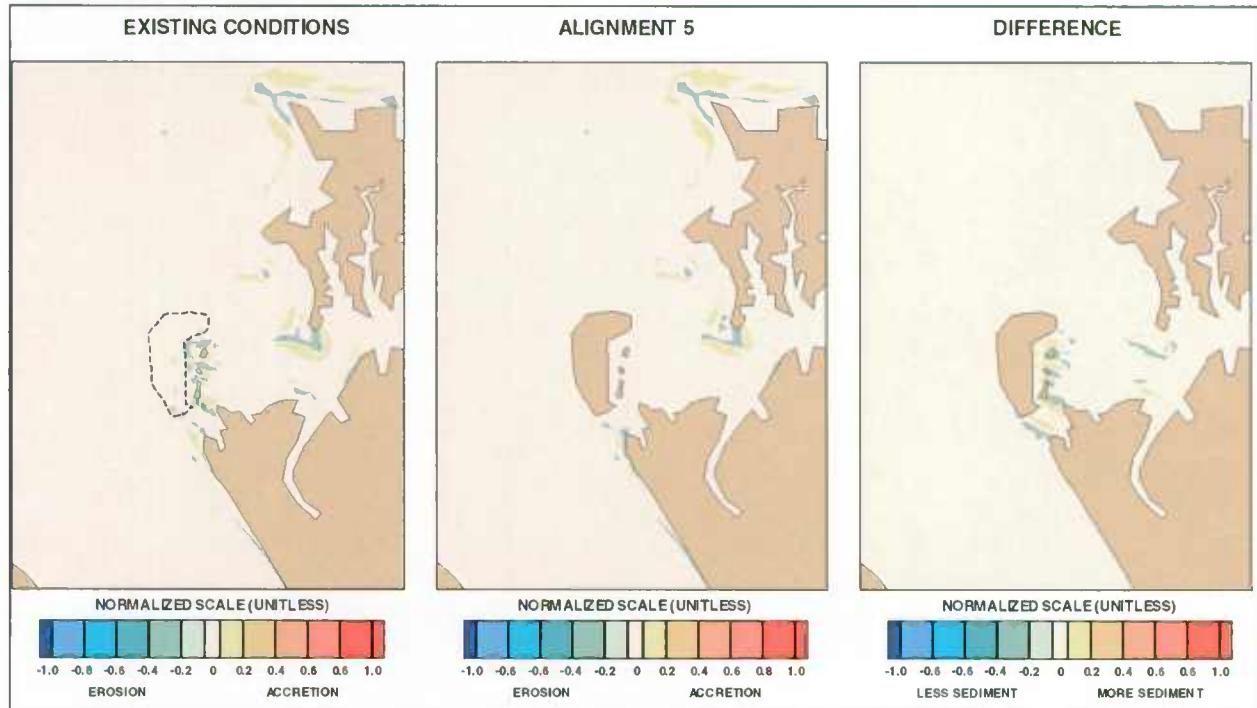


Figure 7-27: Non-Cohesive Sediment – West-Northwest Wind 16 mph – Alignment 5 vs. Existing Conditions

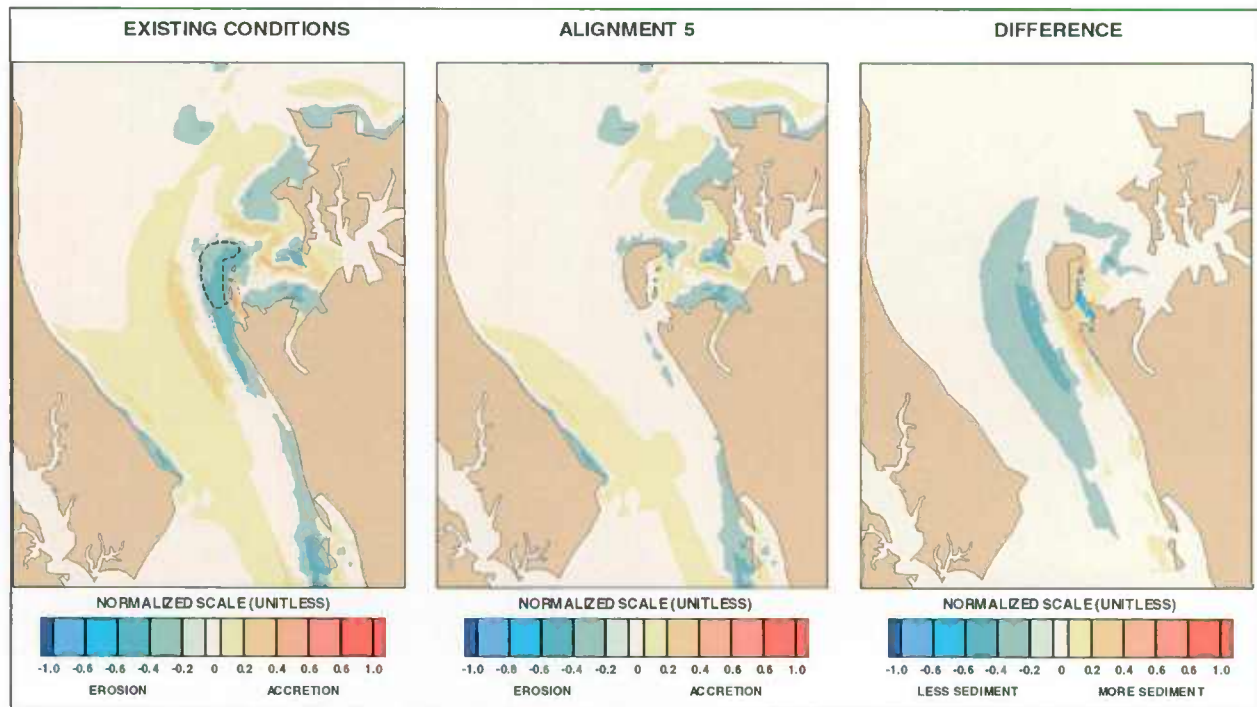


Figure 7-28: Cohesive Sediment – North-Northwest Wind 13 mph Alignment 5 vs. Existing Conditions

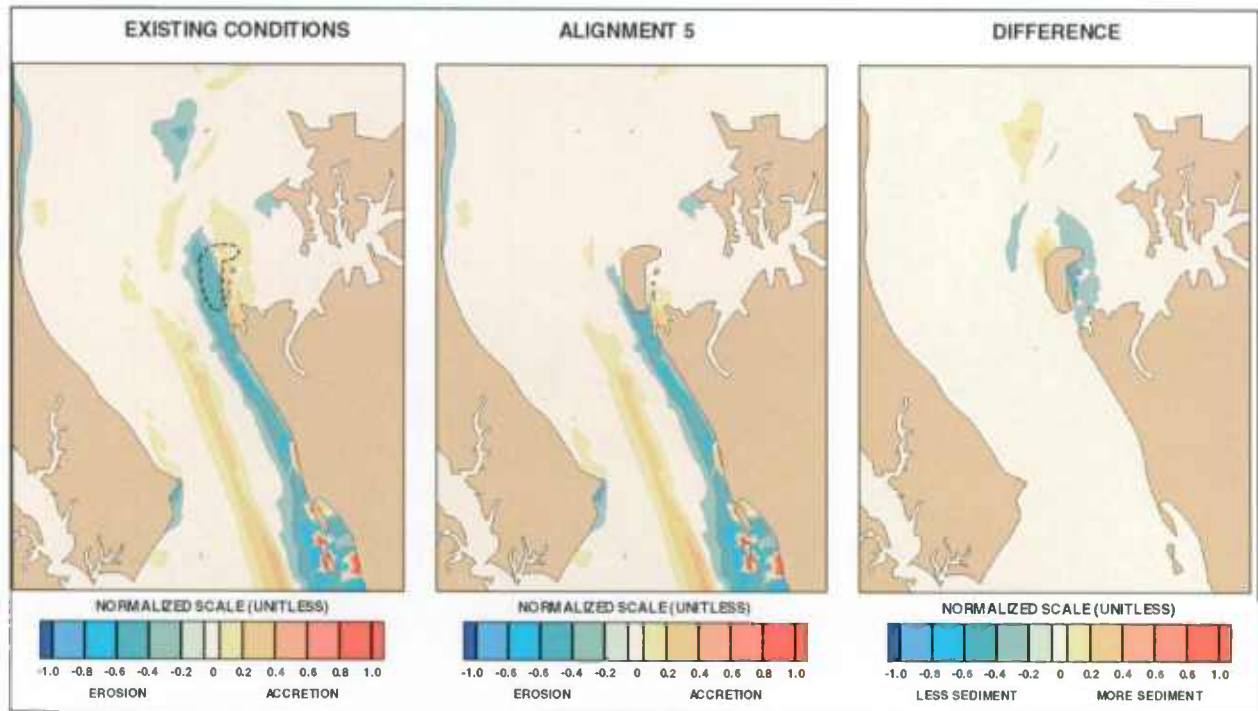


Figure 7-29: Cohesive Sediment – South-Southeast Wind 13 mph – Alignment 5 vs. Existing Conditions

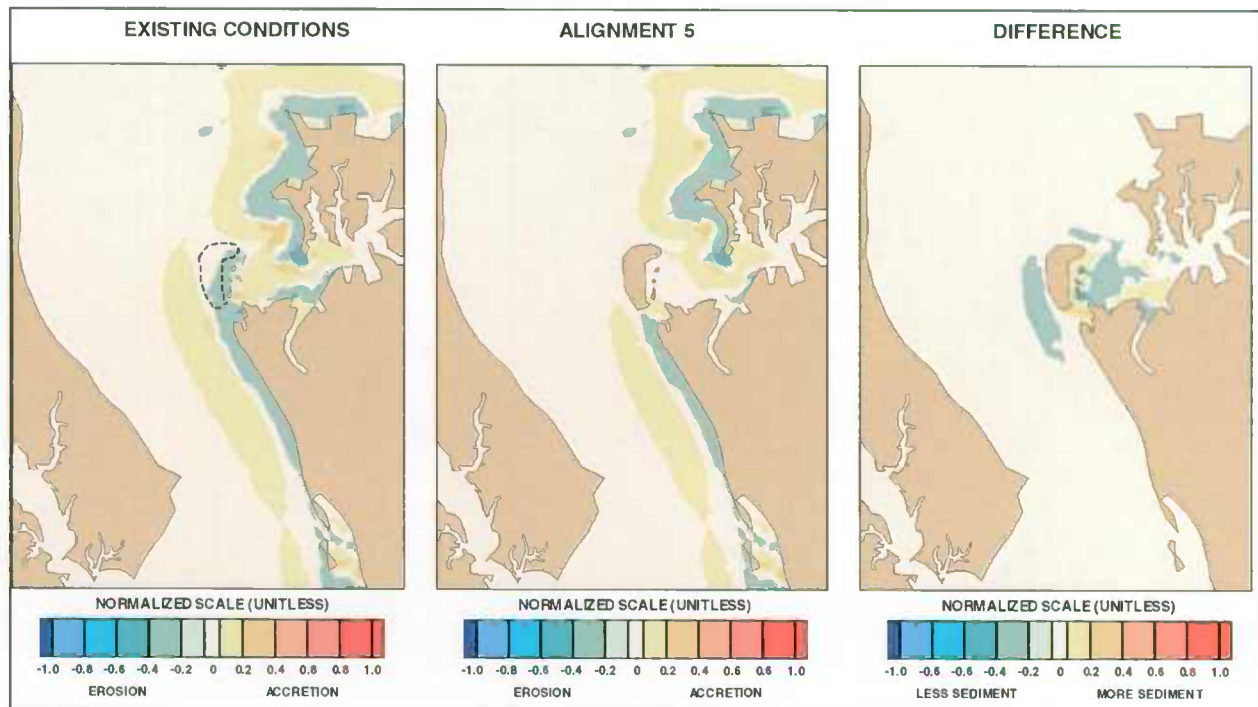


Figure 7-30: Cohesive Sediment – West-Northwest Wind 13 mph – Alignment 5 vs. Existing Conditions

## 1 8. CONCLUSIONS AND RECOMMENDATIONS

### 2 8.1 CONCLUSIONS

3 Results of the Hydrodynamics and Sedimentation Numerical Modeling for the James Island  
4 Reconnaissance Study show that the construction of the island to create additional beneficial use  
5 habitat area would have impacts on local conditions, especially in the area east and south of the  
6 island, and negligible impacts in the far field. The primary impacts on local conditions include  
7 substantial reduction of shoreline erosion along James Island and portions of Taylors Island and  
8 improved water quality within the region due to creation of a quiescent area east of the project.

9 Current velocities around the north of James Island increase on the order of 0.1 to 0.2 ft/sec  
10 current velocities east of the project decrease by 0.4 to 0.5 ft/sec, and current velocities south of  
11 the project increase by about 0.4 to 0.5 ft/sec. Negligible changes are seen in water surface  
12 elevations.

13 Potential changes in tidal current velocities, coupled with wind induced wave conditions, could  
14 cause changes in sedimentation patterns and rates. Non-cohesive sands exhibit reductions in  
15 both erosion and accretion rates following island creation. Cohesive clays have decreased  
16 sedimentation and decreased sediment movement east of James Island.

17 Note that reasonable assumptions, as regards input parameters, were made to perform this  
18 sedimentation modeling study. Because environmental conditions are constantly changing, the  
19 computed sedimentation rate will likely vary as new equilibrium conditions are reached. With  
20 this in mind, the results indicate that there will be localized changes in current velocities and  
21 sedimentation rates and patterns.

### 22 8.2 RECOMMENDATIONS

23 The following recommendations are made to achieve stated objectives for further evaluation and  
24 monitoring of the project area.

25 Further numerical modeling should be performed using three-dimensional models which will

1 more accurately represent hydrodynamics and sedimentation in the Chesapeake Bay. A three-  
2 dimensional model could be used to simulate vertical stratification of currents and sediments due  
3 to winds and salt wedge effects.

4 Additional measured data is required to improve the model calibration. Data needs include  
5 bathymetric survey, current velocity measurements, water surface elevations, and suspended  
6 sediment measurements. Water surface elevations, current velocity and sediment collection  
7 devices installed simultaneously in various locations throughout the bay and project area, and left  
8 in place for a minimum period of one month would serve to verify the model calibration. Water  
9 surface elevation and current velocities would be used to refine the hydrodynamic model;  
10 thickness of sediment and suspended sediment would be used to refine the sedimentation model.

11 Results obtained from the refined model would be used to examine environmental impacts  
12 including water quality as well as to optimize island alignments including fixed jetties and  
13 breakwaters.

14

## 1 9. REFERENCES

- 2 Brigham Young University (BYU). 1995. FastTABS 3.1 Hydrodynamic Modeling Software.  
3 Engineering Computer Graphics Laboratory.
- 4 Maryland Geological Survey (MGS). 1952 through 1999. Aerial Photographs.
- 5 National Ocean Service (NOS). 1988. U.S. Department of Commerce, National Oceanic and  
6 Atmospheric Administration (NOAA). Tide and Tidal Currents in the Chesapeake Bay.  
7 Rockville, MD.
- 8 National Ocean Service (NOS). 1993. U.S. Department of Commerce, National Oceanic and  
9 Atmospheric Administration (NOAA). Chart Number 12230.
- 10 National Ocean Service (NOS). 1993. U.S. Department of Commerce, National Oceanic and  
11 Atmospheric Administration (NOAA). Chart Number 12263.
- 12 National Ocean Service (NOS). 1993. U.S. Department of Commerce, National Oceanic and  
13 Atmospheric Administration (NOAA). Chart Number 12264.
- 14 National Ocean Service (NOS). 1993. U.S. Department of Commerce, National Oceanic and  
15 Atmospheric Administration (NOAA). Chart Number 12266.
- 16 National Ocean Service (NOS). 1993. U.S. Department of Commerce, National Oceanic and  
17 Atmospheric Administration (NOAA). Chart Number 12268.
- 18 National Ocean Service (NOS). 1993. U.S. Department of Commerce, National Oceanic and  
19 Atmospheric Administration (NOAA). Chart Number 12270.
- 20 National Ocean Service (NOS). 1993. U.S. Department of Commerce, National Oceanic and  
21 Atmospheric Administration (NOAA). Chart Number 12272.
- 22 National Ocean Service (NOS). 1993. U.S. Department of Commerce, National Oceanic and  
23 Atmospheric Administration (NOAA). Chart Number 12273.
- 24 National Ocean Service (NOS). 1993. U.S. Department of Commerce, National Oceanic and  
25 Atmospheric Administration (NOAA). Chart Number 12274.
- 26 National Ocean Service (NOS). 1993. U.S. Department of Commerce, National Oceanic and  
27 Atmospheric Administration (NOAA). Chart Number 12278.
- 28 National Ocean Service (NOS). 1996. U.S. Department of Commerce, National Oceanic and  
29 Atmospheric Administration (NOAA). Tidal Currents 1996. Rockville, MD.
- 30 National Ocean Service (NOS). 1997. U.S. Department of Commerce, National Oceanic and  
31 Atmospheric Administration (NOAA). Tide Datums for Selected Stations.

- 1 National Ocean Service (NOS). 2000. U.S. Department of Commerce, National Oceanic and  
2 Atmospheric Administration (NOAA). Web Site: <http://mapfinder.nos.noaa.gov/>.  
3 Digital Elevation Models (DEMs).
- 4 Schubel, J.R. and D.W. Pritchard, 1987. A brief physical description of the Chesapeake Bay, in  
5 Contaminant problems and management of living Chesapeake Bay resources, edited by  
6 S. K. Majumdar, L.W. Hall, Jr., and H. M. Austin, 1-32, Pa Acad. Sci., Philadelphia, PA.
- 7 Thomas, W.A., W.H. McAnally, Jr. and S.A. Adamec, Jr. 1985. A User's Manual for the  
8 Generalized Computer Program, Sediment Transport in Unsteady, 2-Dimensional Flow,  
9 Horizontal Plane (STUDH).
- 10 U.S. Department of Agriculture (USDA), Soil Conservation Service (SCS). 1973. Soil Survey  
11 of Prince Georges County, Maryland.
- 12 U.S. Geological Survey (USGS). 2000. Web Site: <http://md.water.usgs.gov/historical.html>
- 13 Winterwerp, Han. On the dynamics of high-concentrated mud suspensions. Delft: Delft  
14 University of Technology, Faculty of Civil Engineering and Geosciences, 1999; 1 v.  
15 (Communications on hydraulic and geotechnical engineering; rept. no. 99-3). G642 X  
16 no.99-3  
17  
18